

EXAMINING THE ROLE OF THE HOST HELICASE DDX56 DURING
FLAVIVIRUS INFECTIONS

by

Colleen Reid

A thesis submitted in partial fulfillment of the requirements for the degree of

Master of Science

in

Virology

Department of Medical Microbiology and Immunology
University of Alberta

© Colleen Reid, 2015

Abstract

Flaviviruses, such as West Nile virus (WNV), Powassan virus (POW), and Saint Louis encephalitis virus (SLEV), are significant pathogens capable of causing serious neurological disease in both humans and animals. Despite their relevance to human health, treatment and vaccines for these viruses remain limited. Characterizing important cellular host factors during viral infection may identify novel targets for the development of antivirals. Previously, a host nucleolar RNA helicase, DDX56, was identified as an essential host factor for WNV infectivity by utilizing its ATP-dependent helical activity to enhance the packaging of viral RNA. Through extensive microscopy analyses I show that DDX56 localizes to the ER, the site of viral replication and assembly, during WNV infection and colocalizes with markers for viral assembly. Additionally, DDX56 does not play a role in the reorganization of membranes and the induction of viral structural elements in WNV infection. Together, these data support the role of DDX56 in assembly of infectious virions.

I also investigated whether other viruses, POW and SLEV, utilize DDX56 during infection making it a potential target for broad-spectrum antivirals. Interestingly, while I discovered that these viruses affect DDX56 localization and stability, they do not require this helicase for the production of infectious virions. Thus, DDX56 seems to be an essential host factor for WNV while the underlying mechanism of relocalization may not be virus specific. Collectively, my studies further our understanding of the role of DDX56 during WNV infection and further support it as a target for the development of antivirals.

Acknowledgements

I would like to first and foremost thank my supervisor Dr. Tom Hobman for his support, encouragement, knowledge, and enthusiasm during my M.Sc. studies. His advice and expertise helped me during all aspects of research and writing of this thesis. I am thankful to have had the opportunity to work with someone who provides unwavering support for his students and is an excellent scientific mentor.

I would like to thank present and past members of the Hobman lab, including Zack, Adriana, Shangmei, Anil, Joaquin, Justin, Eileen, Valeria, Daniel, Steven, Jae, and Anh. Their technical assistance and helpful discussions greatly aided me in the navigation of this project.

I want to sincerely thank Dr. David Evans and Dr. David Marchant, my supervisory committee, for their advice and helpful suggestions during my M.Sc. studies. Their expertise and immense knowledge aided me in the development of this thesis. I would also like to thank Dr. Ben Montpetit for taking the time to read my thesis and serving as the external examiner during my defense.

Finally, I would like to thank my parents Karen and Lloyd, my siblings Erin and Andrew, and last but certainly not least, my fiancé Joseph. Without their tremendous support, unwavering confidence in me, and encouragement this thesis would not have been completed. I want to especially thank Joe for his companionship and love, and showing me there are more important things in life than work.

Table of Contents

Chapter 1: Introduction	1
1.1 Classification and Clinical Significance of Flaviviruses	2
1.2 Flavivirus Genome and Protein Function(s)	6
1.3 Flavivirus Lifecycle	11
1.3.1 Cellular Tropism and Entry	11
1.3.2 Replication and Translation	12
1.3.3 Assembly, Virion Maturation, and Release	14
1.3.4 Hijacking of Host Membranes	16
1.4 Virus-host Interplay: Host Factors involved in Flavivirus Infection	18
1.4.1 Identification of host factors	18
1.4.2 DEAD-box RNA helicases and virus infection	19
1.4.3 DDX56 is necessary for production of infectious WNV virions	23
1.5 Objectives of Study	26
Chapter 2: Materials and Methods	27
2.1 Materials	28
2.1.1 Reagents	28
2.1.2 Equipment and analyses platforms	30
2.1.3 Commonly used buffers and solutions	31
2.1.4 Antibodies	31
2.2 Methods	33
2.2.1 Cell lines and cell maintenance	33
2.2.2 Cell Transfection	33
2.2.3 RNA Interference	34
2.2.4 Virological Techniques	34
2.2.4.1 Virus Strains and Generation of Stocks	34
2.2.4.2 Virus Infection	34
2.2.4.3 Plaque Assay	35

2.2.5 Protein Electrophoresis and Detection	36
2.2.5.1 Preparation of cell lysates	36
2.2.5.2 Sodium dodecyl-sulphate polyacrylamide gel electrophoresis (SDS-PAGE)	36
2.2.5.3 Western Blot Analysis	36
2.2.5.4 Detection of Fluorescent-conjugated secondary antibodies	37
2.2.6 Analysis of protein-protein interactions	37
2.2.6.1 Cellular Fractionation	37
2.2.6.2 Co-Immunoprecipitation of DDX56-WNV capsid	38
2.2.7 Microscopy Techniques	39
2.2.7.1 Indirect Immunofluorescence	39
2.2.7.2 Confocal Imaging	40
2.2.7.3 Three Dimensional Structured Illumination (3D-SIM) Imaging	40
2.2.7.4 Transmission Electron Microscopy	41
Chapter 3: Visualization of DDX56 at WNV Assembly Complexes	42
3.1 Rationale	43
3.2 Results	45
3.2.1 DDX56 localizes to virus assembly sites during WNV infection	45
3.2.2 Reducing DDX56 expression does not affect formation of virus-induced membrane alterations and virus replication sites	52
3.2.3 Expression of WNV proteins does not affect DDX56 cellular distribution	56
3.2.4 DDX56 and WNV capsid interact in the nucleus during infection	63
3.3 Conclusions	67
Chapter 4: Role of DDX56 during <i>Flavivirus</i> Infection	68
4.1 Rationale	69
4.2 Results	70
4.2.1 POW and SLEV infection causes depletion of DDX56	70
4.2.2 Reducing expression of DDX56 does not significantly affect the infectivity of POW and SLEV	79

4.3 Conclusion	83
Chapter 5: Discussion	84
5.1 Overview	85
5.2 Unraveling the role of DDX56 during WNV Assembly	86
5.2.1 Characterizing DDX56 localization during WNV infection	86
5.2.2 Mechanisms of DDX56 relocalization	89
5.3 DDX56 is a specific host factor for WNV infectivity	91
5.4 Future Directions	93
References	94

List of Tables

Table 2.1 Sources of materials, reagents, and chemicals	28
Table 2.2 Commercially available kits	30
Table 2.3 Detection systems	30
Table 2.4 Analysis software	30
Table 2.5 Buffers and Solutions	31
Table 2.6 Primary Antibodies	31
Table 2.7 Secondary Antibodies	32

List of Figures

Figure 1.1 Schemativ Representation of Flavivirus RNA genome and encoded proteins	8
Figure 1.2 Flavivirus Lifecycle	15
Figure 3.1 DDX56 localizes to the site of virus replication and assembly during WNV infection	47
Figure 3.2 DDX56 colocalizes at viral assembly complexes in the cytoplasm with WNV envelope and calnexin	49
Figure 3.3 DDX56 localizes to punctate regions associated with WNV envelope and calnexin	51
Figure 3.4 DDX56 is not required for WNV-induced membrane rearrangements and ultrastructure	54
Figure 3.5 Expression of WNV proteins does not result in a relocalization or loss of DDX56 from the nucleolus	58
Figure 3.6 Expression of WNV proteins does not induce degradation of DDX56	62
Figure 3.7 DDX56 primarily colocalizes with capsid in the nucleus of WNV infected cells	65
Figure 3.8 DDX56 and WNV capsid interact in the nucleus during infection	66
Figure 4.1 POW and SLEV infection induces a loss of DDX56 in the nucleus of Vero cells	72
Figure 4.2 Flaviviruses WNV, POW, and SLEV induce degradation of DDX56 during infection	76
Figure 4.3 Flaviviruses POW and SLEV do not require DDX56 for infectious virion production	81

Abbreviations

Three-dimensional Structured Illumination Microscopy	3D-SIM
Human aveolar basal epithelial 549 cells	A549
Baby hamster kidney-21 cells	BHK-21
Bovine serum albumin	BSA
Capsid protein	C
Clathrin-dependent endocytosis	CDE
Convoluting membranes	CM
Central nervous system	CNS
4',6-diamidino-2-phenylindole	DAPI
DEAD-box RNA Helicase	DDX
DEAD-box RNA Helicase 56	DDX56
DEAD-box RNA Helicase protein knock down	DDX56-KD
Dengue virus	DENV
Dulbecco's modified Eagle's medium	DMEM
Dimethyl sulphoxide	DMSO
Double-stranded RNA	dsRNA
Envelope protein	E
ethylenediaminetetraacetic acid	EDTA
Electron Microscopy	EM
Endoplasmic Reticulum	ER
Electron Tomography	ET
Fetal bovine serum	FBS
Hours post infection	h.p.i.
Hepatitis C virus	HCV
Human embryonic kidney 293T cells	HEK 293T
4-(2-hydroxyethyl)-1-piperazineethanesulphonic acid	HEPES
Human immunodeficiency virus type 1	HIV-1
Immunofluorescence	IF
Immunoglobulin G	IgG
Immunoprecipitation	IP
Japanese encephalitis virus	JEV
Lipid Droplets	LDs
Multiplicity of infection	MOI
Nuclear Pore Complex	NPC
Non-structural Proteins (viral)	NS
Nuclear Pore Complex proteins	Nup
WNV _{NY99} non-structural protein replicon	NY99
Processing Bodies	P-bodies

Phosphate buffered saline	PBS
Paracrystalline arrays	PC
Pearson's correlation coefficients	PCC
Powassan virus	POW
Precursor membrane protein	prM
Polyvinylidene difluoride	PVDF
RNA-dependent RNA polymerase	RdRp
Ribonucleic acid	RNA
Region of interest	ROI
WNV Structural Cassette (C/prM/E)	SC
Sodium dodecyl-sulphate polyacrylamide gel	SDS-PAGE
Pooled siRNA-targeting DDX56	siDDX56
siRNA nonsilencing control	siNC
Small-interfering RNA	siRNA
Saint Louis encephalitis virus	SLEV
Tick-borne encephalitis virus	TBEV
Transmission Electron Microscopy	TEM
N,N,N',N'-tetramethylethylenediamine	TEMED
Enzymatic units	U
Untranslated region	UTR
Volume per volume	v/v
Vesicular Packets	VPs
Viral Replication Complex	VRC
Weight per volume	w/v
West Nile virus	WNV
Kunjin virus (Australian attenuated strain of WNV)	WNV _{KUN}
West Nile virus (New York 1999 strain, highly pathogenic)	WNV _{NY99}
Yeast-2-hybrid	Y2H
Yellow fever virus	YFV

Chapter 1

Introduction

1.1 Classification and Clinical Significance of Flaviviruses

The family *Flaviviridae* is comprised of animal viruses divided into three genera: *Flavivirus*, *Pestivirus*, and *Hepacivirus*. Members of this family are small, enveloped, positive-sense, single-stranded RNA viruses. The *Flavivirus* genus is comprised of 50 defined species, 40 of which cause disease in humans (reviewed in (Sips, Wilschut et al. 2012)). Notable human pathogenic members include Yellow Fever virus (YFV), West Nile virus (WNV), Japanese encephalitis virus (JEV), Dengue virus (DENV), Saint Louis encephalitis virus (SLEV), and Tick-borne encephalitis viruses (TBEV). Some of these viruses, such as WNV and SLEV, are capable of crossing the blood-brain barrier leading to encephalitis and meningitis, while others, like DENV, cause vascular leakage and hemorrhagic fever, and thus pose a serious health threat to humans, mammals, and other vertebrates that contract them.

Viruses within the *Flavivirus* genus are primarily spread via arthropod vectors, mosquitos and ticks. The viruses used in my research, WNV and SLEV are carried by *Culex* species of mosquitos while Powassan virus (POW), a member of the TBEV clade, is carried by *Ixodes* species of ticks (Calisher 1994, Weaver 2005, Ebel 2010, Gray and Webb 2014). The transmission of these viruses is dependent on contact and feeding by an infected vector. Due to the abundance of the *Culex* species, WNV and SLEV transmission occurs readily across North America. Interestingly, the use of the same vector and the emergence of WNV in North America has resulted in a decline of SLEV in the bird and mosquito population (Reisen, Lothrop et al. 2008). POW is generally confined to heavily wooded areas, such as the northeastern United States and regions within Canada (Ebel 2010). Transmission of WNV and SLEV in North America

normally occurs between sentinel birds and *Culex spp.* mosquitos. Human infection occurs through biting of infected mosquitos. However, due to the low viral titers in human blood, mosquitos do not transmit the virus from human to human, which means humans are dead-end hosts. WNV can be transmitted via organ donors or blood transfusion, a situation that often results in severe neuroinvasive disease onset (Rhee, Eaton et al. 2011, Winston, Vikram et al. 2014). The virus can also be transmitted vertically from mother to child during pregnancy or through breast milk (Hayes and O'Leary 2004). POW transmission occurs naturally between snowshoe hares or marmots and *Ixodes* species of ticks (Calisher 1994). Similar to WNV and SLEV, incidental infection of humans with POW is a dead-end process.

Comparing the coding sequences of SLEV strains with POW and other TBEV strains suggests that transmission of these viruses and their introduction into the New World (the Americas) from the Old World (Africa, Europe, and Asia) occurred over many thousands of years rather than during a single event (Moureau, Cook et al. 2015). In contrast, WNV was introduced in North America during a single event. Human WNV cases in North America were first identified during a large outbreak in New York City, USA in 1999. During this outbreak there were 62 cases of invasive neurologic disease and 7 deaths (Mostashari, Bunning et al. 2001, Nash, Mostashari et al. 2001). Since 1999, there have been thousands of cases reported annually in North America with geographic distribution of cases gradually spreading east to west as well as both north and south (Hayes, Sejvar et al. 2005). In Canada, annual case numbers vary greatly. During a peak year (2007), 2215 cases of human disease were reported (Public Health Agency of Canada, Surveillance of West Nile). The largest WNV outbreak in the United

States occurred in 2012, with over 5600 human disease cases, most of these occurring in the state of Texas where 1800 cases and 89 deaths were reported (Center for Disease Control and Prevention). SLEV was first isolated in 1933 during a large outbreak in Saint Louis, Missouri, U.S.A (Calisher 1994). An earlier outbreak with similar clinical manifestations occurred in the previous year. While SLEV is found throughout North America, most clinical cases are confined to the southern United States, with approximately 7 cases of neuroinvasive disease per year (Center for Disease Control and Prevention). The largest outbreak of SLEV in North America occurred between 1974-1976 where over 2000 cases were reported. POW was first isolated in 1958 from an infected child who died of encephalitis in Powassan, Ontario, Canada (Calisher 1994). Due to the relatively poor transmission between vector and humans, prevalence remains low with only 60 cases reported in the last 10 years in the U.S.A. (Center for Disease Control and Prevention). The incidence of infection by these viruses is heavily dependent on the abundance of the vector and the rate of exposure of humans to them. Use of insecticides or repellents, reducing insect habitat and/or numbers, and reducing potential contact with the vector are the most effective ways to prevent contraction of these viruses.

When humans become infected with WNV, SLEV, or POW, most cases are asymptomatic. For example, ~80% of WNV infections in human do not result in clinical disease (Sejvar 2014). Clinical manifestations are usually mild and present as a transient febrile illness with fever, cough, and general malaise. Of clinical cases, <1% manifest in severe neurological infections of encephalitis, meningitis, and flaccid paralysis which can be fatal. For SLEV, it is estimated that <1% of people infected will develop clinical

symptoms, that include mild fever and headache (Calisher 1994). Of those that develop encephalitis, neurological sequelae can persist up to 3 years after infection. Elderly persons are more susceptible to severe disease as persons over 70 years old have a fatality rate of 23% (Day 2001). However, in individuals between 0-49 years, the fatality rate is lower (less than 5%). Less is known about POW infection, since there are so few known clinical cases. It's expected that most cases are subclinical, as is true for SLEV and WNV. Children are more likely to develop clinical manifestations of disease, which include headache, fever, and convulsions. Long-term neurological sequelae have been demonstrated following acute infection. As reported by the Public Health Agency of Canada, the fatality rate among individuals infected with POW that develop severe clinical disease can be as high as 60%, which is the highest reported fatality rate for Arboviruses.

Unfortunately, no vaccines or antivirals are available for WNV, SLEV, or POW. Vaccines against TBEV Europe, Far Eastern, and Siberian strains have been developed and are licensed for human use in Europe and Asia (reviewed in (Ishikawa, Yamanaka et al. 2014)). Treatment of patients with severe disease consists of supportive care to minimize damage to internal organs and to reduce the possibility for development of long-term neurological sequelae. Currently, there are no vaccines undergoing clinical trials for SLEV or POW, and this is likely due to the low numbers of clinical cases observed each year. For WNV, however, there are several human vaccines that have progressed to phase I and II clinical trials. ChimeriVAX-WN02 (Sanofi Pasteur) is a chimeric vaccine encoding the WNV prM/E proteins on a YFV-17D backbone. In phase II clinical trials >96% seroconversion rate was observed in all age groups (Biedenbender,

Bevilacqua et al. 2011). Another promising candidate, chimeric WN/DEN4Delta30 vaccine, protects against WNV and DENV serotype 4, and had a 74% seroconversion rate from a single low dose in phase I trials (Durbin, Wright et al. 2013). Additionally, a subunit vaccine WN-80E consisting of prM and 80% E protein (Merck & Co.), has shown to be protective in rhesus monkeys (Lieberman, Nerurkar et al. 2009). Currently, there are four vaccines approved for livestock and equine use (reviewed in (Ishikawa, Yamanaka et al. 2014)). In addition to vaccine strategies, there is need for the development of antivirals to treat flavivirus infections, specifically those that can reduce effects of severe disease and resulting long-term neurological sequelae. Current strategies being investigated use compounds to pharmacologically block activity of viral proteins or the neutralization of virions through therapeutic antibodies (reviewed in (Lim and Shi 2013)). The most promising approach thus far is the use of therapeutic antibodies, specifically hE16, which showed efficacy in mouse model infections when administered at 5 days post infection (Oliphant, Engle et al. 2005). Phase I clinical trials were completed to determine the tolerated dose but, thus far, phase II clinical trials have not proceeded. Clearly there is a need for the development and licensure of therapies for the treatments of these viruses. The development of broad-spectrum antivirals would be very beneficial as these viruses display similar symptoms during early onset when the antiviral action would be most needed.

1.2 Flavivirus Genome and Protein Function(s)

Flaviviral genomes are single, positive sense RNA molecules ~ 11kb in size. The 5' and 3' untranslated regions that flank the coding region form stem loop structures,

which aid in RNA translation and replication (Chiu, Kinney et al. 2005, Tilgner, Deas et al. 2005). The RNA has a conserved type-1 (m^7GpppN) 5' cap but contains no polyadenylation tail at the 3' end (Chiu, Kinney et al. 2005). The viral RNA contains one open reading frame and is translated as a single polyprotein. Following translation, processing of the polyprotein by host and viral proteases gives rise to three structural and seven non-structural (NS) proteins (Figure 1.1). Structural proteins capsid (C), membrane (prM), and envelope (E) are the components of the infectious virions. Capsid protein is a small charged protein that binds the viral RNA during assembly (assembly described in section 1.3.3). Both prM and E are transmembrane proteins that are associated with host-derived lipid membranes. Functions of prM include maturation of the virion and acting as a chaperone for E folding and assembly (Lorenz, Allison et al. 2002). Envelope protein is involved in the binding and fusion of the virion with the host cell membrane during entry (Kimura and Ohyama 1988). Besides forming the nucleocapsid core of the virion, our lab and others have shown that flaviviral capsid proteins have many roles during infection, including localization to the nucleus and interfering with cellular signaling (Makino, Tadano et al. 1989, Tadano, Makino et al. 1989, Mori, Okabayashi et al. 2005, Hunt, Urbanowski et al. 2007, Xu, Anderson et al. 2011, Xu and Hobman 2012, Bhuvanakantham and Ng 2013, Urbanowski and Hobman 2013).

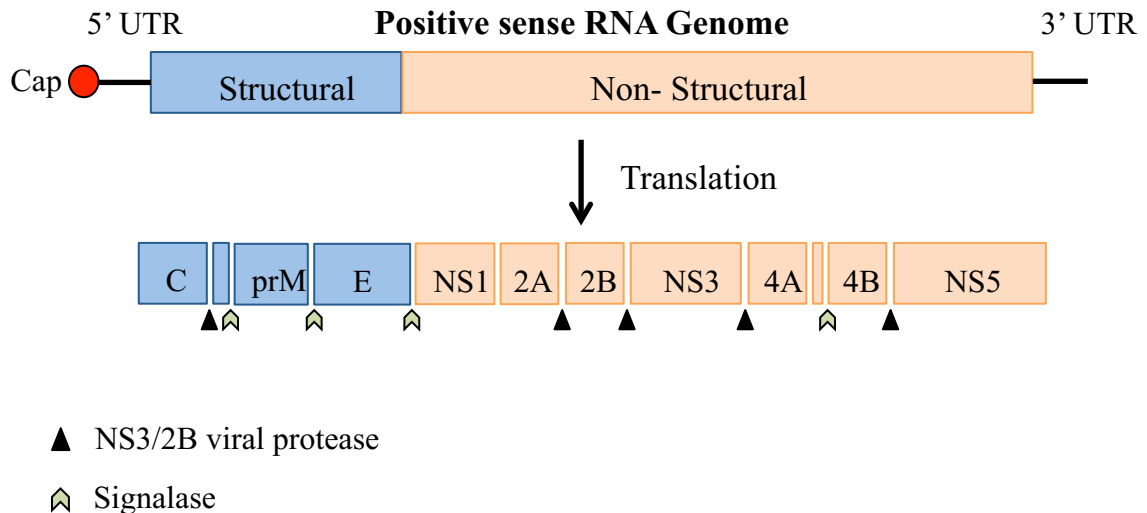


Figure 1.1 Schematic Representation of Flavivirus RNA genome and encoded proteins. The Flavivirus genome is a single strand of positive-sense RNA ~11kb. It is flanked by 5' and 3' untranslated regions (UTRs) which aid in transcription and replication. The genome has a 5' cap but no polyadenylated tail. The genome is transcribed as a single polyprotein encoding for three structural proteins: Capsid (C), Membrane (prM), and Envelope (E); and seven non-structural proteins: NS1, 2A, 2B, 3, 4A, 4B, and 5. The polyprotein is processed by both host (signalase) and viral (NS3/2B) proteolytic enzymes giving rise to the ten proteins listed above.

The non-structural (NS) proteins 1, 2A, 2B, 3, 4A, 4B, 5, which are not packaged into the virion, are expressed following translation of the viral RNA. NS1 is a multifunctional glycosylated protein capable of associating with membranes. Recently, both DENV and WNV NS1 crystal structures were determined. Interestingly, both adopt dimeric and hexameric forms (Akey, Brown et al. 2014, Edeling, Diamond et al. 2014). Dimerized NS1 is a cofactor for viral replication that colocalizes with the replication intermediate, double-stranded RNA (dsRNA), and is important for the formation of the replication complex (Westaway 1997, Youn, Ambrose et al. 2013). Hexameric NS1 associates with lipoproteins and is secreted. Secreted NS1 is detectable in the plasma of WNV infected patients and elevated levels of NS1 are associated with severe disease (Macdonald, Tonry et al. 2005).

NS3 has multiple roles during infection. The N-terminus of NS3 together with NS2B forms the viral serine protease responsible for cleavage of the viral polyprotein during processing (Figure 1.1) (Chambers, Grakoui et al. 1991, Zhang and Padmanabhan 1993, Jan, Yang et al. 1995). The C-terminal end of NS3 has both NTPase and helicase activities, classified under DEAH/D box helicase superfamily 2 (Li, Clum et al. 1999). This second activity is important during replication, viral RNA capping, and possibly functions in assembly of virions. Crystalization of various flaviviral NS3 proteins revealed that the protein has two segregated globular domains, which may explain its ability to perform diverse functions during infection (Xu, Sampath et al. 2005, Assenberg, Mastrangelo et al. 2009).

Another well-characterized flaviviral protein is NS5. It has high sequence conservation between flaviviruses and possesses two essential enzymatic activities, as a

methyltransferase (MTase) and RNA-polymerase, spatially separated by an interdomain region. Interestingly, the N-terminus has both N7 and 2'-O MTase activity, which are required for the formation of the 5' RNA cap on newly synthesized genomes (Egloff, Benarroch et al. 2002, Ray, Shah et al. 2006, Assenberg, Ren et al. 2007, Zhou, Ray et al. 2007). The C-terminus contains the RNA-dependent RNA polymerase (RdRp) activity, which is essential for genome replication (Grun and Brinton 1986, Chu and Westaway 1987, Tan, Fu et al. 1996, Guyatt, Westaway et al. 2001). NS5 associates with the 3'UTR of the genome and initiates RNA replication (Chen, Kuo et al. 1997), and regulates NS3 NTPase activity (Cui, Sugrue et al. 1998).

NS2A, NS4A, NS4B, are small hydrophobic proteins and largely remain uncharacterized due to the lack of identifiable enzymatic motifs. However, while no structural information exists, it is apparent that they have important roles during infection. Recently, the association of NS2A with membranes was shown to be important for the DENV virion biogenesis and assembly (Wu, Tsai et al. 2015, Xie, Zou et al. 2015). NS2A also plays a critical role in immune evasion by inhibiting the production in IFN- β , thereby enhancing virulence (Liu, Chen et al. 2004, Liu, Wang et al. 2006). NS4A, specifically the 2K peptide generated during proteolytic processing, is important for the expansion of ER membranes and localization of NS4B to the ER (Roosendaal, Westaway et al. 2006). The critical association of NS4A and NS4B with the ER membrane results in initial membrane curvature and formation of the viral replication complexes (Miller, Kastner et al. 2007, Kaufusi, Kelley et al. 2014).

1.3 Flavivirus Lifecycle

1.3.1 Cellular Tropism and Entry

All Flaviviruses have wide cellular tropism allowing them to infect insect vectors and a variety of hosts, including birds, reptiles, and mammals. Infection of mammals and birds by WNV occurs through the skin following the bite of an infected mosquito. The virus first infects surrounding keratinocytes, epithelial cells, and cells of the draining lymph node (reviewed in (Suthar, Diamond et al. 2013)). After a primary viremia is established, the virus spreads to the spleen where a second round of replication occurs followed by dissemination into the blood stream. Breakdown of the blood brain barrier allows the virus to invade the central nervous system (CNS) (Roe, Kumar et al. 2012, Xu, Waeckerlin et al. 2012). In the CNS, WNV can infect neurons and myeloid cells. In laboratory, WNV, SLEV, and POW can infect many cell lines derived from various mammals including rodent, monkey, and human.

The wide tissue tropism range of Flaviviruses can be attributed to their ability to utilize commonly expressed receptors found on multiple cell types. Initially, interaction between the virion and sulfated glycosaminoglycans, such as heparin sulfate, allows for low affinity binding and concentration of the virion on the cell surface (Chen, Maguire et al. 1997). This interaction is mediated by domain III of E (Lee and Lobigs 2000, Lee and Lobigs 2002, Watterson, Kobe et al. 2012). Next, E protein binds to a receptor, which can vary between cell types. For dendritic cells, particularly those found in the skin and lymph node, DC-SIGN is thought to be the main entry receptor (Navarro-Sanchez, Altmeyer et al. 2003, Tassaneeritthep, Burgess et al. 2003, Davis, Nguyen et al. 2006). Another receptor, $\alpha\beta 3$ integrin, can also contribute to internalization of WNV in

mammalian cells (Chu and Ng 2004, Lee, Chu et al. 2006). However, entry receptors for neurons and macrophages remain to be identified.

Following binding, entry of the virion into the cell is mediated by clathrin-dependent endocytosis (CDE). Pharmacological inhibition of clathrin-coated pit formation or cellular trafficking prevented the establishment of WNV infection, whereas blockage of caveolin-mediated entry had no effect on infection (Chu and Ng 2004). Entry by the virions follows a canonical CDE pathway; entry via clathrin-coated pits and formation of endosomes, decreasing pH maturation leading to formation of lysosomes (reviewed in (Kaufmann and Rossmann 2011)). In a mildly acidic pH environment, the E protein undergoes a large conformational shift from a homodimeric pre-fusion state to an active fusion state. This facilitates fusion between the virion envelope and the host endosomal membrane and the formation of a fusion pore. Pore formation is independent of host protein interactions and interaction between E and the host membrane in an acidic environment is sufficient for fusion (Moesker, Rodenhuis-Zybert et al. 2010). Following formation of the fusion pore, the viral RNA is released into the cytoplasm.

1.3.2 Replication and Translation

The +RNA genomes of flaviviruses can be directly translated for the production of viral proteins and also serve as templates for the synthesis of an antisense (-) strand. The latter is used as a template for genome replication. Upon release of the viral RNA into the cytoplasm, translation by host ribosomes at the ER membrane occurs, giving rise to a single polyprotein. Co-translational insertion into the ER membrane and posttranslational processing of the viral protein by host and viral proteases allows for the production of seven viral proteins (discussed in section 1.2). Production of these proteins

induces the formation of replication complex structures at the ER membrane (discussed further in section 1.3.4). Regions of the 5' and 3' UTRs of the viral genome, such as those that form structural elements or stem loops, are important for translational and replication regulation (reviewed in (Villordo and Gamarnik 2009)). At early time points, translation occurs readily in the infected cell. This allows for the build up of necessary factors for replication, such as NS5 and NS3, and the concentration of structural proteins needed for virion formation. Since the viral RNA is translated as a single polyprotein, there seems to be no obvious translational control for the stoichiometric production of structural to non-structural proteins. Therefore, translation needs to occur readily and frequently to produce enough structural proteins for the production of virions.

Replication of the viral RNA is dependent on NS5, and its RNA-dependent RNA polymerase activity. Initiation of replication occurs *de novo*, meaning NS5 does not require a primer, and can occur this way on either the 5' or 3' ends of the viral RNA (Selisko, Dutartre et al. 2006). Production of an antisense (-) strand is necessary to serve as a template for genome replication. Genomic replication on the antisense strand results in a double-stranded replication intermediate (dsRNA), and is often used as a marker for visualization of replication complexes in infected cells by microscopy. Overall, replication favors the production of the + sense RNA (Khromykh and Westaway 1997). Additionally, many host factors have been shown to be important for Flavivirus replication (reviewed in (Brinton 2001, Nagy and Pogany 2012)).

1.3.3 Assembly, Virion Maturation, and Release

The majority of research to date has focused on the mechanisms and dynamics of *Flavivirus* replication. Unfortunately, little is known about the process of virion assembly, which also takes place at ER-derived membranes (discussed further in section 1.3.4). The production of nucleocapsids requires interactions between the capsid protein and the viral RNA. Packaging sequences on viral RNA have not been identified and it is possible that the interactions between the viral RNA and capsid are non-specific. Interestingly, only newly replicated +RNA genomes are packaged, indicating a coupling between replication and packaging (Khromykh, Varnavski et al. 2001). Nascent virions bud into the ER lumen spiked with 180 copies each of E and prM. At this stage, immature virions have trimeric spikes of heterodimers of E and prM and are non-infectious (Zhang, Corver et al. 2003, Zhang, Kaufmann et al. 2007). Virions exit the ER and traverse the Golgi before release from the plasma membrane. In the *trans*-Golgi network, a host protease furin cleaves prM to generate mature M resulting in a conformational change of the glycoproteins. Mature virions are smooth and have a classical $T=3$, icosahedral symmetry. Release of mosaic particles and immature particles during DENV infection has been reported indicating that furin cleavage is not 100% efficient (Junjhon, Edwards et al. 2010).

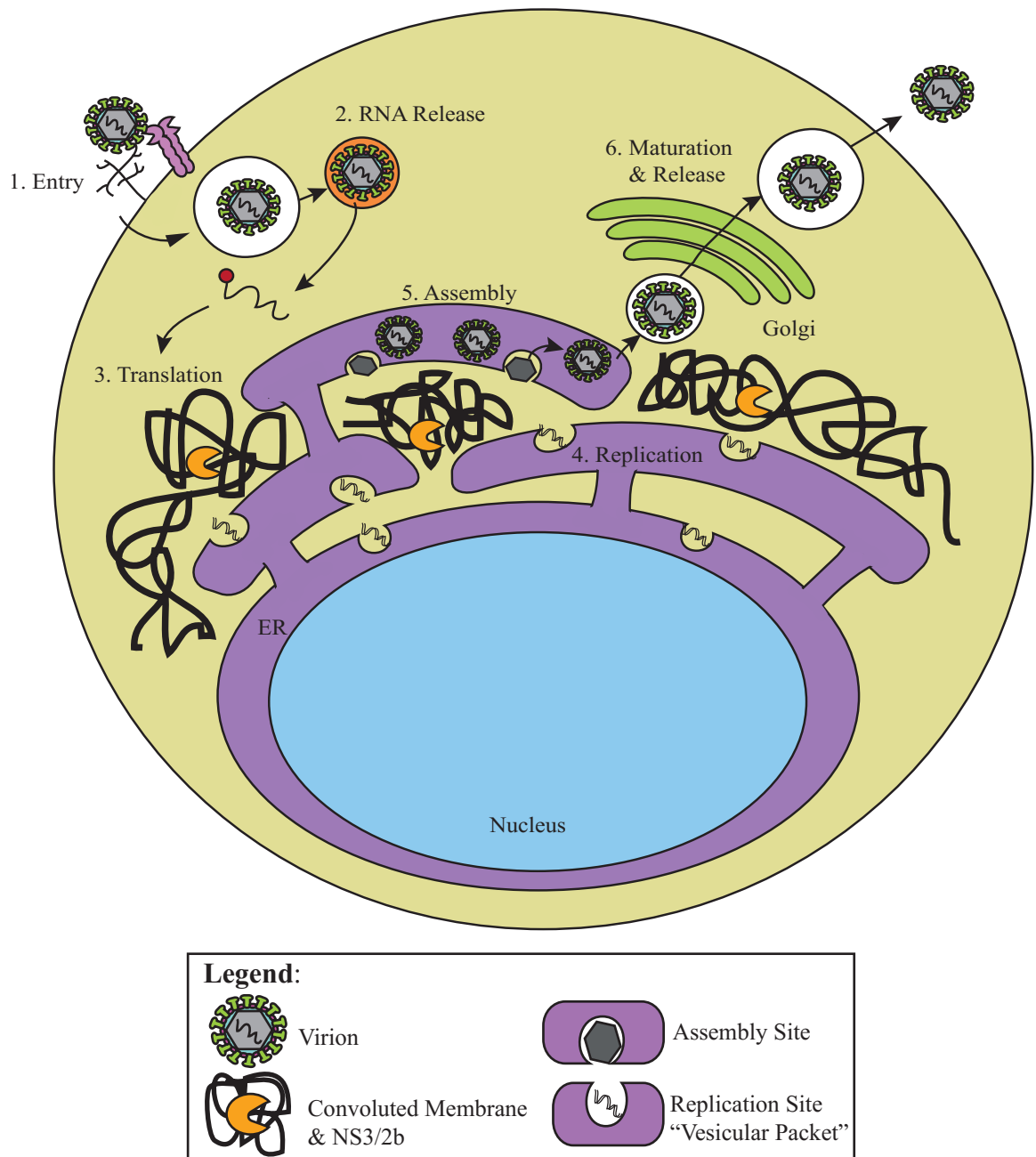


Figure 1.2 Flavivirus Lifecycle. 1) Upon binding with cell surface receptors, the virion enters the cell via clathrin-dependent endocytosis. 2) Maturation and decreasing pH of the endosome allows for fusion and the release of the viral RNA into the cytoplasm. Viral translation, replication, and assembly all occur at modified cellular membranes. 4) Replication occurs in vesicular packets containing dsRNA. 5) Virion assembly occurs on opposing ER membranes. 6) Once the virion is assembled it is released via the secretory pathway and the viral prM protein undergoes cleavage by the host protein furin in the Golgi. Diagram not to scale.

1.3.4 Hijacking of Host Membranes

As with all +RNA viruses, *Flaviviruses* hijack cellular membranes and organelles for the formation of their replication and assembly compartments. The function of these structures is two-fold; concentration of necessary factors for efficient replication and shielding of viral components from cellular immune sensors. Understanding of this complex process occurred through key studies utilizing electron microscopy (EM) and tomography (ET) studies on DENV and WNV infected cells. Infection by WNV_{KUN}, an attenuated strain from Australia, or highly pathogenic WNV_{NY99} results in similar phenotypic alterations (Westaway 1997, Whiteman, Popov et al. 2015). Early EM studies showed a dramatic reorganization of perinuclear membranes into vesicular packets (VPs) and convoluted membranes (CM) that were closely associated to the rough-ER (Mackenzie, Jones et al. 1996, Westaway 1997). Paracrystalline arrays (PC) were also described in WNV_{KUN}-infected cells (Westaway 1997). This type of reorganization seems to be conserved as infection of mosquito cells with DENV or WNV also led to dramatic alterations of membranes resulting in spherules associated with ER membranes (Girard, Popov et al. 2005, Gangodkar, Jain et al. 2010). The formation of these different structures may be important for segregation of viral replication from protein translation (Uchil and Satchidanandam 2003).

VPs contain dsRNA, NS1, NS3, and NS5, the viral RNA-dependent RNA polymerase, suggesting this is the site of viral replication (Mackenzie, Jones et al. 1996, Westaway 1997, Westaway, Khromykh et al. 1999, Mackenzie, Kenney et al. 2007, Welsch, Miller et al. 2009). In contrast, CMs do not contain dsRNA and associate with NS3/2b, the viral protease important for post-translational processing, indicating they are

the sites of translation and/or proteolytic processing (Westaway 1997, Welsch, Miller et al. 2009). While all of these virus-induced structures arise in the perinuclear space and are in close proximity to the nucleus, they vary considerably depending upon the particular flavivirus. For instance, DENV VPs contain the ER-resident protein calnexin and protein disulphide isomerase (PDI), suggesting they are derived from ER membranes (Welsch, Miller et al. 2009). Similarly, WNV_{NY99} VPs colocalize with PDI (Whiteman, Popov et al. 2015). In contrast, WNV_{KUN} VPs contain the *trans*-Golgi network protein galactosyltransferase, indicating their possible derivation from the Golgi apparatus (Mackenzie, Jones et al. 1999). Recent advances in ET have allowed further characterization of the viral replication complexes for DENV (Welsch, Miller et al. 2009), WNV_{KUN} (Westaway 1997, Gillespie, Hoenen et al. 2010), WNV_{NY99} (Kaufusi, Kelley et al. 2014), and TBEV-like virus TBFV Langat (Offerdahl, Dorward et al. 2012). Interestingly, VPs appear to be invaginations of the ER membrane with small neck-like openings (~11.2nm for DENV) that may facilitate trafficking of molecules into and out of these replication sites. During DENV infection electron dense invaginations (~60nm), presumed sites of assembly, are observed on opposing cisternae from VPs (Welsch, Miller et al. 2009). This suggests that viral replication and assembly occurs in distinct localizations. Despite these elegant structural studies on DENV and WNV VRCs, the exact mechanism of biogenesis remains unclear.

1.4 Virus-host Interplay: Host Factors involved in Flavivirus Infection

1.4.1 Identification of host factors

Flaviviruses have limited coding capacity and thus rely on their multifunctional viral proteins (discussed in section 1.2) and a wide range of cellular host factors. Targeting viral proteins has been the traditional approach in the development of antiviral therapies. However, the occurrence of escape mutants (viruses with mutations in encoded viral proteins allowing avoidance of antiviral action) poses a serious challenge in the development of potent antivirals. Thus, in recent years, a switch to understanding key host factors that viruses utilize may provide targets for new antiviral drugs (reviewed in (Krishnan and Garcia-Blanco 2014)). The likelihood of escape mutations to host-cell protein targeting drugs is theoretically much lower and thus gives promise for effective treatment and viral clearance. Identification of these host factors and understanding their mechanisms of action during the viral lifecycle is crucial in the development of targeted antivirals.

To date, a large number of host factors that are needed for generation of WNV replication complexes, the process of viral replication, and the dampening of cellular immune response have been identified (reviewed in (Brinton 2001, Lazear and Diamond 2015, Reid, Airo et al. 2015)). A seminal study conducted by Krishnan *et al.*, utilized RNA interference to identify 305 human genes that affect WNV infection. These genes function in diverse cellular pathways and processes including metabolism and growth, signal transduction, and genetic regulation (Krishnan, Ng et al. 2008). Other systematic genomic and proteomic screens have been performed for DENV (Sessions, Barrows et al. 2009, Mishra, Diwaker et al. 2012, Mairiang, Zhang et al. 2013, Campbell, Harrison et

al. 2014) and JEV (Saha 2003, Zhang, Chai et al. 2013, Sengupta, Ghosh et al. 2014). Like WNV, cellular pathways strongly affected during DENV or JEV infection include those that modulate metabolism, signal transduction, and genetic regulation. Therefore, commonalities of the pathways affected between these *Flaviviruses* suggest conserved mechanisms of host cellular manipulation exist within this genus. To date, there has not been published genomic or proteomic screens for host factors important for POW and SLEV. While these screening methods are important for the identification of host factors and common pathways, functional validation and mechanistic studies are still needed.

1.4.2 DEAD-box RNA helicases and virus infection

Previously, our lab performed a yeast-2-hybrid (Y2H) screen to identify WNV capsid binding proteins. Of the many interactors identified, the role of a host RNA helicase, DDX56, was further investigated (Xu, Anderson et al. 2011). DDX56 belongs to the highly conserved helicase superfamily 2: DEAD-box RNA helicases. Helicases serve essential functions in the cell. RNA helicases utilize ATP hydrolysis to bind and unwind RNA duplexes or remodel RNA-protein complexes. These enzymes are found in all living organisms and have diverse roles in RNA metabolism (reviewed in (Rocak and Linder 2004)). They contain nine conserved motifs and are named after a highly conserved D-E-A-D (Asp-Glu-Ala-Asp) motif. While the conserved motifs are necessary for ATP hydrolysis and RNA binding, the amino and carboxy termini of these proteins tend to be very diverse in sequence, which may allow these proteins to perform a wide variety of functions. In addition to their diverse functional roles, DEAD-box RNA helicases are found in the nucleus, cytoplasm, or shuttle between these regions via nuclear pore complexes (reviewed in (Linder and Jankowsky 2011)).

DEAD-box RNA Helicase 3 (DDX3)

Most RNA viruses encode their own RNA helicases (e.g. NS3 for *Flaviviruses*), however, many host cell DEAD-box RNA helicases have been demonstrated to play functional roles in diverse viral infections. The first such DDX protein identified was DDX3, which interacts with the HCV core protein (Owsianka and Patel 1999, You, Chen et al. 1999). Expression of the HCV structural proteins resulted in relocalization of DDX3 to distinct puncta at perinuclear sites that colocalized with HCV core protein. With the advent of a HCV cell culture system, DDX3 was shown to be required for viral RNA replication (Ariumi, Kuroki et al. 2007), however, this effect did not seem to be due to its interaction with HCV core protein (Angus, Dalrymple et al. 2010). DDX3 is also involved in HIV-1 Rev function (Yedavalli, Neuveut et al. 2004, Ishaq, Hu et al. 2008, Yedavalli, Zhang et al. 2008, Yasuda-Inoue, Kuroki et al. 2013), which is important in the export of viral mRNA from the nucleus, and enhancing the function of HIV-1 transcription regulator Tat (Yasuda-Inoue, Kuroki et al. 2013).

During JEV infection, a close relative of WNV and SLEV, DDX3 binds to the 5' and 3' UTR of the genome and regulates viral replication (Li, Ge et al. 2014). Interestingly, during WNV infection, DDX3 colocalizes with NS3 near the nucleus suggesting it is recruited to WNV replication and/or translation sites (Chahar, Chen et al. 2013). Normal cellular functioning of this helicase suggests it has multiple roles in export of mRNA and translation initiation, assembly of 80S ribosomes, and innate immune signaling (Mulhern and Bowie 2010, Geissler, Golbik et al. 2012, Soto-Rifo, Rubilar et al. 2012).

DEAD-box RNA Helicase 5 (DDX5, p68)

DDX5 is another extensively studied helicase that is essential for cell growth, and is known to act with DDX3 during mRNA export and splicing (Choi and Lee 2012). It was identified as an interacting partner of HCV NS5B, the virus-encoded RNA dependent RNA polymerase, during a Y2H assay (Goh, Tan et al. 2004). Expression of NS5B in HeLa cells leads to a redistribution of DDX5 from the nucleus to the cytoplasm. Interactions between DDX5 and viral proteins, and other host factors, may lead to a dysregulation in cellular checkpoints and contribute to HCV-associated liver cancers (reviewed in (McGivern and Lemon 2009)). DDX5 is also recruited to the cytoplasm during JEV infection, and is essential for replication by interacting with the 3' UTR of the genome (Li, Ge et al. 2013). Additionally, DDX5 interacts with JEV capsid, NS3, and NS5, but the significance of these interactions remains to be determined. Recently, DDX5 was shown to bind the NS5A protein of the *Pestivirus* Classical swine fever virus (Zhang, He et al. 2014). This helicase is also a cofactor of the HIV-1 mRNA export protein, Rev (Zhou, Luo et al. 2013) and was recently identified as an important host factor for HIV-1 replication through a small-interfering RNA screen (Williams, Abbink et al. 2015).

DEAD-box RNA Helicase 6 (DDX6, rck/p54)

The RNA helicase DDX6, which has been implicated in multiple viral infections, is normally involved in translational regulation, mRNA degradation, and is a component of processing bodies (P-bodies) (reviewed in (Weston and Sommerville 2006)). It was first identified as being highly upregulated in ~90% of cases of chronic hepatitis and all cases of hepatocellular carcinoma examined that were related to HCV infection (Miyaji,

Nakagawa et al. 2003). DDX6 is important for both viral translation and replication as evidenced by studies showing that reducing expression of this helicase results in a reduction of viral proteins and RNA (Scheller, Mina et al. 2009). Interestingly, DDX6 and HCV core protein interact and DDX6 is redistributed from P-bodies to sites of HCV replication in close association with lipid droplets (Ariumi, Kuroki et al. 2011, Pérez-Vilaró, Scheller et al. 2012, Chatel-Chaix, Germain et al. 2013). However, this interaction is not required for replication of subgenomic RNA lacking core protein (Jangra, Yi et al. 2010). Thus, DDX6 while seems to be important for HCV replication and translation, the purpose of its interaction with HCV core remains unknown. DDX6 was identified during a screen for interacting partners of the DENV-2 genome (Ward, Bidet et al. 2011). DDX6 interacts with the 3' UTR of the DENV-2 genome and its assembly on this region is necessary for viral replication. Additionally, during DENV-2 infection DDX6 is redistributed in the cytoplasm and colocalizes with the replication complex. As is true with the other DDX proteins listed, DDX6 is also important for HIV-1 propagation. Interestingly, expression of DDX6 prevents the association of viral mRNA with polysomes for translation, suggesting that DDX6 is a negative regulator of viral gene expression (Chable-Bessia, Meziane et al. 2009). Recently, DDX6 was shown to be important for enhancing HIV-1 Gag function during the assembly of viral capsids in primary human T lymphocytes (Reed, Molter et al. 2012). This suggests that DDX6 may be involved in the switch between viral translation and assembly of virions during HIV-1 infection.

DEAD-box RNA Helicase 56 (DDX56, NOH61)

Less is known about DDX56, the helicase of interest in this study. Microscopy localization studies indicate that DDX56 is primarily found in the nucleolus. Functional information about its normal role in the uninfected cell is limited, but evidence suggests its involvement in the biogenesis of the large 60S ribosomal subunit (Zirwes, Eilbracht et al. 2000). Similar to DDX3 and DDX5, DDX56 acts to enhance Rev function during HIV-1 infection (Yasuda-Inoue, Kuroki et al. 2013). Recently, a temporal proteomics study demonstrated that DDX56 protein levels are down-regulated during infection with an *Alphavirus* Chikungunya (Treffers, Tas et al. 2015).

The study of RNA helicases, specifically DEAD-box RNA helicases, has shown that these proteins play diverse roles during viral infection. Since many viruses, including *Flaviviruses*, utilize specialized compartments for replication and assembly (discussed in section 1.3.4), DDX proteins are often relocalized during infection to the sites of viral replication and/or assembly. This relocalization likely affects the normal functions of these enzymes by altering their interaction with cellular or viral substrates. The identification of the mechanisms used by these DDX proteins during viral infection may lead to the development of specific antiviral therapies in treatment of these viruses.

1.4.3 DDX56 is necessary for production of infectious WNV virions

As previously stated, our lab identified DDX56 as a WNV capsid interacting partner during a Y2H screen (Xu, Anderson et al. 2011). Immunoprecipitation of DDX56 with WNV capsid in infected A549 cells 48 hours post infection (h.p.i) indicated that this interaction also occurs during infection. Next, the stability of DDX56 during WNV infection was examined. DDX56 staining in the nucleolus was lost over time during

WNV infection of A549 cells, with the peak loss seen at 72 h.p.i. Interestingly, infection with a Togavirus, Rubella virus, or the related *Flavivirus*, DENV-2, did not alter DDX56 staining intensity in the nucleolus. Additionally, the localization of another nuclear protein Nucleolin was unaffected by WNV infection, suggesting that the loss of DDX56 during WNV infection is specific.

Pharmacologically blocking degradation pathways demonstrated that DDX56 is degraded by the 26S proteasome during infection. The proteasome is a large multi-protein complex that degrades proteins in the cytoplasm, often those that are misfolded at the ER (reviewed in (Bhattacharyya, Yu et al. 2014)). Interestingly, upon closer examination of WNV infected cells treated with a proteasome blocker, DDX56 was observed on distinct perinuclear puncta. This suggests that DDX56 may be relocalized to the cytoplasm from the nucleolus during infection. However, blocking of CRM-1 dependent nuclear export did not prevent DDX56 proteasomal degradation (Xu, Anderson et al. 2011). Other mechanisms of nuclear export have not been explored. Alternatively, once DDX56 is translated and folded at the ER it may be sequestered by the virus and prevented from being imported into the nucleus. This could explain why DDX56 is lost slowly during infection from the nucleolus.

Generation of stable DDX56 knock down cells using a lentivirus carrying a DDX56-specific shRNA (DDX56-KD) was done to further investigate the role of DDX56 during WNV infection. Uninfected cells appeared to grow and divide normally, suggesting that DDX56 functionality may be dispensable for cell viability *in vitro*. WNV infection of DDX56-KD cells did not affect viral translation, as evidenced by the fact that capsid and NS3 protein levels were unchanged compared to mock-infected cells.

Additionally, similar levels of viral RNA were found in control and DDX56-KD cells (Xu, Anderson et al. 2011). This suggested that DDX56 acts at a late step during WNV infection. Isolation and quantitation of capsid protein from extracellular (secreted) virions revealed that DDX56 does not affect the number of virions generated. However, the virions produced from these knock down cells were ~100X less infectious and contained 3-4X less viral RNA packaged (Xu, Anderson et al. 2011). Given that DDX56-KD does not result in a reduction of viral RNA replication or production of virions, it appears that the viral RNA is not efficiently incorporated into virions during the assembly process in DDX56-KD cells. This suggests that DDX56 acts to enhance viral RNA packaging possibly through facilitating interactions between WNV capsid and viral RNA. This packaging phenotype is dependent on DDX56 ATP-dependent helicase activity as introduction of helicase-dead mutants into DDX56-KD cells also results in less infectious virions containing less viral RNA (Xu and Hobman 2012). Thus, a functional helicase domain is required for the efficient packaging of viral RNA.

These studies suggest that DDX56 is an important host factor for the production of infectious WNV virions by enhancing packaging of viral RNA. This effect is dependent on functional helicase activity of DDX56 possibly by unwinding dsRNA replication intermediates, or facilitating interactions between WNV capsid and viral RNA. Additionally, DDX56 localizes to as yet undefined sites in the cytoplasm during infection, but it is tempting to speculate that these sites are where WNV virions are assembled. Based on these previous data, I hypothesize that DDX56 localizes to sites of WNV assembly where it is involved in enhancing viral RNA packaging, possibly through mediating interactions between WNV capsid and the + stranded genomic RNA.

1.5 Objectives of Study

While DDX56 is relocalized to the cytoplasm during WNV infection, its precise location is not known. Identifying this intracellular site may provide insight into its functional role during virus infection. I also determined whether this host factor was important for other members of the *Flavivirus* genus. The first study was carried out to examine the cytoplasmic location of DDX56 during WNV infection in relation to markers for viral replication and assembly. I also investigated whether DDX56 relocalization from the nucleus to the cytoplasm was a result of viral protein expression. The second study was carried out to determine whether SLEV or POW require DDX56 for the production of infectious virions. This would allow us to determine whether DDX56 could be a helicase used broadly within the *Flavivirus* genus and give implications for the development of antivirals.

Chapter 2

Materials and Methods

2.1 Materials

2.1.1 Reagents

The following reagents and supplies were purchased from their indicated suppliers and used according to the manufacturing guidelines.

Table 2.1 Sources of materials, reagents, and chemicals

<i>Reagent</i>	<i>Source</i>
0.25% Trypsin-EDTA	Invitrogen
0.45 µm Millex-HV PVDF Syringe Filter	EMD Millipore
13 mm Nunc™ Thermanox™ Plastic Coverslips	Thermo Fisher Scientific
18 mm #1 ½ Micro Coverglass	Electron Microscopy Sciences
2-Mercaptoethanol (βME)	Thermo Fischer Scientific
4', 6-diamidino-2-phenylindole (DAPI)	Sigma-Aldrich
40% Acrylamide/Bis-acrylamide solution	Bio-Rad
AllStars Negative Control siRNA Alexa-488	QIAGEN
Ammonium Chloride	Sigma-Aldrich
Ammonium Persulphate	Sigma-Aldrich
Benzonase® Nuclease	EMD Millipore
Bovine Serum Albumin (BSA)	Sigma-Aldrich
Bromophenol blue	Sigma-Aldrich
Carboxy-Methylcellulose	Sigma-Aldrich
Complete™ EDTA-free protease inhibitors (25X)	Roche
Crystal Violet	Sigma-Aldrich
Dimethyl sulphoxide (DMSO)	Sigma-Aldrich
Dulbecco's modified Eagle's medium (DMEM)	Invitrogen
Ethanol	Commercial Alcohols
Fetal bovine serum (FBS)	Invitrogen
Formaldehyde, 37% (v/v)	Sigma-Aldrich
Glycerol	Fischer Scientific
HEPES 1M (cell culture grade)	Gibco Life Technologies
Immobilon®-P PVDF Membrane	EMD Millipore

Isopropanol	Commercial Alcohols
L-Glutamine	Invitrogen
Lipofectamine LTX	Invitrogen
Magnesium chloride	EMD Chemicals
Methanol	Thermo Fischer Scientific
MG132	Sigma-Aldrich
Microscope slides (25x75x1mm)	Thermo Fisher Scientific
N,N,N',N'-tetramethylethylenediamine (TEMED)	Sigma-Aldrich
Nonidet P-40/IGEPAL CA-630	Sigma-Aldrich
OptiMEM	Invitrogen
Paraformaldehyde	Thermo Fischer Scientific
Penicillin-streptomycin solution (100X)	Invitrogen
Poly-L-lysine	Sigma-Aldrich
ProLong® Gold Antifade reagent with DAPI	Invitrogen
Protein A-sepharose	GE Healthcare
Protein G-sepharose	GE Healthcare
PVDF membrane (0.45µM)	Millipore
Puromycin	Sigma-Aldrich
Restore™ Western Blot Stripping Buffer	Thermo Scientific
Skim milk powder	Carnation
SlowFade® Gold Antifade reagent	Invitrogen
SMARTpool: ON-TARGETplus siRNA against DDX56	Dharmacon GE
Sodium azide	Sigma-Aldrich
Sodium chloride	Sigma-Aldrich
Sodium dodecyl sulphate (SDS)	Bio-Rad
Triton X-100	VWR International
Tween® 20 (polyoxyethylenesorbitan monolaureate)	Sigma-Aldrich

Table 2.2 Commercially available kits

<i>Kit Name</i>	<i>Source</i>
Lipofectamine LTX with Plus Reagent	Life Technologies
Lipofectamine RNAiMAX	Life Technologies
Pierce BCA protein Assay kit	Thermo Scientific

2.1.2 Equipment and analyses platforms

Table 2.3 Detection Systems

<i>System</i>	<i>Source</i>
DeltaVision® OMX	GE Healthcare Life Sciences
Hitachi H-7650	Hitachi High Technologies, Inc
Moxi Z Automated Cell Counter	Orflo
NanoDrop ND-1000 Spectrophotometer	Thermo Scientific
Odyssey Infrared Imaging System	LiCor
Olympus IX-81 with Hamamatsu EMCCD	Quorum Technologies

Table 2.4 Analysis software

<i>Software</i>	<i>Use</i>	<i>Source</i>
DeltaVision® OMX Master Control	3D-SIM Image Acquisition	GELifeSciences
Fiji (ImageJ)	EM Image Analysis	Open Source
Image Studio™ Lite	Analysis of Western Blot Images	LI-COR
Odyssey V3.0	Western Blot Image Acquisition	LI-COR
Prism 6	Graphing and Statistical Analysis	GraphPad
softWoRx V6.1	3D-SIM Image Reconstruction	GELifeSciences
Volocity® 3D Image Analysis (v6.3)	Image Acquisition and Analysis	PerkinElmer

2.1.3 Commonly used buffers and solutions

Table 2.5 Buffers and Solutions

Name	Composition
5x Protein sample buffer	62.5 mM Tris-HCl (pH 6.8), 25% (v/v) glycerol, 2% (w/v) SDS, 0.01% (w/v) bromophenol blue, 1% (v/v) β -mercaptoethanol
NP-40 Lysis buffer (REAP)	150 mM NaCl, 50mM Tris HCl, 0.1% NP-40
PBS-T	137 mM NaCl, 2.7 mM KCl, 8 mM Na ₂ HPO ₄ (pH 7.4), 0.05% (v/v) Tween-20
PBSCM	137 mM NaCl, 2.7 mM KCl, 8 mM Na ₂ HPO ₄ , 0.5 mM CaCl ₂ , 1 mM MgCl ₂ , pH 7.4
Phosphate buffered saline (PBS)	137 mM NaCl, 2.7 mM KCl, 8 mM Na ₂ HPO ₄ (pH 7.4)
RIPA Buffer	50 mM Tris-HCl (pH 7.4), 150 mM NaCl, 0.1% SDS, 1% Triton X-100, 1% sodium deoxycholate, 1 mM EDTA
SDS-PAGE Resolving gel buffer	0.1% SDS, 374 mM Tris-HCl (pH 8.8)
SDS-PAGE Running buffer	250 mM glycine, 0.1% SDS, 100mM Tris Base (pH 8.3)
SDS-PAGE Stacking gel buffer	0.1% SDS, 250mM Tris-HCl (pH 6.8)
Transfer Buffer	200mM Glycine, 25mM Tris base (pH 8.3), 20% (v/v) methanol, 0.1% (w/v) SDS

2.1.4 Antibodies

Table 2.6 Primary antibodies

<i>Antibody</i>	<i>Dilution</i>	<i>Application</i>	<i>Source</i>
Guinea pig anti-WNV capsid	1:1000, 1:1000, 1:500	WB, IF, IP	This Laboratory
Human anti-WNV envelope (hE16)	1:15,000	IF	Dr. M. Diamond, Wash. U

Mouse anti-dsRNA (J2)	1:500	IF	English and Scientific Consulting Kft
Mouse anti-SLEV E	1:1000, 1:1000	WB, IF	LS Biosciences
Mouse anti-WNV NS3	1:3000	WB	R & D Systems
Mouse anti-WNV NS3/2b	1:700	IF	R & D Systems
Mouse anti- β -actin	1:2000	WB	Abcam
Mouse anti-DDX56	1:3000, 1:1000, 1:500	WB, IF, IP	PROGEN Biotechnik
Rabbit anti-Calnexin	1:100	IF	Dr. T. Simmen, UA
Rabbit anti-GAPDH	1:2500	WB	Abcam
Rabbit anti-Histone H3	1:2000	WB	Abcam
Rabbit anti-Lamin B	1:1000	WB	Abcam
Rabbit anti-TBEV E	1:500	IF	Dr. F. Heinz, Med. U Vienna

* WB: Western Blot; IF: Immunofluorescence; IP: Immunoprecipitation

Table 2.7 Secondary Antibodies

<i>Antibody:Conjugate</i>	<i>Dilution</i>	<i>Application</i>	<i>Source</i>
Donkey anti-guinea pig:Alexa 488	1:1000	IF	Life Technologies
Donkey anti-mouse:Alexa 546	1:1000	IF	Life Technologies
Donkey anti-mouse:Alexa 680	1:5000	WB	Life Technologies
Donkey anti-rabbit:Alexa 488	1:500	IF	Life Technologies
Donkey anti-rabbit:Alexa 568	1:500	IF	Life Technologies
Donkey anti-rabbit:Alexa 680	1:5000	WB	Life Technologies
Goat anti-guinea pig:Alexa 568	1:1000	IF	Life Technologies
Goat anti-guinea pig:Alexa 680	1:10,000	WB	Thermo Scientific

Goat anti-human:Alexa 488	1:1000	IF	Life Technologies
Goat anti-mouse IgG1:Alexa			Jackson
647	1:1000	IF	ImmunoResearch
Goat anti-mouse IgG2A:Alexa			Jackson
488	1:500	IF	ImmunoResearch
			Jackson
Goat anti-mouse IgG2A:RhRed	1:500	IF	ImmunoResearch
Goat anti-mouse IgG3:Cy3	1:500	IF	Jackson ImmunoResearch

* WB: Western Blot; IF: Immunofluorescence

2.2 Methods

2.2.1 Cell lines and cell maintenance

A549 (human lung epithelial), HEK 293T (human embryonic kidney), BHK-21 (baby hamster kidney), and Vero (African green monkey fibroblast) cell lines were purchased from the American Type Culture Collection (Manassas, VA). A549 and HEK 293T cells were maintained in Dulbecco's modified Eagle's medium (DMEM) supplemented with 10% heat-inactivated fetal bovine serum (FBS), 4.5 g/L D-glucose, 2mM glutamine, 25 mM HEPES (pH 7.4), 110 mg/L sodium pyruvate, 1% penicillin-streptomycin. Vero and BHK-21 cells were maintained in similar DMEM as above except it was supplemented with only 5% heat-inactivated FBS.

2.2.2 Cell Transfection

HEK 293T cells (5×10^4) were seeded on sterile poly-L-lysine coated glass coverslips in 12-well plates for microscopy experiments or (2×10^5) in 6-well plates for lysate collection. Cells were seeded in media without antibiotics 24h before transfection. The day of transfection expression plasmids were mixed with Plus reagent and Lipofectamine LTX reagent (Table 2.2) in Opti-MEM before being added to cells. Transfection was

allowed to proceed for 6 hours after which the transfection mixture was replaced with DMEM supplemented with 10% FBS lacking antibiotics. Cells were collected 24-48 hours post transfection and then processed for indirect immunofluorescence or SDS-PAGE analysis, respectively.

2.2.3 RNA Interference

A549 or HEK 293T cells (5×10^4) were seeded in 12-well plates 24 hours before transfection. To transiently knock down DDX56, cells were transfected with ON-TARGET plus SMARTpool® siRNA targeting human DDX56 mRNA (Table 2.1) or non-silencing control siRNA Alexa Fluor 488 (Table 2.1). The siRNAs (10nM, final concentration) were mixed with Lipofectamine RNAiMAX™ reagent (Table 2.2) in Opti-MEM and then added to cells. Cell lysates were collected 24-96 hours post transfection to assay for DDX56 knock down efficiency.

2.2.4 Virological Techniques

2.2.4.1 Virus Strains and Generation of Stocks

West Nile virus (NY99 strain), Tick-borne encephalitis virus (Powassan virus, strain M5/725) and Saint Louis encephalitis virus (ATCC strain, passage 7) were provided by Drs. Mike Drebot and Maya Andonova (Public Health Agency of Canada, Winnipeg, MB). Virus stocks were generated in and titer was determined using Vero E6 cells. Aliquots of stocks were stored at -80°C until use.

2.2.4.2 Virus Infection

All virus manipulations were performed in the Glaxo Biosafety Containment (CL-3) facility or the Canada Foundation for Innovation CL-3 facility (both located at the

University of Alberta). WNV, TBEV, or SLEV stocks were diluted in DMEM without FBS or antibiotics and added directly to cells for 1hr at 37°C with occasional rocking. Following this, the virus inoculum was removed and “regular” culture media was added. Infected cells were maintained at 37°C, 5% CO₂ until harvesting for experimental analysis. Cells were infected at a multiplicity of infection (MOI) of 1-5.

2.2.4.3 Plaque Assay

The day before infection, Vero cells (2×10^5) were seeded into 24-well dishes or BHK-21 cells (3×10^5) were seeded into 6 well dishes. Supernatants from virus-infected cells were passed through Millex-HV 0.45 µm PVDF filters (Table 2.1). Filtered supernatants were serially diluted 10-fold in serum-free DMEM. Infection with 100 µL or 450 µL (24-well or 6-well format, respectively) from each dilution was added to the well, in duplicate, and infection was allowed to proceed 1hr at 37°C with occasional rocking. After this, the inoculum was removed and serum-free DMEM supplemented with 1.5% (Vero) or 3.5% (BHK-21) carboxymethylcellulose was added. 48h (WNV), or 96h (TBEV and SLEV) post-infection Vero cells were fixed with 1mL of 10% formaldehyde for 30 minutes. The methylcellulose/formaldehyde media was removed and wells were gently washed under running tap water. Plaques were stained with 10% ethanol, 0.1% crystal violet solution for 15 minutes and washed with water as before. When BHK-21 cells were used, samples were collected 5 days post infection following the same staining protocol as above. Average plaque counts were calculated from duplicate wells to determine particle-forming units/mL (pfu/mL).

2.2.5 Protein Electrophoresis and Detection

2.2.5.1 Preparation of cell lysates

Virus-infected or transfected cells were washed two times with cold PBS and then lysed with RIPA buffer containing proteinase inhibitors (Table 2.5) for 30 minutes on ice. Lysates were clarified by centrifugation at 13,000 x g for 10 minutes at 4°C. Protein concentrations were determined using BCA assay (Table 2.2) following manufacturer's instructions. Equal amounts of protein were loaded into and resolved on a 5% stacking/12% resolving SDS-PAGE gel, transferred to Immobilon-polyvinylidene fluoride (PVDF) membranes (Table 2.1) and detected by Western blot (see below).

2.2.5.2 Sodium dodecyl-sulphate polyacrylamide gel electrophoresis (SDS-PAGE)

Separation of proteins was done by discontinuous polyacrylamide gel electrophoresis with a 5% stacking and 12% resolving gel. Stacking gels were prepared by adding acrylamide/bis-acrylamide (final concentration 5%) to 375 mM Tris-HCl (pH 8.8), 0.1% SDS, 0.1% ammonium persulphate, and 0.1% TEMED. Resolving gels were prepared by combining acrylamide/bis-acrylamide (final concentration 12%) to 125 mM Tris-HCl (pH 6.8), 0.1% SDS, 0.1% ammonium persulphate, and 0.1% TEMED. Protein samples (prepared as described above) were mixed with 5x Protein Sample buffer (Table 2.5), containing 1% (v/v) β -mercaptoethanol, and then denatured 95°C for 10 minutes. Bio-Rad Mini Protean III systems with SDS-PAGE running buffer (Table 2.5), set at 90-120V, were used for gel electrophoresis.

2.2.5.3 Western Blot Analysis

Following separation by SDS-PAGE, proteins were transferred to 0.45 μ m PVDF membranes. The membranes were activated with methanol for 1-2 minutes and then

equilibrated in Transfer Buffer (Table 2.5) for 5 minutes with rocking. A Bio-Rad Mini Transblot Electrophoresis transfer cell apparatus, filled with 4° C Transfer buffer and placed in an ice bucket, was run under a constant current of 300-350mA for up to 3 hours. Once transfer was complete, membranes were dried, re-wet with methanol, and then blocked with 5% (w/v) skim milk PBS-T for 1 hour at room temperature, with rocking. Membranes were then incubated with primary antibodies (Table 2.6) diluted in 5% (w/v) skim milk PBS-T for 3 hours at room temperature or overnight at 4°C. Following this membranes were washed with PBS-T three times (15 minutes per wash). Fluorescent (Alexa-680 conjugated) secondary antibodies (Table 2.7) diluted in 2% (w/v) skim milk PBS-T were added for detection of primary antibodies for 1 hour at room temperature. Membranes were again washed three times (15 minutes per wash) with PBS-T then rinsed with PBS before detection, as described below.

2.2.5.4 Detection of Fluorescent-conjugated secondary antibodies

Membranes were placed protein side down on the scanner bed of an Odyssey Infrared Imaging system (Table 2.3). Membranes were scanned at 84µm resolution on “high” quality setting. Quantitation of proteins was performed following the protocol (http://www.licor.com/bio/products/software/image_studio_lite/support.html) for Image Studio™ Lite LI-COR Software (Table 2.4).

2.2.6 Analysis of protein-protein interactions

2.2.6.1 Cellular Fractionation

A549 cells (2×10^5) were seeded into 6-well plates the day before infection. Cells were infected with WNV (MOI, 3) for 24 or 48 hours as described previously (section 2.2.4.2).

The use of Rapid Efficient and Practical (REAP) for subcellular fractionation has previously been described in detail elsewhere (Suzuki, Bose et al. 2010). All steps were carried out at 4°C or on ice as applicable. Briefly cells were washed with cold PBS two times and, following collection by scrapping, were quickly pelleted at 10,000 x g for 30 seconds. The cell pellets were resuspended in 0.1% NP-40 lysis buffer (Table 2.5) containing protease inhibitors and mixed by pipetting quickly. An aliquot of each whole cell lysate was saved and the remaining lysates were centrifuged at 10,000 x g for 10 seconds. The supernatants were removed and labeled “cytosolic fraction”. The pellets were washed with 0.1% NP-40 lysis buffer and centrifuged again at 10,000 x g for 10 seconds. The supernatants were removed and the pellets were resuspended in 0.1% NP-40 lysis buffer containing 1% (v/v) (approximately 250 U/μL) of Benzonase (Table 2.1), to degrade genomic DNA. These samples were referred as “nuclear fractions”.

2.2.6.2 Co-Immunoprecipitation of DDX56-WNV capsid

Aliquots of REAP-fractionated cells were kept for loading controls. Remaining lysates were pre-cleared with protein G-sepharose or protein A-sepharose beads (50% suspension) for 1 hour at 4°C, with rotation. Immunoprecipitations of lysates were performed with guinea pig anti-WNV capsid antibody (1:500) or mouse anti-DDX56 antibody (1:500) for at least 4 hours at 4°C, with rotation. Twenty-five microliters of protein A-sepharose or protein G-sepharose were added and samples were incubated for 2 hours at 4°C, with rotation. Beads were pelleted at 500 x g and washed three times with 0.1% NP-40 lysis buffer (Table 2.5). Bound proteins were eluted in Protein sample buffer (Table 2.5) by heating samples at 95°C for 10 minutes. Samples were separated by SDS-

PAGE and transferred to PVDF membranes for Western blot analysis as described above (section 2.2.5).

2.2.7 Microscopy Techniques

2.2.7.1 Indirect Immunofluorescence

A549, HEK 293T, and Vero cells were cultured on sterile 18mm glass coverslips (Table 2.1) in 12-well plates and then subjected to virus infection or transfection for 24, 36, 48, or 72 hours, as indicated. For examination of virus assembly and replication complexes, cells were treated 24 hpi with 50 μ M MG132 or DMSO vehicle control for 12 hours and collected at 36hpi. At time of collection, cells were washed twice with PBSCM (PBS containing 0.5 mM CaCl_2 and 1 mM MgCl_2 , Table 2.5) and then fixed with 4% (w/v) paraformaldehyde for 20 minutes. The fixative was then quenched with 50 mM ammonium chloride in PBSCM for 5 minutes. Fixed cells were rinsed three times with PBSCM and then permeabilized with 0.2% (v/v) TritonX-100 PBSCM solution for up to 10 minutes. Following permeabilization, coverslips were rinsed three times with PBSCM and then blocked with 3% (w/v) BSA PBSCM for 1 hour at room temperature. Primary antibodies (Table 2.6) diluted in 3% BSA PBSCM were incubated with coverslips for 1 hour at room temperature or overnight at 4°C in a humid chamber. Coverslips were washed three times with PBSCM containing 0.3% BSA (w/v) for a total of 45 minutes, with rocking. Secondary antibodies conjugated to the appropriate fluorochromes (Table 2.7) were diluted in 1% BSA PBSCM and incubated with coverslips for 30 minutes in a humid chamber at room temperature in the dark. For cells to be imaged by three-dimensional structured illumination microscopy (3D-SIM), DAPI (1 μ g/mL) was added to

the secondary antibody incubation to label nuclei. Coverslips were again washed three times with 0.3% BSA PBSCM for a total of 45 minutes. One mm thickness glass slides (Table 2.1) were used for confocal and 3D-SIM Imaging. Coverslips that were to be examined by confocal microscopy were mounted in ProLong® Gold Antifade reagent containing DAPI (Table 2.1) and dried for 1 hour at room temperature in the dark. Coverslips to be examined by 3D-SIM were mounted in SlowFade® Gold Antifade reagent (Table 2.1) and sealed with nail polish. Samples were stored at -20°C overnight if not being visualized same day.

2.2.7.2 Confocal Imaging

Mounted coverslips were visualized on an Olympus IX-81 fluorescence confocal microscope with a Hamamatsu EMCCD camera. Acquisition of images was done with an ApoN 60X/1.42 aperture oil lens and laser beam intensity was adjusted to show no background staining in mock-infected or untransfected cells. Compressed z-stack images composed of 0.25 µm sections were obtained. Images were acquired and analyzed using Volocity® 3D Image Analysis Software (Table 2.4).

2.2.7.3 Three Dimensional Structured Illumination (3D-SIM) Imaging

Cells on mounted coverslips were visualized using a DeltaVision OMX® microscope system (Table 2.3) equipped with three sCMOS cameras, capable of 3D-SIM. Image acquisition was done with an Olympus ApoN 60X/1.42 aperture oil lens and Applied Precision 518 immersion oil (N=1.518). DeltaVision OMX® Master Control software (Table 2.4) was set for SI capture at 512 x 512 pixel size and 1x1 binning. Z-stack images were acquired with 0.125 µm spacing. Following acquisition, images underwent

reconstruction and image registration processes using SoftWoRx version 6.1 (Table 2.4). Files were imported into Volocity® libraries for visualization.

2.2.7.4 Transmission Electron Microscopy

A549 cells (5×10^4) were cultured on 13mm poly-L-lysine coated coverslips (Table 2.1), three samples per group, in 12-well dishes. Twenty-four hours after transfection of siRNAs (described in section 2.2.3) cells were infected with WNV (MOI, 3) for 48 hours. Following infection, cells were fixed with 4% glutaraldehyde/2% paraformaldehyde, 0.2 M sucrose and 4 mM CaCl_2 in 1.6 M sodium cacodylate buffer (pH 7.2) at 37°C for 1 hour. Woo Jung Cho (FoMD Microscopy Facility, University of Alberta) performed all subsequent steps of sample preparation. Following fixation, coverslips were washed with 0.05 M sodium cacodylate buffer and then lipids were fixed with 1% ice-cold osmium tetroxide in 0.05 M sodium cacodylate buffer. Samples were again washed with 0.05 M sodium cacodylate buffer to remove excess osmium tetroxide. Samples were stained with 1% uranyl acetate in 0.1 M sodium acetate buffer (pH 5.2) for 10 minutes. Coverslips were washed with sodium acetate buffer and then Milli-Q water before being dehydrated with increasing concentrations of ethanol in propylene oxide. Samples were embedded in Spurr epoxy resin and thermally polymerized at 60°C for 48h prior to generation of ultra-thin sections (70 nm) using a Leica UC7 ultramicrotome. To increase contrast, Reynolds lead citrate was added as a final step. Samples were imaged with a 16 mega pixel TEM camera on a Hitachi H-7650 Transmission electron microscope (Table 2.3) set at 70.0 kV. Image analysis of spherule size was performed using Fiji (ImageJ) open source software (Table 2.4).

Chapter 3

Visualization of DDX56 at WNV Assembly Complexes

3.1 Rationale:

Research focusing on identification and function of host factors required for replication and propagation of *Flaviviruses*, specifically WNV and DENV, has intensified over the last several years. Despite a multitude of studies demonstrating the complex interplay between flavivirus proteins and host factors, many are based on large scale genomic or proteomic screen that do not provide mechanistic data (Saha 2003, Krishnan, Ng et al. 2008, Sessions, Barrows et al. 2009, Mairiang, Zhang et al. 2013, Zhang, Chai et al. 2013, Sengupta, Ghosh et al. 2014). Previously, our lab identified 22 novel host cell-encoded interacting partners of WNV capsid protein using a Y2H assay (Xu, Anderson et al. 2011). Among these was an RNA helicase, DDX56, which normally localizes to the nucleolus. DDX56 purportedly functions in 60S ribosome biogenesis (Zirwes, Eilbracht et al. 2000). The interaction between WNV capsid and DDX56 during WNV infection was confirmed by reciprocal co-immunoprecipitation. Transient or stable knock-down of DDX56 has been observed to reduce the yield of infectious WNV by more than 100-fold in some cases, thus demonstrating DDX56 as a critical host factor for WNV infectivity (Xu, Anderson et al. 2011). Efficiency of viral replication and translation was assessed to determine where in the viral lifecycle DDX56 functions. Replication of WNV viral RNA in DDX56-KD and control cells was similar, as was the production of viral proteins NS3 and capsid. This suggests that DDX56 is important for a process that occurs after replication of viral RNA and translation of viral proteins. Interestingly, reducing DDX56 does not appear to affect assembly of WNV *per se*, however virions produced from DDX56-KD cells contain 3-4x less viral RNA. WNV virions produced from cells expressing DDX56-helicase dead mutants also contained 3-

4x less viral RNA and were ~100x less infectious, confirming that the helicase activity of DDX56 is required for assembly of infectious WNV virions (Xu and Hobman 2012).

As mentioned in Chapter 1, all known steps in the lifecycle of flaviviruses occur in the cytoplasm whereas DDX56 is normally localized to nucleoli. These viruses use modified ER membranes for replication, translation, and assembly. If DDX56 is involved in the latter, we expect that at a significant fraction of this enzyme to be present at or near virus assembly sites. Assessment of the steady state of DDX56 during WNV infection demonstrated that it is lost from the nucleoli during WNV infection. DDX56 protein levels are reduced as infection progresses and this process is dependent upon the proteasome. Since the proteasome is localized to the cytoplasm, this indicated that DDX56 might be relocalized from the nucleus during infection. Inhibition of the proteasome with MG132 in WNV-infected cells results in the build up of DDX56 on cytoplasmic reticular structures (Xu et al, 2011). These structures are reminiscent of the ER but their identity was not confirmed until the present study.

Based on the observations discussed above, I hypothesize that DDX56 is involved in the enhancement of WNV RNA packaging at viral assembly sites. To this end, I examined that distribution of DDX56 during WNV infection by confocal and super-resolution microscopy. The distribution of DDX56 relative to viral markers for replication (dsRNA), assembly sites (capsid and envelope) as well as the ER-localized chaperone calnexin was determined. In addition, I examined whether DDX56 expression was required for WNV-induced membrane rearrangements that give rise to replication complexes. Finally, as a first step toward understanding how DDX56 is relocalized from the nucleolus to the ER, I examined where DDX56-capsid interactions occur and if/how

the expression of WNV structural and non-structural proteins contribute to loss of DDX56 from the nucleus.

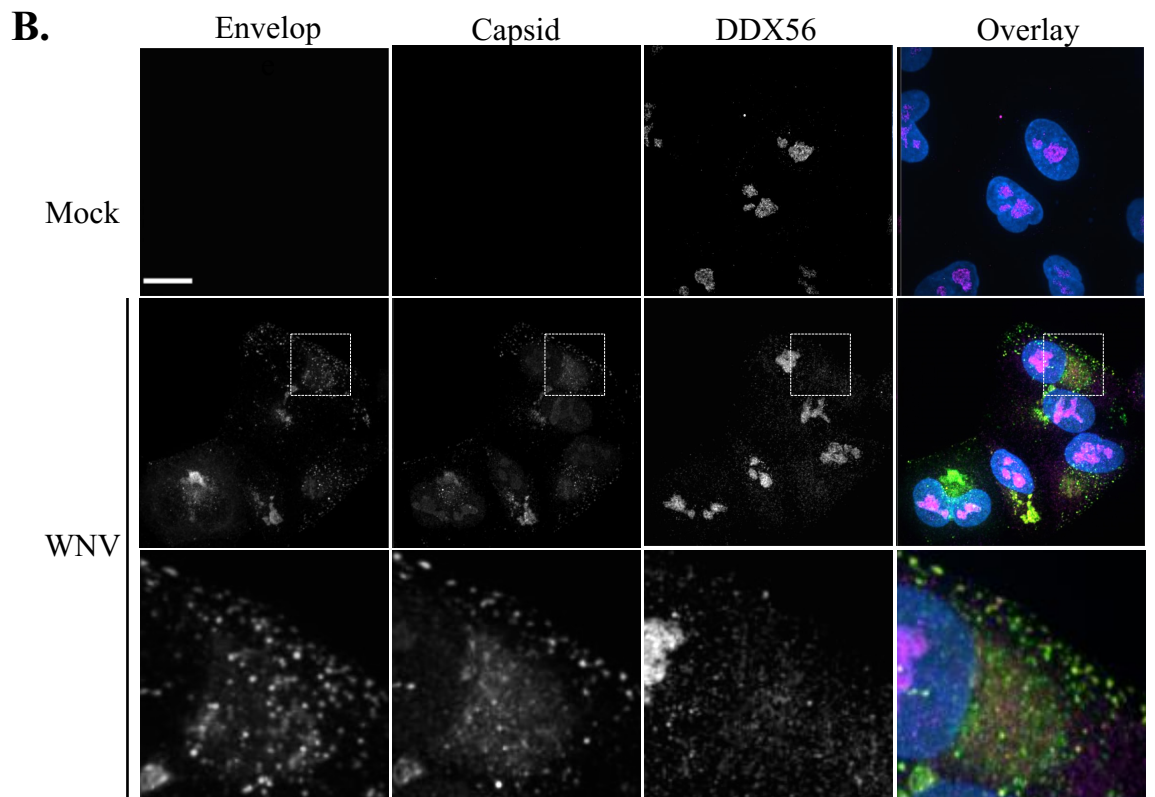
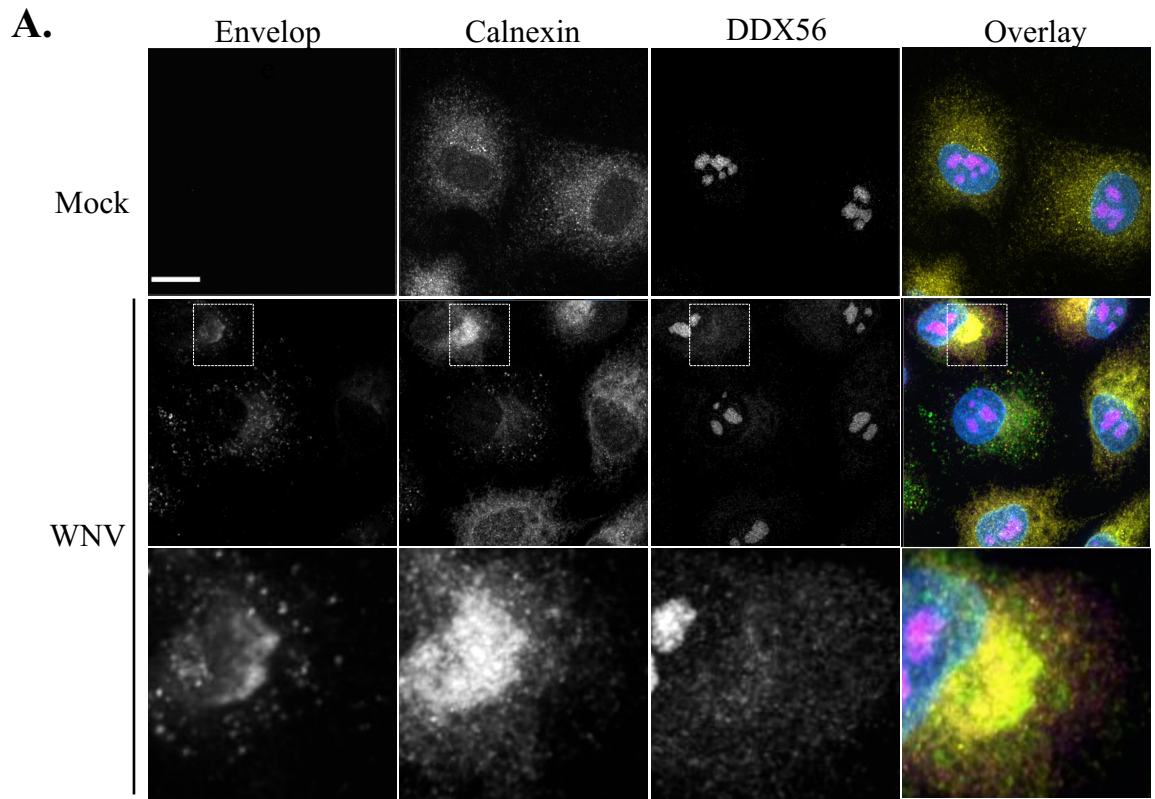
3.2 Results

3.2.1 DDX56 localizes to virus assembly sites during WNV infection

As mentioned above, I used indirect immunofluorescence (described in section 2.2.7.1) to examine the distribution of DDX56 in relation to viral markers and calnexin. Specifically, the localizations of two WNV structural proteins (capsid and envelope protein) and a replication intermediate (dsRNA) were examined. Confocal microscopy (described in section 2.2.7.2) was first used to examine DDX56 distribution in mock and WNV-infected cells. At 36 hours post-infection, the majority of DDX56 was still in nucleoli, however, a pool of this helicase was visible in the cytoplasm at perinuclear sites (Figure 3.1). Enlarged insets of images show staining of DDX56 in relation to dsRNA, envelope, capsid, and calnexin. While overlap between DDX56 and dsRNA or capsid was not evident, the helicase was present in regions of the ER where envelope protein and calnexin staining was prominent. To quantitatively and objectively assess the localization of DDX56 relative to viral and ER markers, Volocity® 3D image analysis software was employed (Table 2.4). In this analysis, the nucleus was excluded by use of ROI gates, thereby allowing colocalization values for cytoplasmic DDX56. Pearson's correlation coefficients (PCC) are represented on a scale from -1.0 (anti-correlation) to 1.0 (perfect correlation) with 0 indicating no spatial relationship between two proteins. PCC values derived from confocal microscopic analyses of WNV-infected cells revealed that there was virtually no overlap between dsRNA (marker for replication sites) and

capsid or envelope protein (assembly site markers) (Figure 3.2A). This indicates that replication and assembly sites on the ER can be distinguished from each other.

All three viral proteins colocalized with calnexin to some degree, with envelope protein having the highest amount of overlap. DDX56 colocalized with WNV envelope protein and calnexin, but not with dsRNA, thus supporting the hypothesis that DDX56 localizes to WNV assembly sites. Surprisingly, DDX56 did not colocalize with capsid in the cytoplasm. Because of the relatively low amount of DDX56 in the cytoplasm compared to viral and ER markers, I examined the percent overlap between the DDX56 signal with viral proteins and calnexin. Limited overlap of DDX56 with dsRNA was observed, further confirming the lack of correlation between these two markers (Figure 3.2B). Degrees of overlap between DDX56 and capsid varied widely between cells, suggesting that their correlation may be transient in the cytoplasm. In contrast, consistent overlap between DDX56 and WNV envelope protein and calnexin was observed, further validating the colocalization analysis. Thus, lower correlation values observed between DDX56 and other markers are a result of low DDX56 signal in the cytoplasm during infection.



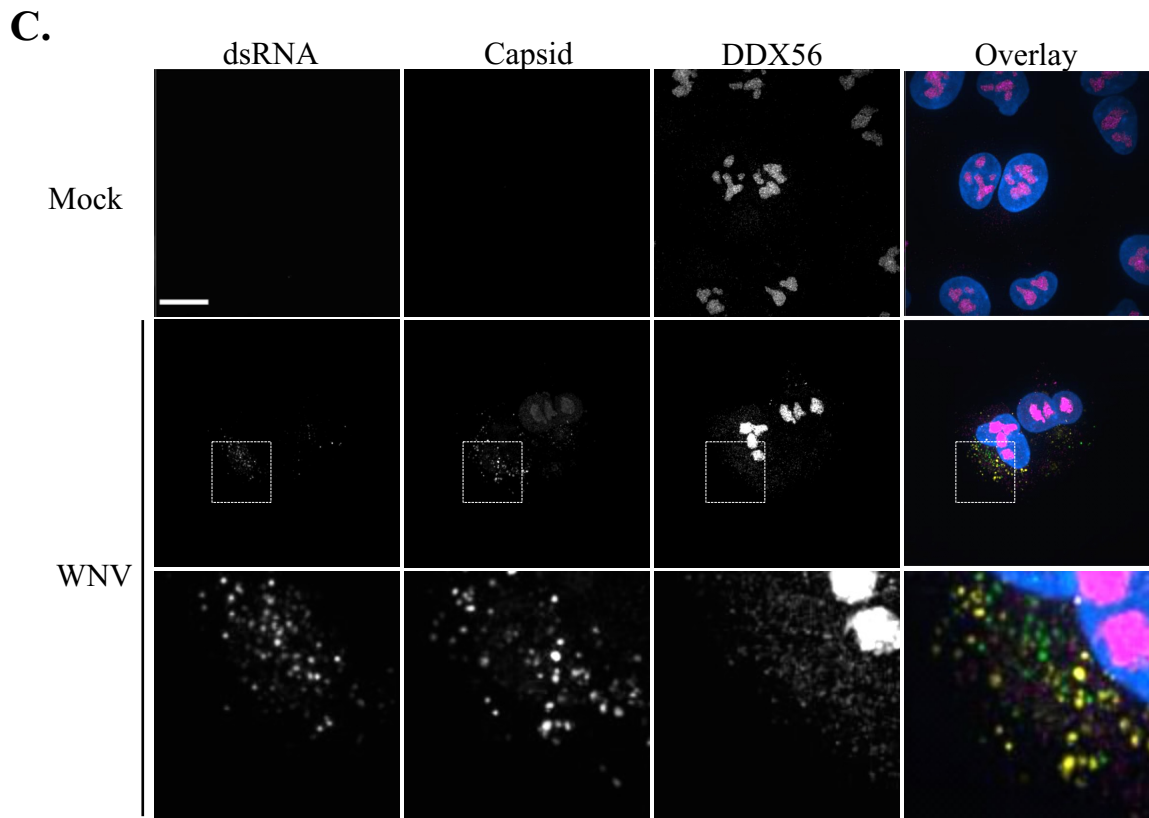


Figure 3.1 DDX56 localizes to the site of virus replication and assembly during WNV infection. A549 cells were infected with WNV (MOI, 3) for 36h and then processed for indirect immunofluorescence. A) Cells were stained using a humanized anti-WNV envelope antibody detected with a goat anti-human Alexa 488, a rabbit anti-calnexin antibody detected with a donkey anti-rabbit Alexa , and a mouse monoclonal against DDX56 detected with a goat anti-mouse IgG1 Alexa 647. B) Cells were stained using a humanized anti-WNV envelope antibody detected with a goat anti-human Alexa 488, a guinea pig anti-WNV capsid detected with a donkey anti-guinea pig Alexa 568, and mouse monoclonal against DDX56 detected with a goat anti-mouse IgG1 Alexa 647. C) Cells were stained using a mouse monoclonal against dsRNA (J2) detected with a goat anti-mouse IgG2A Alexa 488, a guinea pig anti-WNV capsid detected with a donkey anti-guinea pig Alexa 568, and a mouse monoclonal against DDX56 detected with a goat anti-mouse IgG1 Alexa 647. All samples were mounted in ProLong® Gold antifade reagent containing DAPI. Images were captured using an Olympus IX-81 confocal spinning disk microscope. Enlarged images of indicated perinuclear regions in WNV infected cells are given. Bars=15 μ m.

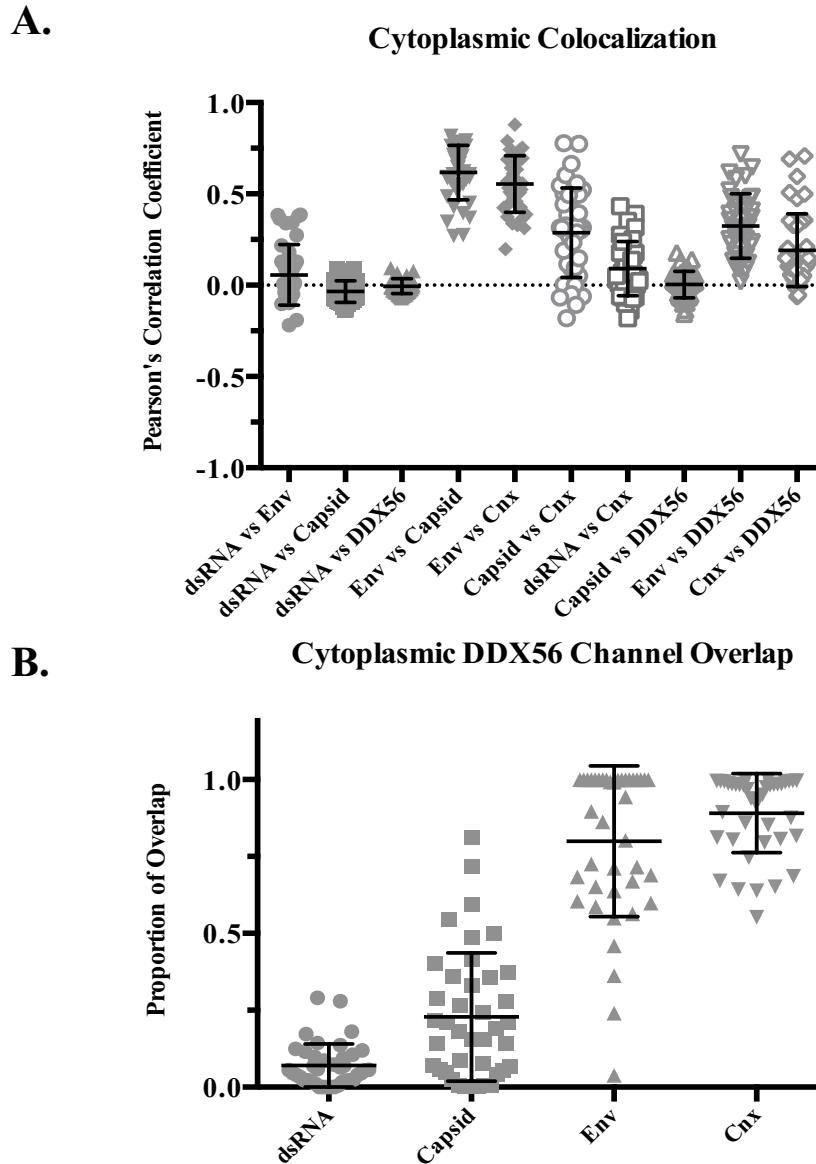


Figure 3.2 DDX56 colocalizes at viral assembly complexes in the cytoplasm with WNV envelope protein and calnexin. A) A549 cells infected with WNV (MOI, 3) for 36 hours were collected and were stained for DDX56 and a variety of WNV markers of assembly, capsid and envelope (Env), and a replication marker (dsRNA) as well as a marker for the endoplasmic reticulum, calnexin (Cnx). The experiment was performed in triplicate and 40 cells were selected for analysis using Volocity 6.3 Image Analysis (Perkin Elmer). The nucleus was excluded by utilizing ROI gates. Mock cells stained with the same markers were used to set thresholding gates so that no relationship occurred between the gates compared. Pearson's colocalization coefficient (PCC) was calculated for each cell. B) For each cell the amount of DDX56 channel overlap with their respective marker is shown. Note: 1 is a perfect 100% overlap and 0 is no overlap.

To gain further insight into the nature of DDX56 localization during WNV infection, the distributions of envelope protein, capsid, calnexin, and DDX56 were examined using 3D Structured Illumination Microscopy (3D-SIM) (section 2.2.7.3). This method allows for an 8-fold increase in resolution compared conventional fluorescence microscopy (reviewed in (Schermele, Heintzmann et al. 2010)). By 3D-SIM, DDX56 was clearly discernable in the cytoplasm at 36 h.p.i. (Figure 3.3). Close examination of z-stack images of perinuclear regions revealed that there were multiple regions in which DDX56 was closely associated with WNV envelope protein and calnexin (Figure 3.3, numbered boxes). By confocal imaging, overlap between DDX56 and WNV capsid was not evident, however, when 3D-SIM was employed, pools of DDX56 that were closely associated with capsid-positive areas of the ER were observed. Together these data suggest that DDX56 localizes to WNV assembly complexes at modified-ER membranes; which is consistent with our hypothesis that this helicase functions in packaging of viral RNA.

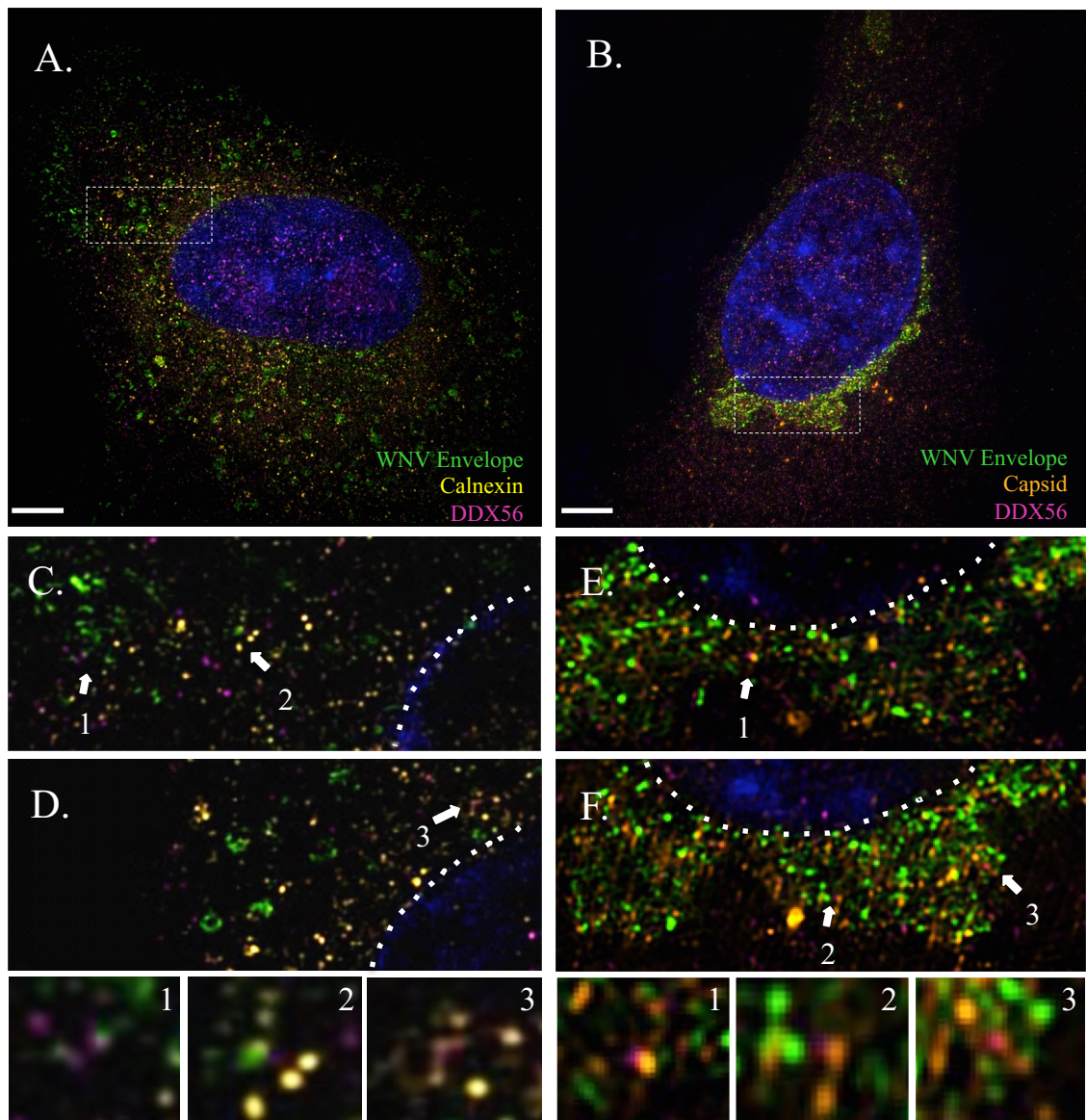


Figure 3.3 DDX56 localizes to punctate regions associated with WNV envelope and calnexin. A549 cells were infected with WNV (MOI, 3) for 36h and then processed for indirect immunofluorescence. Cells were stained using DAPI (blue), a humanized antibody against WNV Envelope, detected with a goat anti-human Alexa 488, and a mouse monoclonal antibody to DDX56, detected with a goat anti-mouse IgG1 Alexa 647. Cells were stained with a guinea-pig antibody against WNV Capsid (A), detected with a goat anti-guinea pig Alexa 568, or a rabbit antibody to Calnexin (B), detected with a donkey anti-rabbit Alexa 568. Images were captured on a DeltaVision OMX® microscope system capable of 3D-SIM. Bar = 4µm. Reticular regions with large amounts of viral envelope protein staining with Calnexin and DDX56 (C-D) or Capsid and DDX56 (E-F) were closely examined. Single Z-stacks with representative staining are shown at higher magnification. Arrows and numbers indicate areas of close association between DDX56 and WNV E protein or calnexin.

3.2.2 Reducing DDX56 expression does not affect formation of virus-induced membrane alterations and virus replication sites

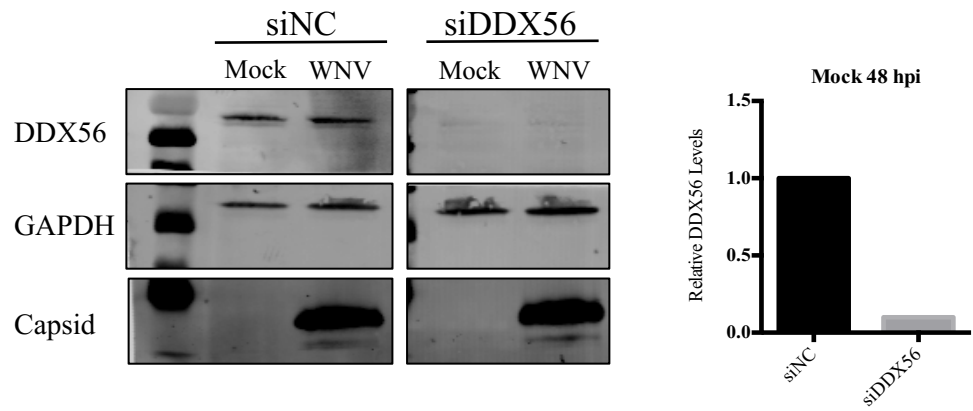
Formation of WNV replication and assembly sites entails dramatic rearrangements of ER membranes (Westaway 1997, Gillespie, Hoenen et al. 2010, Whiteman, Popov et al. 2015). Because of the purported role of DDX56 in packaging of viral RNA into nascent virions, I questioned whether the helicase was important for the virus-induced ER membrane rearrangements. To address this question, cells in which DDX56 levels were reduced or “knocked down” (DDX56-KD) by siRNA transfection (described in section 2.2.3) were infected with WNV for 48 hours after which the samples were processed for transmission electron microscopy (TEM, section 2.2.7.4). Transient knock down of DDX56 was quite efficient and stable over the course of the time frame used for infection. Specifically, at 72 hours post transfection, DDX56 levels were reduced by 90% (Figure 3.4, A). Importantly for my analyses, the intracellular ultrastructure as examined by TEM, did not seem to be affected by transfection with either a control non-targeting siRNA (siNC) or a DDX56-targeting siRNA (siDDX56) in mock infected cells (Figure 3.4, B).

Examination of WNV infected cells by TEM showed that decreased expression of DDX56 did not hinder the formation of virus-induced membrane structures in the cytoplasm (Figure 3. 4, B). The presumably ER-derived structures seen in DDX56-depleted cells were indistinguishable in morphology from the control siRNA transfected cells. In both cases, the structures are similar to those, which have previously been described for DENV- and WNV_{KUN}-infected cells (Westaway 1997, Welsch, Miller et al. 2009). Spherule structures that lack electron density (white arrows), as well as

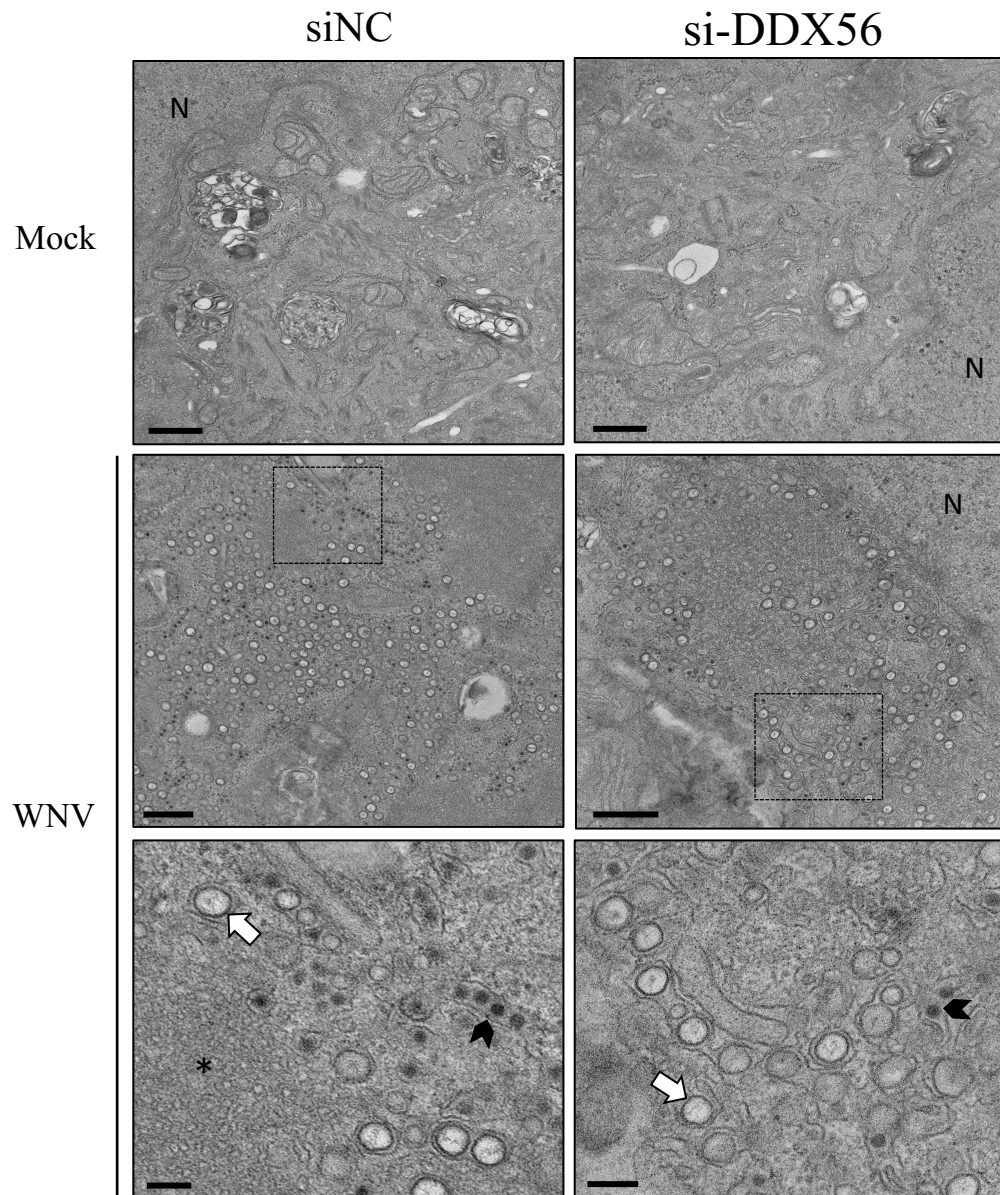
convoluted membranes, were observed in WNV-infected cells transfected with DDX56-specific siRNAs as well as control siRNA expressing cells. Close examination of the spherules, which are presumed replication sites, indicated that they contain invaginations or porous necks rather than being closed structures. This is similar to what has been described in DENV and WNV_{KUN}-infected cells; that the spherules are invaginations into the ER membrane and are connected to the cytoplasm through a small neck-like opening (Welsch, Miller et al. 2009, Gillespie, Hoenen et al. 2010).

Next, I examined whether the size of the spherules differed between control and DDX56-KD cells. In total, the diameters of 150 spherules were measured using ImageJ software (Table 2.4). For control cells and DDX56-KD cells the average spherule diameter was $82.9 \text{ nm} \pm 0.69 \text{ nm}$ and $81.2 \text{ nm} \pm 0.74 \text{ nm}$, respectively (Figure 3.4, C). This size is similar to what has been reported for DENV-2 infected cells in which the average spherule diameter is 87.5 nm (Welsch, Miller et al. 2009). My analyses showed that statistically, the diameters of the WNV-induced spherules in DDX56-depleted cells were the same size as those in control siRNA-transfected cells ($p=0.089$, $t= 1.706$, $df=296.5$). In addition, loss of DDX56 expression did not result in discernable differences in the morphologies of nascent virions or other virus-induced structures. Taken together the data suggest that DDX56 is not required for the formation of WNV-induced membrane alterations, specifically those involved in replication. This is consistent with our hypothesis that DDX56 is not important for WNV replication and therefore would not affect cellular ultrastructure during infection.

A.



B.



C.

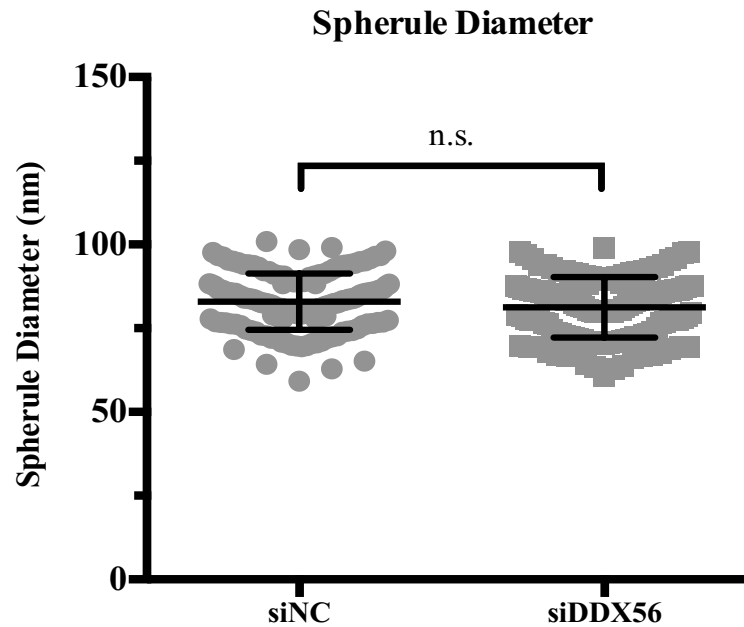


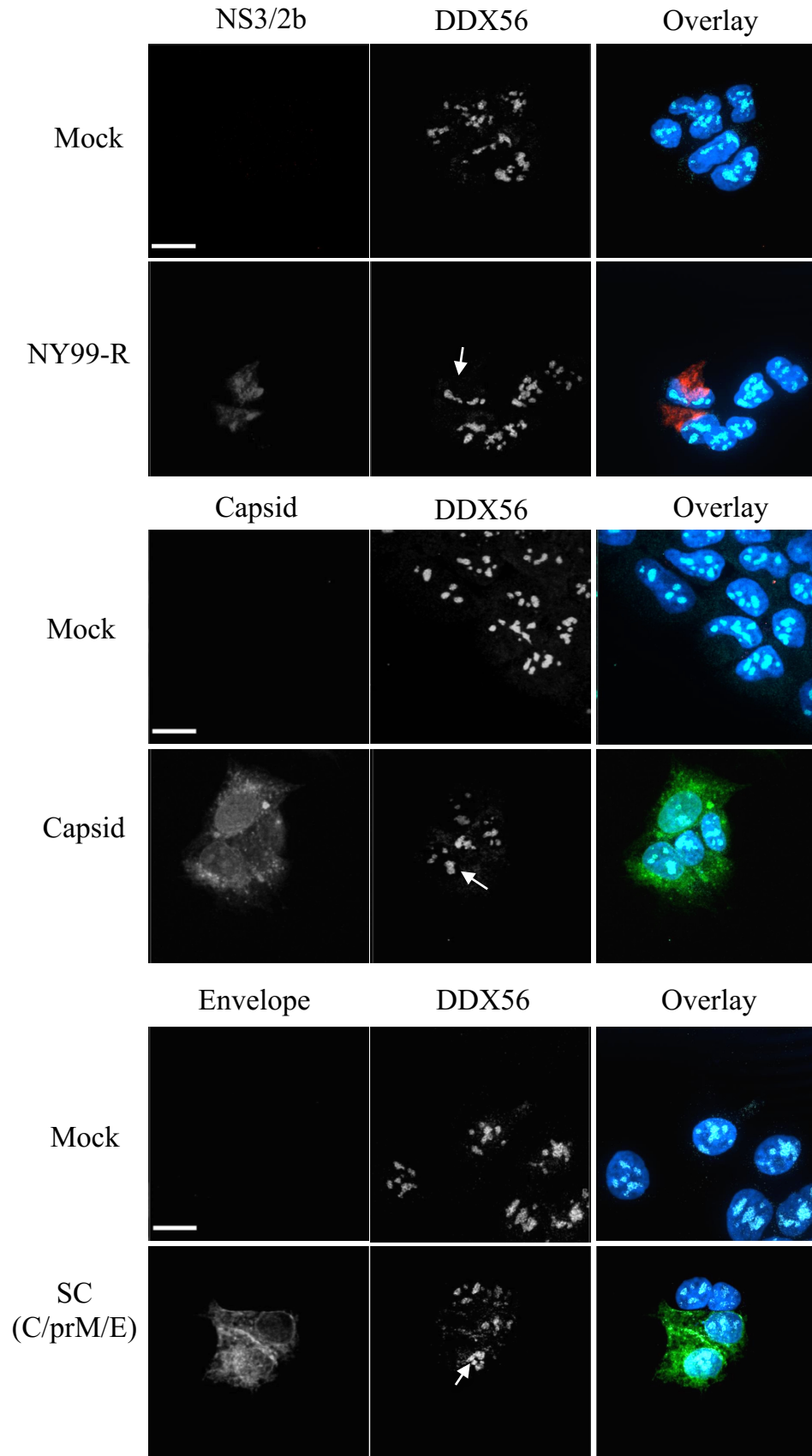
Figure 3.4 DDX56 is not required for WNV-induced membrane rearrangements and ultrastructure. A549 cells were transfected with a non-silencing control siRNA (siNC) or a DDX56-targeting siRNA (siDDX56) for 24 hours and then infected with WNV (MOI, 3) for an additional 48 hours. A) Immunoblot analysis was used to determine the relative amounts of viral (WNV-capsid) and cellular (DDX56 and GAPDH [loading control]) in cell lysates. B) Cells transfected with siRNAs and infected with WNV were collected at forty-eight hours post infection and were fixed and sectioned for TEM visualization. Images were acquired with a Hitachi H-7650 transmission electron microscope. Images of indicated regions were taken at a larger magnification and shown below. Bar = 500nm, 100nm for increased magnification. The nucleus (N) and nuclear envelope are seen in some images. Replication spherules (white arrows), virions (black arrow heads), and convoluted membranes (asterisk) are indicated. C) Diameters of presumed replication complexes (spherules) were measured between inner membranes (n=150). A *t*-test comparison with Welch's correction determined that there is no significant difference between the samples.

3.2.3 Expression of WNV proteins does not affect DDX56 cellular distribution

Viruses have evolved efficient mechanisms to recruit and/or sequester host proteins in order to aid in virus entry, replication and/or assembly or to interfere with critical anti-viral signaling. The use of host nuclear proteins during viral infection has been demonstrated for many viruses including members of the *Flaviviridae* family. Hepatitis C virus interacts with and recruits nuclear pore complex proteins (Nups) to the cytoplasm, the site of virus replication and assembly. Here, Nups are thought to facilitate the establishment of the membranous web (Neufeldt, Joyce et al. 2013, Levin, Neufeldt et al. 2014). Interestingly, WNV capsid protein localizes to the nucleus and cytoplasm, a process that is reportedly affected by the phosphorylation state of the protein, (Westaway, Khromykh et al. 1997, Cheong and Ng 2011). Whereas a large pool of cytoplasmic capsid is likely involved in virus assembly, the role of nuclear capsid is not yet understood but it does interact with the nucleolar helicase DDX56. During WNV infection, DDX56 is depleted from the nucleus, followed by proteasome-dependent degradation, but the mechanism by which this occurs is not well understood. We do know that expression of WNV capsid alone is not sufficient for relocalization of DDX56 from the nucleolus (Xu, Anderson et al. 2011). Moreover, treatment of cells with Leptomycin B, an inhibitor of CRM1-dependent nuclear export, did not prevent DDX56 degradation during WNV infection. CRM1 is only one of many nuclear export factors and as such, it is possible that other exportins promote loss of DDX56 from the nucleus. Alternatively, WNV infection may also prevent import of DDX56 into the nucleus.

Here I sought to better understand the process by which DDX56 is translocated to the ER during WNV infection. First, I transfected cells with WNV replicons (plasmid-

based expression systems that encode virus non-structural proteins) and then examined the intracellular distribution of DDX56 by indirect immunofluorescence. Expression of WNV capsid, a WNV replicon plasmid (kindly provided by Dr. Vladimir Yamshchikov, Southern Research Institute, Birmingham, AL), and/or a virus structural protein cassette did not result in any obvious change in DDX56 localization at 24 hours post-transfection (Figure 3.5). Additionally, longer transfection times (48h or 72h) did not result in any noticeable difference in DDX56 localization (data not shown).



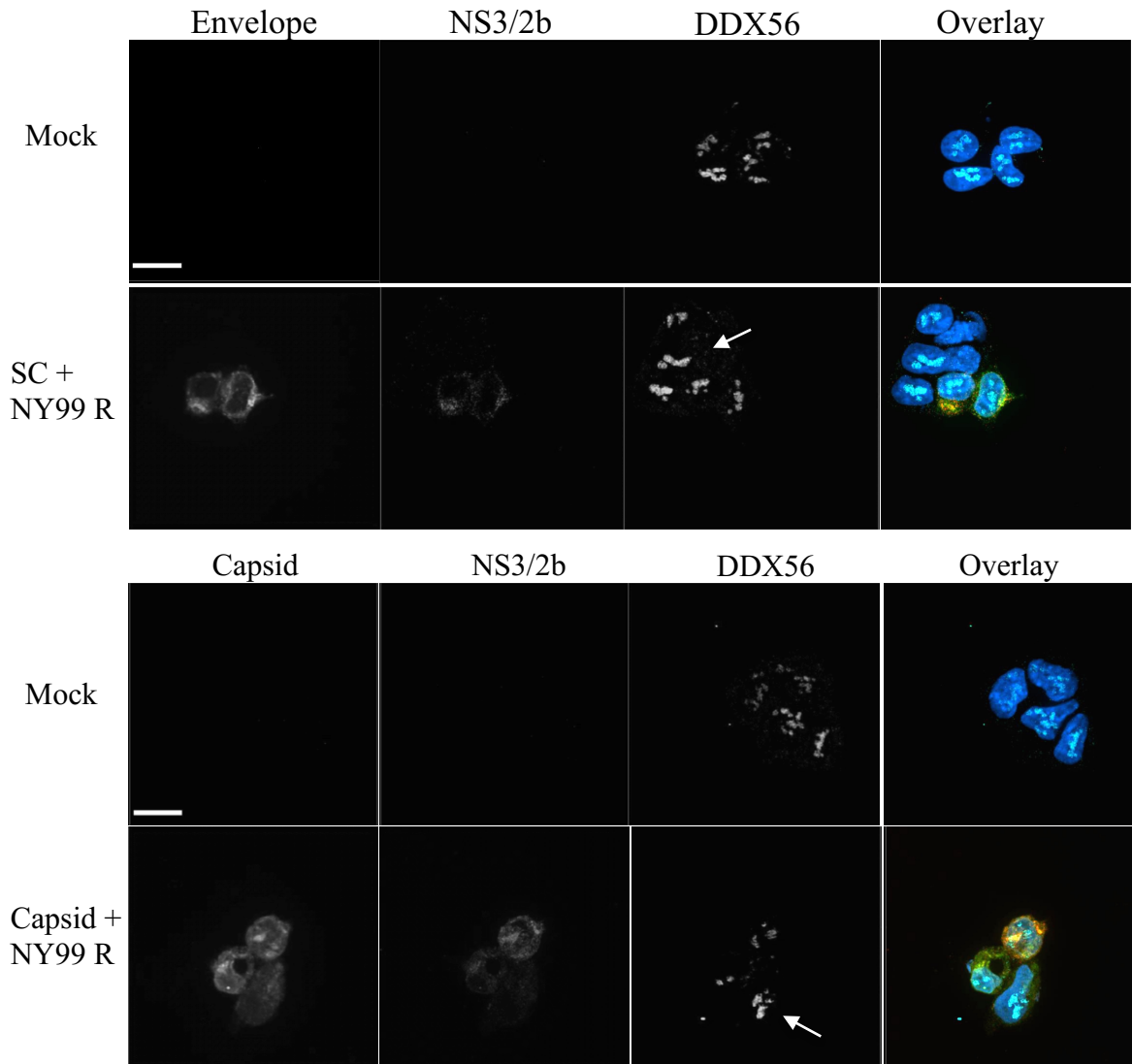


Figure 3.5 Expression of WNV proteins does not result in a relocalization or loss of DDX56 from the nucleolus. HEK 293T cells were transfected with a subgenomic replicon expressing all non-structural proteins from a WNV_{NY99} backbone (NY99-R), a plasmid encoding capsid protein alone (Capsid), a cassette encoding all structural genes (SC), or combinations of the above. Mock cells were transfected with no vector but given same amounts of transfection reagent to check to cytotoxicity. 24 hours post transfection, samples were processed for indirect immunofluorescence using a monoclonal mouse anti-WNV NS3/2b detected with a goat anti-mouse IgG3 Cy3, a human anti-WNV envelope, detected with a goat anti-human Alexa 488, a guinea-pig anti-WNV capsid detected with a goat anti-guinea pig Alexa 488, and a monoclonal mouse anti-DDX56 detected with a goat anti-mouse IgG1 Alexa 647. Images were captured using an Olympus IX-81 confocal spinning disk microscope. No difference in DDX56 pixel intensity in the nucleolus was observed (arrows). Bars=15 μ m

Next I examined if transient expression of WNV proteins resulted in the degradation of DDX56, which would be expected to occur if the mis-localized helicase was targeted for degradation by the proteasome. Briefly, cells were transfected with the aforementioned constructs and 24 hours post-transfection, cell lysates were subjected to SDS-PAGE and immunoblotting (section 2.2.5). Unfortunately, the structural protein cassette resulted in low expression levels and the viral proteins were not detectable by immunoblotting. Very low levels of capsid were detected when the structural cassette and non-structural replicon were co-transfected, indicating that the expression of the structural cassette may be limited during co-transfection (Figure 3.6A). Data from three independent experiments were used to quantitate relative DDX56 levels to the loading control GAPDH in cells expressing WNV proteins (Figure 3.6 B). No significant differences in DDX56 protein levels were observed between mock transfected cells and cells expressing WNV proteins by 1-way ANOVA ($F(4,10)=2.863$, $p=0.0808$). Expression of WNV proteins alone, even those that could potentially produce infectious virions (SC+NY99), may not be sufficient for DDX56 degradation. However, it is possible that the structural proteins were not processed correctly as capsid is normally cleaved by the viral protease, which is not present during transfection (see Figure 1.1). This cleavage facilitates the release of capsid from its membrane anchor. The lack of viral protease activity could explain the undetectable level of mature capsid by immunoblot during cassette transfection. It appears as though this effect could be rescued in *trans* to some extent by expression of the nonstructural replicon, given the low level of capsid during co-transfection. Therefore, we cannot conclude whether expression of some or all WNV structural proteins affects the distribution of DDX56. Further investigation using a

structural protein cassette with an autocatalytic cleavage site in capsid is needed to determine whether these proteins are required. At this point I can conclude that expression of capsid or nonstructural proteins alone does not affect DDX56 distribution.

The redistribution of DDX56 from the nucleolus to the cytoplasm may require an active WNV infection. Alternatively, it is possible that WNV infection inhibits host cell nuclear import, thus preventing newly synthesized DDX56 from gaining entry into the nucleus. However, it was shown that nucleolin, another nucleolar-localized host protein is not relocalized or degraded during infection, suggesting that DDX56 is unique to WNV (Xu, Anderson et al. 2011). Loss of DDX56 from the nucleolus could be a result of protein-turnover. Further investigation into how WNV infection results in DDX56 localizing to the ER is needed.

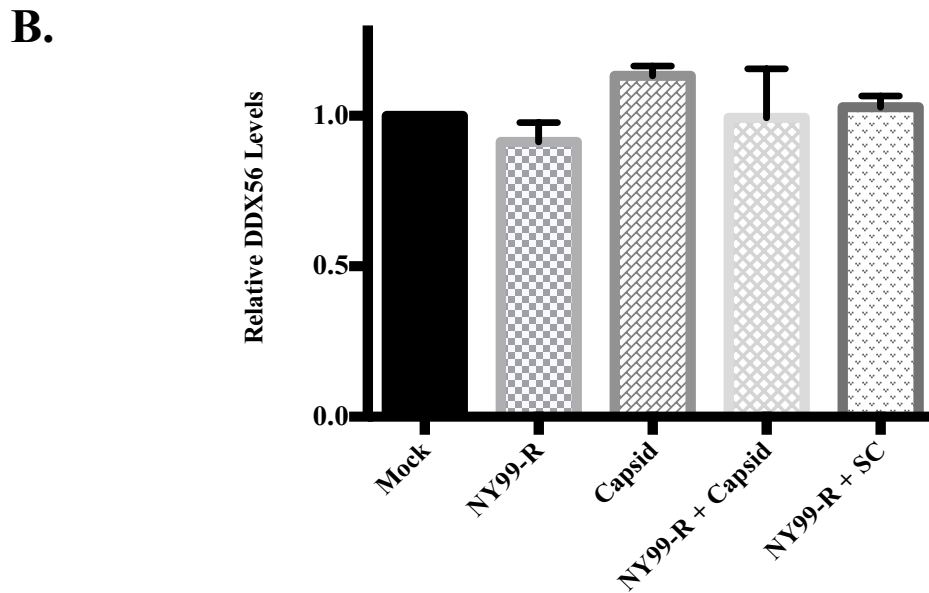
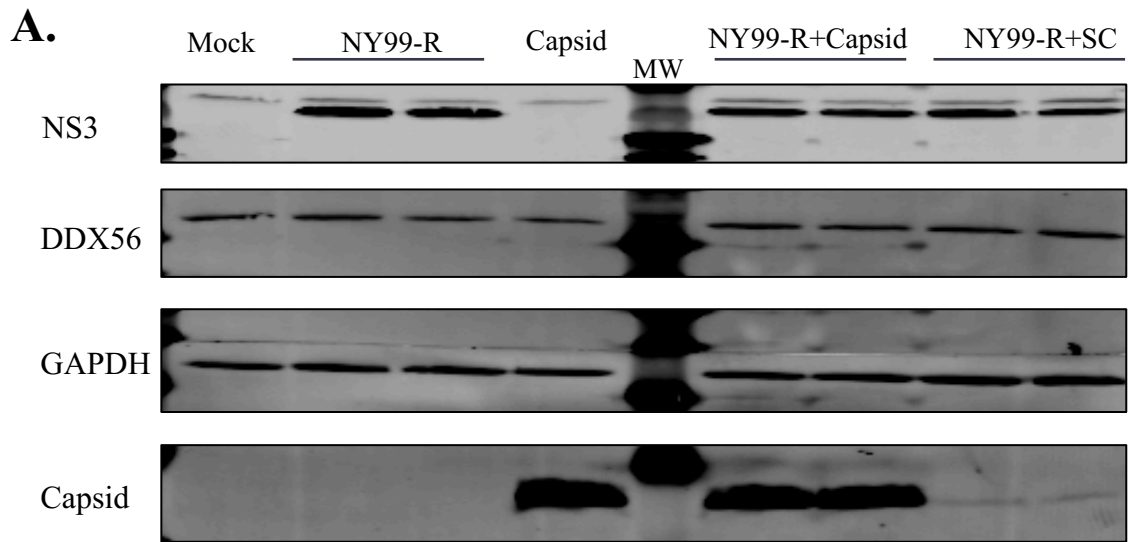


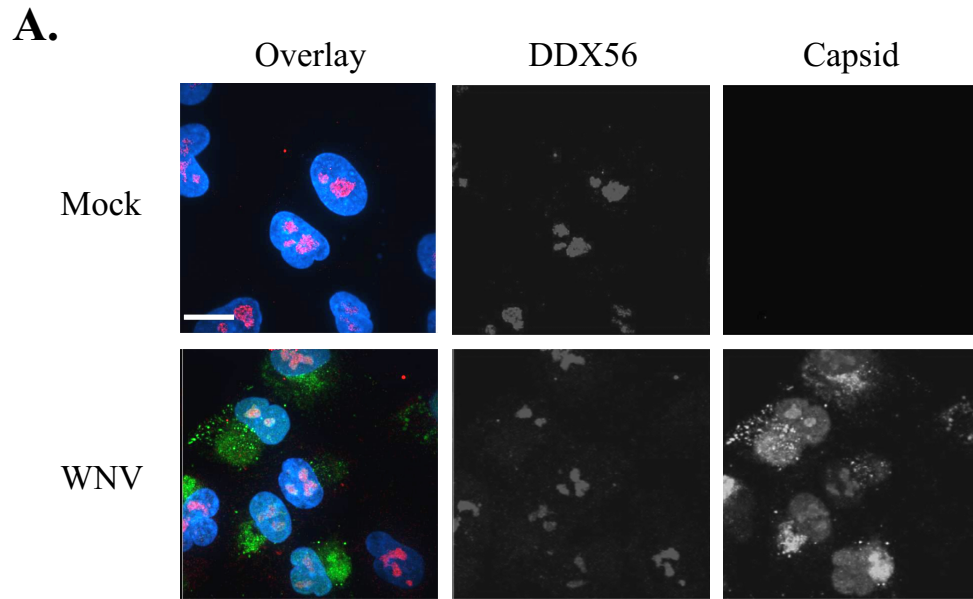
Figure 3.6 Expression of WNV proteins does not induce degradation of DDX56. A) HEK 293T cells were transfected with plasmids encoding nonstructural protein replicon (NY99-R), WNV capsid, a cassette encoding all structural proteins (SC), or combinations of the above. Mock cells have had transfection media added to them without any plasmid DNA. 24 hours post transfection, lysates were collected and subject to SDS-PAGE and immunoblotting for NS3 (detecting NY99-R), Capsid (detecting capsid and SC), DDX56, and GAPDH (loading control). MW indicates the molecular weight protein ladder used to determine correct size of bands present. B) Data from three independent experiments were used to determine the normalized level of DDX56 (relative to GAPDH).

3.2.4 DDX56 and WNV capsid interact in the nucleus during infection

Given the theorized function of DDX56 at WNV assembly sites, the lack of colocalization between this helicase and capsid protein in the cytoplasm (section 3.2.1) was unexpected. Understanding when and where these two proteins interact should provide further insight as to how WNV infection leads to relocalization and repurposing of DDX56. As such, I re-examined the localizations of capsid and DDX56 in infected cells using quantitative confocal microscopy (Figure 3.7, A). At 36 h.p.i., extensive overlap between capsid and DDX56 was observed in the nucleus whereas little colocalization was evident in the cytoplasm (Figure 3.7, B). These data are consistent with a scenario in which capsid and DDX56 interact primarily occur in the nucleus, at least at 36 hpi. However, because colocalization is not direct evidence of interaction, I used co-immunoprecipitation to further, A549 cells were infected with WNV (MOI, 3) for 48 hours after which crude nuclear and cytoplasmic fractions were prepared and then subjected to immunoblot analysis (section 2.2.6). The relative purity of the fractions was assessed by immunoblotting for GAPDH, a cytoplasmic marker, and histone H3, a nuclear marker. Data in Figure 3.8A show that I was able to separate nuclear and cytoplasmic compartments using this rapid procedure. DDX56 and capsid interaction was detected in the whole cell lysates and nuclear fractions prepared from WNV infected cells (Figure 3.8, B and C). Co-immunoprecipitation of DDX56 and capsid was not observed in cytoplasmic fractions. Taken together, these data suggest that the interaction between capsid and DDX56 occurs primarily in the nucleus.

Because the interaction between WNV capsid and enzymatically active DDX56 is important for infectious virion production (Xu and Hobman 2012), these data are

surprising. This is because WNV assembles and packages its viral RNA in the cytoplasm at ER-derived membranes. One explanation for this is that the interaction between WNV capsid and DDX56 is transient and/or unstable at virus assembly sites thereby making it difficult to detect by either immunoblotting or colocalization. As well, the importance of the DDX56-capsid interaction in the nucleus remains to be determined.



B. Capsid and DDX56 Colocalization

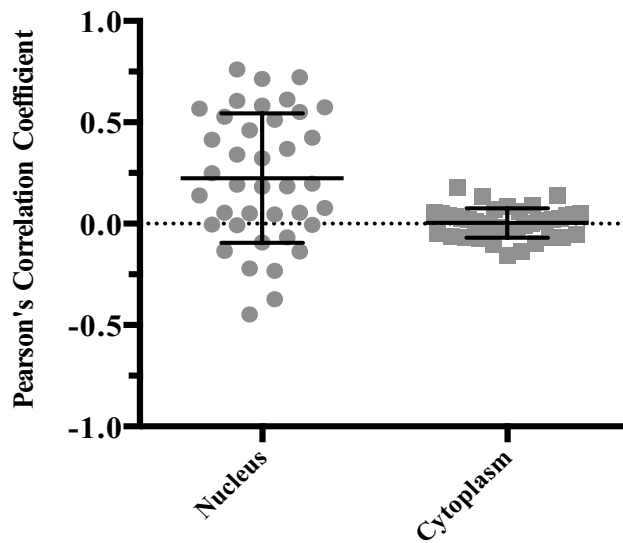


Figure 3.7 DDX56 primarily colocalizes with capsid in the nucleus of WNV infected cells. A) A549 cells were infected with WNV (MOI,3) and collected at 36 hours post infection. Samples were processed for indirect immunofluorescence using a mouse antibody to DDX56 which was detected by a goat anti-mouse IgG₁ Alexa 647 secondary. Viral capsid was detected with a guinea pig antibody and a goat-anti-guinea pig Alexa 568 secondary. Images are false colored to show colocalization. Bars= 15uM B) Colocalization analysis was performed on selected regions of interest (nucleus alone or cytoplasm alone) in Volocity 6.3. Cells (n=40) were selected from three independent experiments and the Pearson's colocalization coefficient (PCC) was determined.

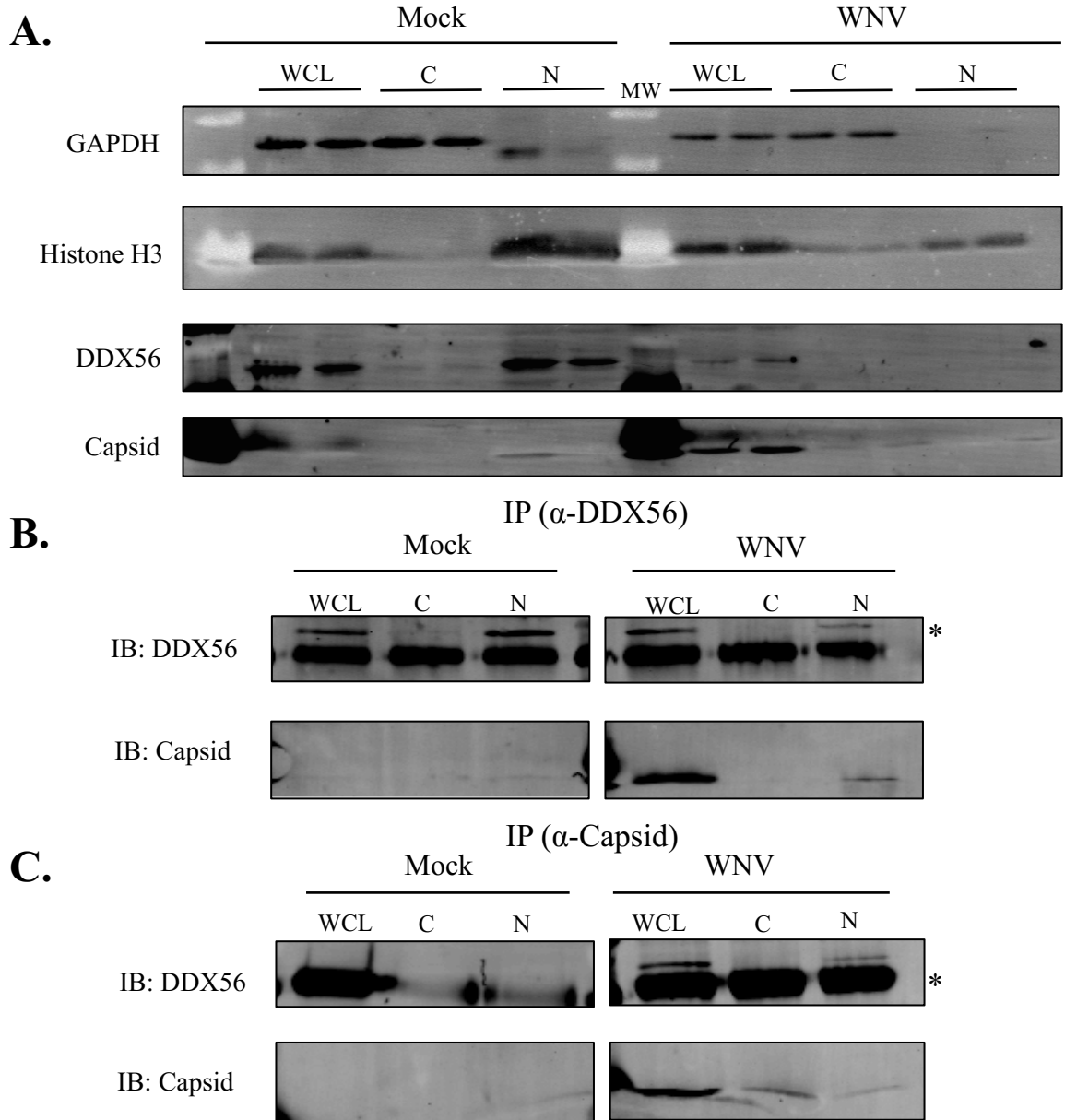


Figure 3.8 DDX56 and WNV capsid interact in the nucleus during infection. A549 cells were infected with WNV (MOI, 5) for 48 hours and then cells lysates were fractionated via REAP method. A) Prelysates (2%) were subject to SDS-PAGE and immunoblotting for Histone H3 and GAPDH to determine fractionation efficiency. Histone H3 is a control for nuclear fractionation and GAPDH is a cytoplasmic fractionation control. A protein molecular weight marker (MW) was used to confirm size of expected bands. Immunoblotting with DDX56 and WNV Capsid shows levels of these proteins prior to immunoprecipitation. Remaining lysates were subject to coimmunoprecipitation with a mouse anti-DDX56 antibody (B) or a guinea pig anti-capsid antibody (C) followed by SDS-PAGE and immunoblotting (IB) with antibodies against DDX56 and WNV Capsid. IgG heavy chain is indicated with an asterisk (*).

3.3 Conclusions

In this chapter, I used confocal and 3D-structured illumination microscopy to visualize DDX56 at specific regions in the ER. DDX56 visualization in the cytoplasm was optimal at 36 h.p.i. prior to degradation by the proteasome. Colocalization between WNV envelope protein, calnexin, and DDX56 suggest that DDX56 localizes to sites of virus assembly. Consistent with this was the lack of colocalization of DDX56 with dsRNA, a marker for replication sites. Examination of WNV-induced ER membrane rearrangements demonstrated that DDX56 is not required for the formation of these structures which are thought to function in replication. This confirms previous data showing that DDX56 is not required for replication or translation of virus-encoded proteins during infection. I did not observe relocalization of DDX56 to the cytoplasm and/or a block in its nuclear import in cells expressing different combinations of WNV structural and/or non-structural proteins. However, it is possible that the structural proteins were not correctly processed in the transfected cells. Use of a self-processing viral protein cassette would be helpful in determining their role in altering DDX56 localization. Also, it could be that active WNV infection, not the expression of viral proteins *per se*, is required for localization of DDX56 to the cytoplasm followed by degradation by the proteasome. Clearly, additional experiments are needed to distinguish between these possibilities. Finally, the interaction between DDX56 and WNV capsid is most stable in the nucleus; however, its role at this site is unknown. Together, all these observations confirm our hypothesis that DDX56 is important for the packaging of viral RNA at WNV assembly sites at the ER.

Chapter 4

Role of DDX56 in *Flavivirus* Infection

4.1 Rationale

Often, similar host factors or cellular pathways are utilized by related viruses, and understanding these connections is crucial in the development of broad-spectrum antivirals (reviewed in (Reid, Airo et al. 2015)). The requirement of various host cell-encoded DEAD-box RNA helicase members for virus infection has been demonstrated, including members of the *Flaviviridae* family (discussed in section 1.4.2). Previously, our lab demonstrated that DDX56 is a critical host factor for WNV infection (Xu, Anderson et al. 2011). DDX56 has also been shown to be important for HIV-1 Rev function (Yasuda-Inoue, Kuroki et al. 2013). Investigation into the role of DDX56 for other viruses showed that during infection with *Flaviviridae* members DENV-2, HCV, or another +RNA, rubella virus, DDX56 was not lost from the nucleolus (Xu, Anderson et al. 2011, Xu 2013). Nor was DDX56 degraded during rubella virus infection, suggesting that DDX56 may be a specific host factor for WNV. Indeed knock-down of DDX56 resulted in ~100x less infectious WNV virions produced, titers of rubella virus were not affected (Xu, Anderson et al. 2011).

The *Flavivirus* genus contains the important human pathogens WNV and SLEV (both in the Japanese encephalitis serocomplex), and Powassan virus (in the Tick-borne encephalitis serocomplex), and DENV serotypes 1-4 comprise the Dengue serocomplex (reviewed in (Mukhopadhyay, Kuhn et al. 2005)). Although DDX56 does not seem to be required for DENV-2 infection, I was interested in determining whether this helicase played a role in the life cycle of other *Flaviviruses*. If so, targeting this host enzyme could possibly serve as a novel broad-spectrum antiviral therapy. Due to the relatedness of WNV and SLEV, we hypothesize that DDX56 is an important host factor for members

of the Japanese encephalitis serocomplex. Presently, relatively little is known about the host factors required for SLEV infection. Here, I investigated the role of DDX56 during infection with SLEV and another flavivirus POW. First I examined if DDX56 is lost from the nucleolus of cells infected with SLEV or POW, as was previously described for WNV. Next I examined the steady state of DDX56 during infection with these flaviviruses. Finally, I assayed POW and SLEV infectivity of virions produced from DDX56 knockdown cells.

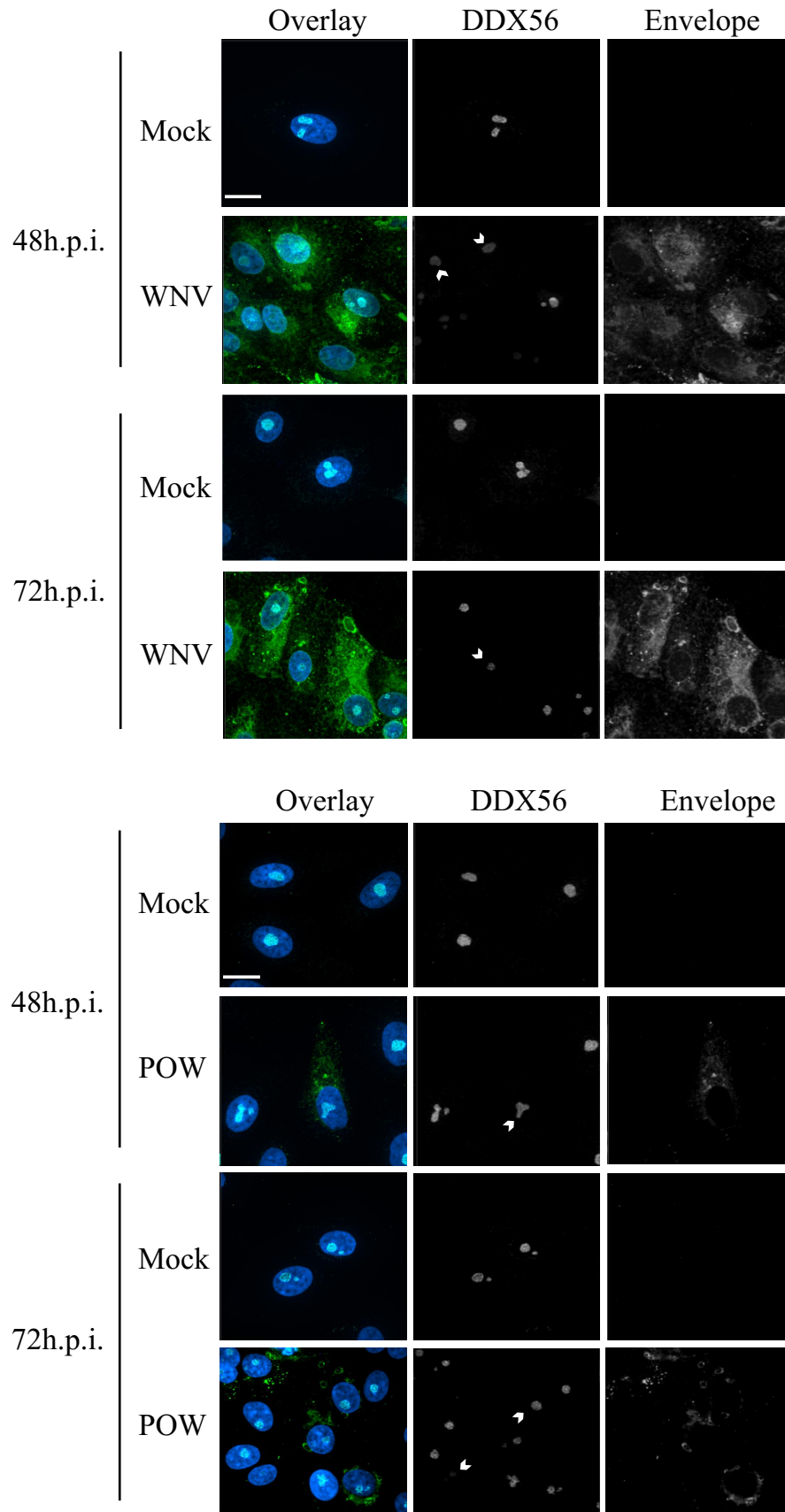
4.2 Results

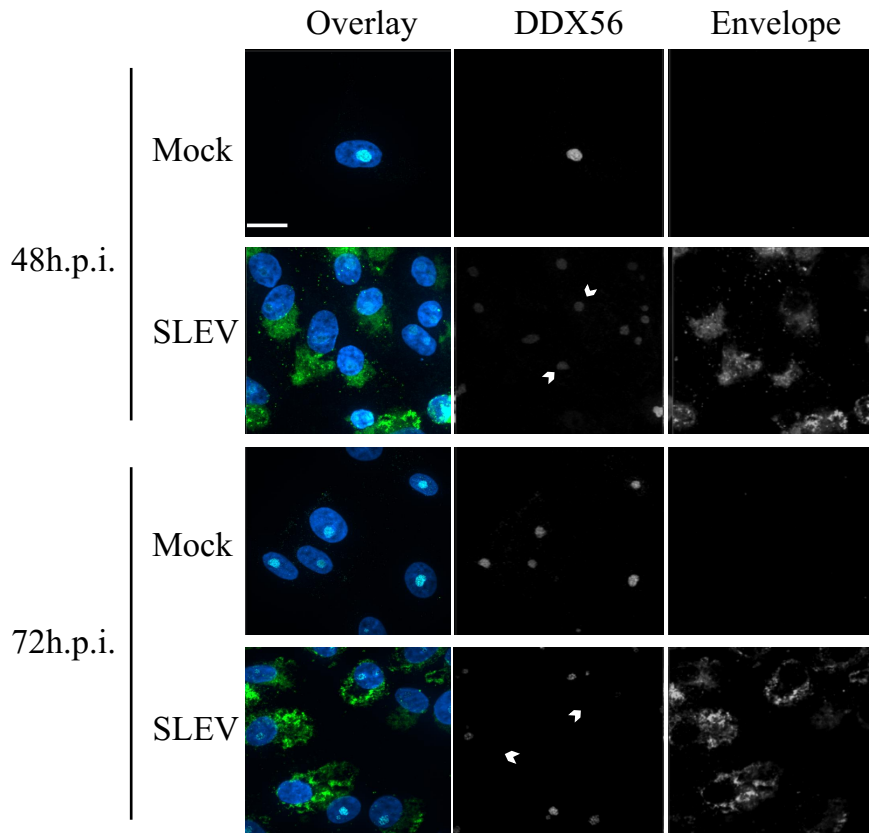
4.2.1 POW and SLEV infection causes depletion of DDX56

As stated above, DDX56 was identified as a WNV capsid binding protein, which interestingly is lost from the nucleolus during WNV infection and degraded by the proteasome. Infection with a related flavivirus, DENV-2 did not result in loss of DDX56 from nucleoli. To determine if the effect on DDX56 localization and stability was unique to WNV, I examined the localization of this helicase in POW- and SLEV-infected cells. Briefly, Vero cells were infected with WNV, POW, or SLEV for 48 or 72 hours and then processed for indirect immunofluorescence (section 2.2.7.1). DDX56 staining in the nucleolus diminished in POW- and SLEV-infected cells in a time-dependent manner (Figure 4.1, A, arrows). As a positive control, it can be seen that WNV infection resulted in diminished nucleolar DDX56 staining in Vero cells (Figure 4.1, A). Quantitation of DDX56 levels in nuclei of infected cells (n=50) was determined in three independent experiments by measuring pixel intensity using Volocity® 3D analysis software (Table 2.4). Compared to mock-infected cells, the DDX56 signal in nuclei of infected cells was

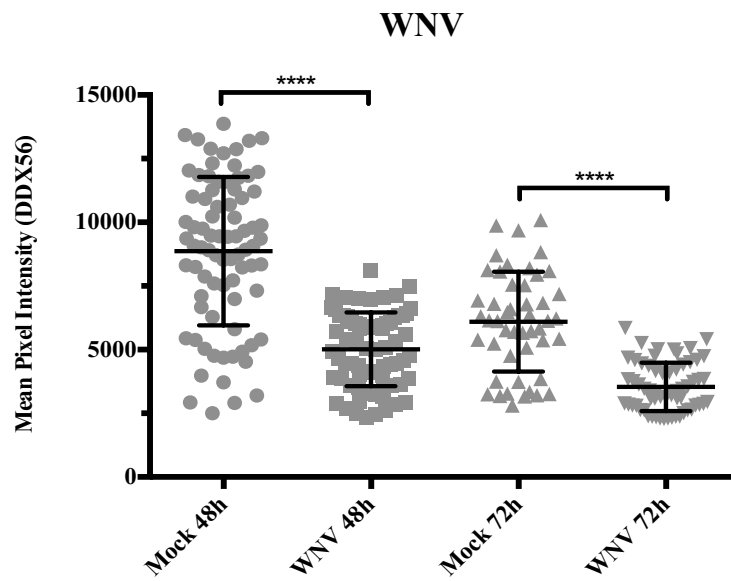
significantly decreased ($p < 0.001$) at 48 and 72 hours post infection for both POW and SLEV (Figure 4.1, B).

A.





B.



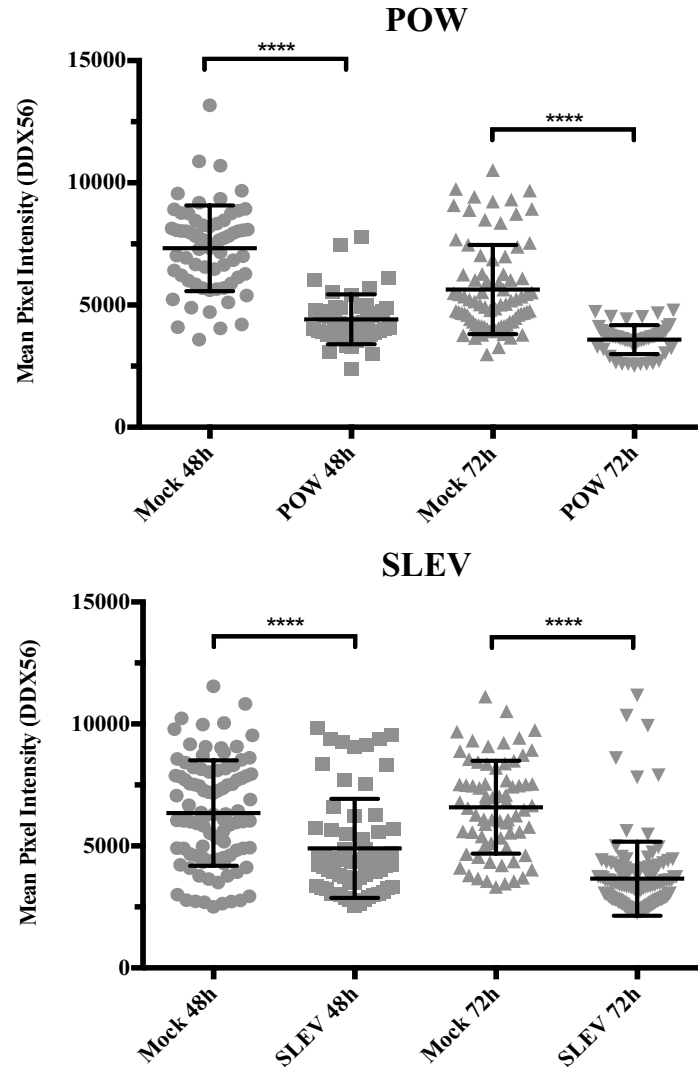
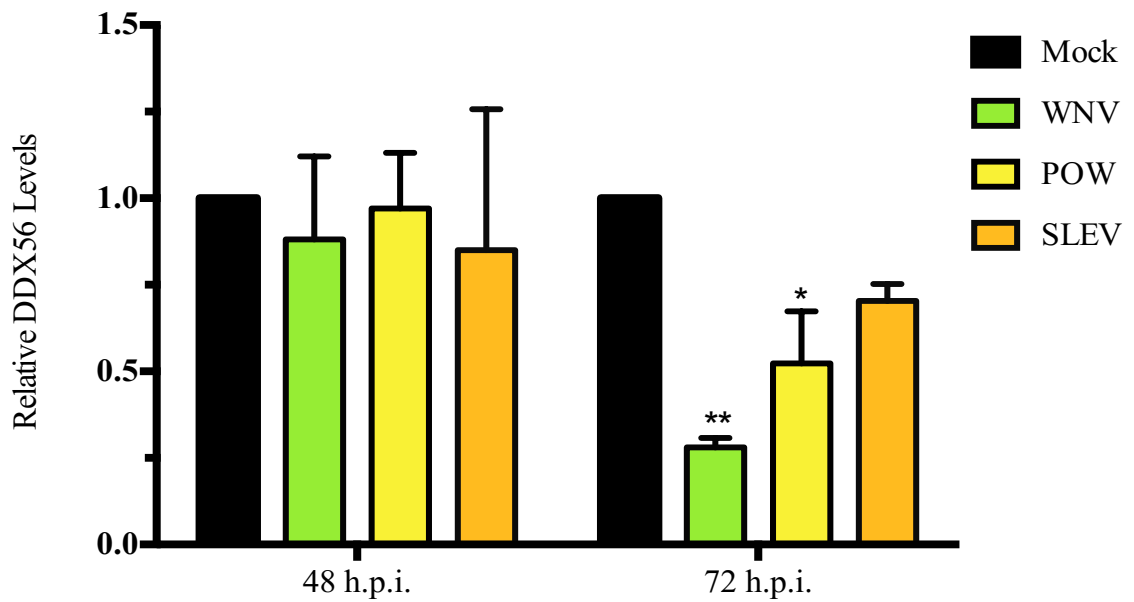
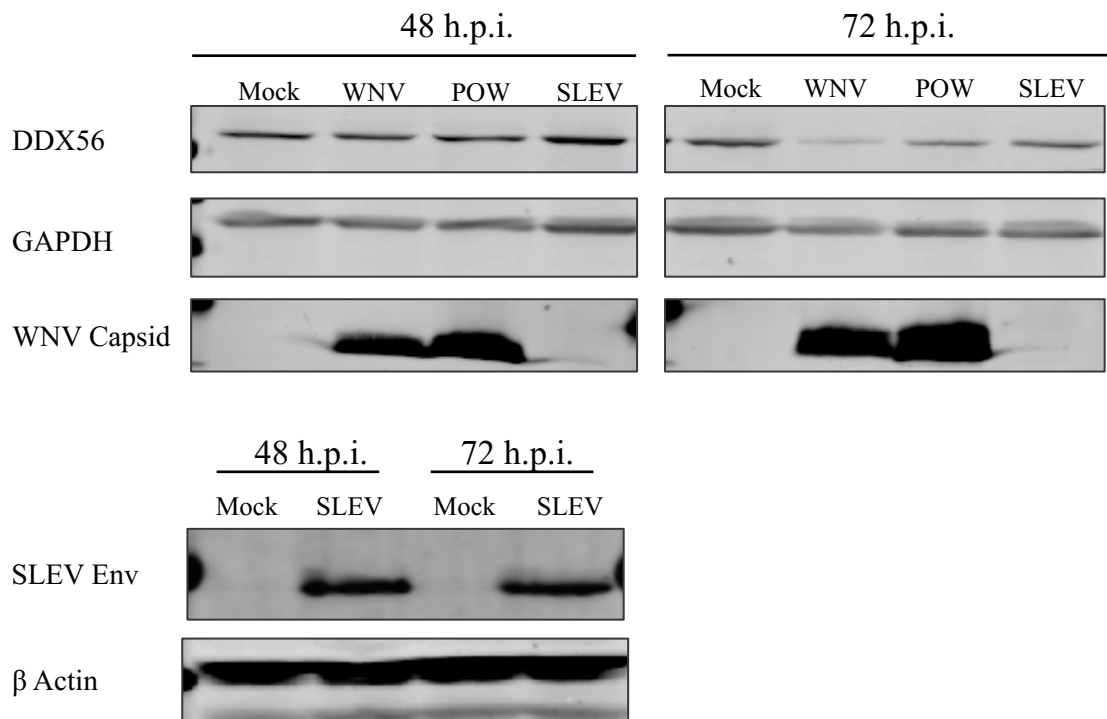


Figure 4.1 POW and SLEV infection induces loss of DDX56 in the nucleolus of Vero cells. A) Vero cells were infected with WNV (MOI, 3), POW (MOI, 1), or SLEV (MOI, 3). Cells were collected at 48 and 72 hours post infection (h.p.i.) and processed for indirect immunofluorescence using a mouse antibody to DDX56 which was detected by a goat anti-mouse IgG₁ Alexa 647. Viral envelope protein was detected with human, rabbit, or mouse antibodies for WNV, POW, and SLEV, respectively. Primary antibodies against viral envelope were detected using goat anti-human Alexa 488, goat anti-rabbit Alexa 488, or goat-anti mouse IgG2A Alexa 488. Images were captured using an Olympus IX-81 confocal spinning disk microscope. Arrows point to infected cells that have decreased levels of DDX56 in the nucleoli. Bars=15 μ m. B) Mock and Infected Vero cells from A were analyzed using Velocity to determine mean DDX56 pixel intensity in the nucleus for each whole cell in the field of view. A total of 50 cells from 3 experiments were used in the analysis. Statistical significance was determined with unpaired *t*-tests with Welch's correction. **** denotes a P value < 0.001.

It is possible that the decrease in DDX56 nuclear signal was due to diffuse localization in the cytoplasm rather than degradation by the proteasome. As such, I next used Immunoblot analyses to measure the relative levels of DDX56 in POW- or SLEV-infected cells. HEK 293T and Vero cells were infected with WNV, POW, or SLEV for 48 and 72 hours after which cell lysates were analyzed by SDS-PAGE and immunoblotting (described in section 2.2.5). A549 cells, which were not permissive for SLEV, were also infected with WNV or POW for these experiments. POW infection caused degradation of DDX56 in HEK 293T, Vero, and A549 cells (Figure 4.2). This decrease was statistically significant in all cell types at 72 h.p.i. as determined by 2-way ANOVA with Tukey's multiple comparison. Similarly, SLEV infection lead to a statistically significant decrease in DDX56 protein levels at 48 h.p.i. in HEK 293T cells and 72 h.p.i. in both HEK 293T and Vero cells (Figure 4.2, A and B). As expected, WNV infection, which was used as a positive control, reduced DDX56 protein levels over time, in all cell types. Together, these data suggest that other flaviviruses affect the localization and stability of DDX56. Whether POW or SLEV infection induce degradation of DDX56 by the proteasome remains to be determined.

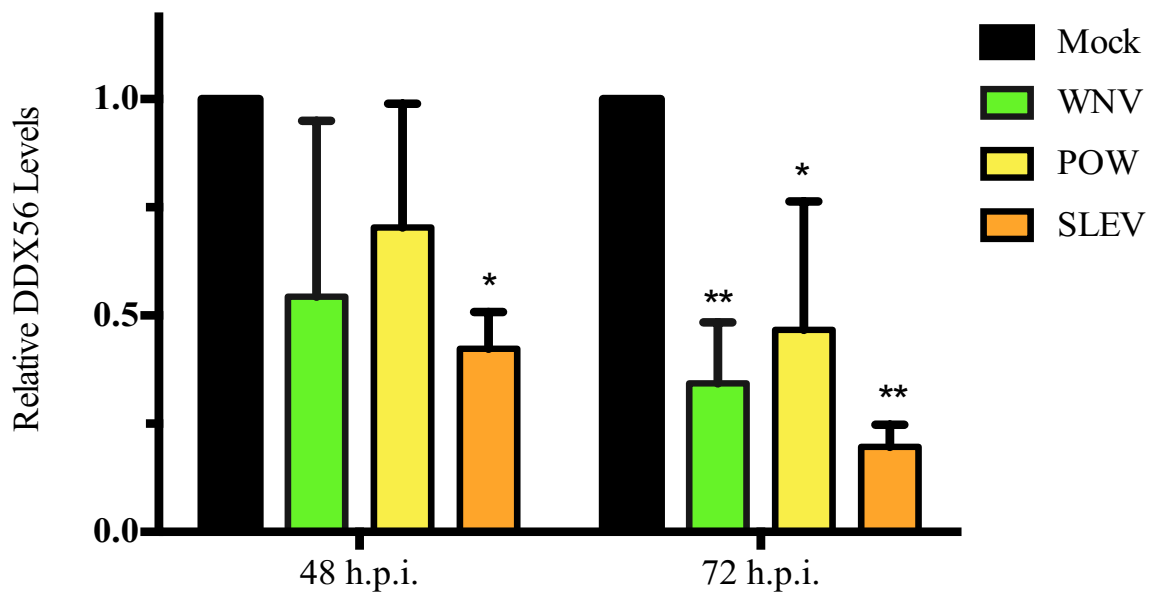
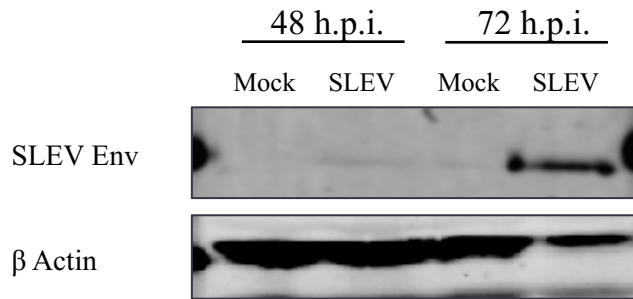
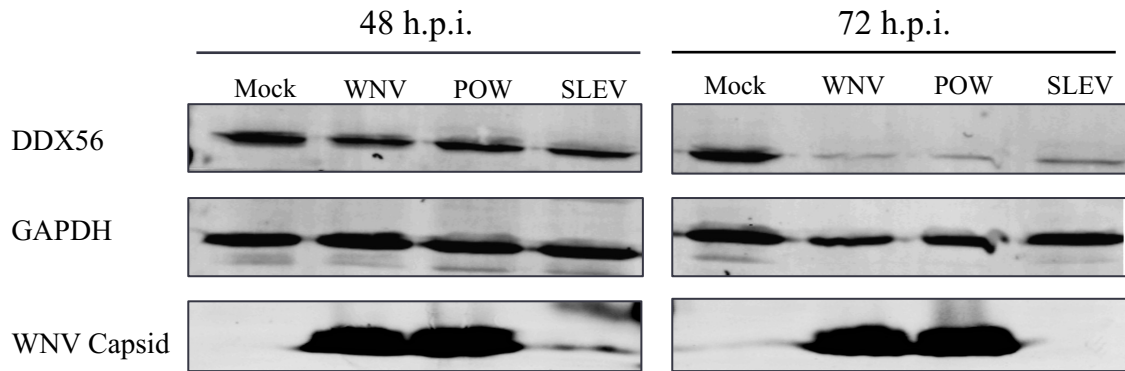
A.

Vero



B.

HEK 293T



C.

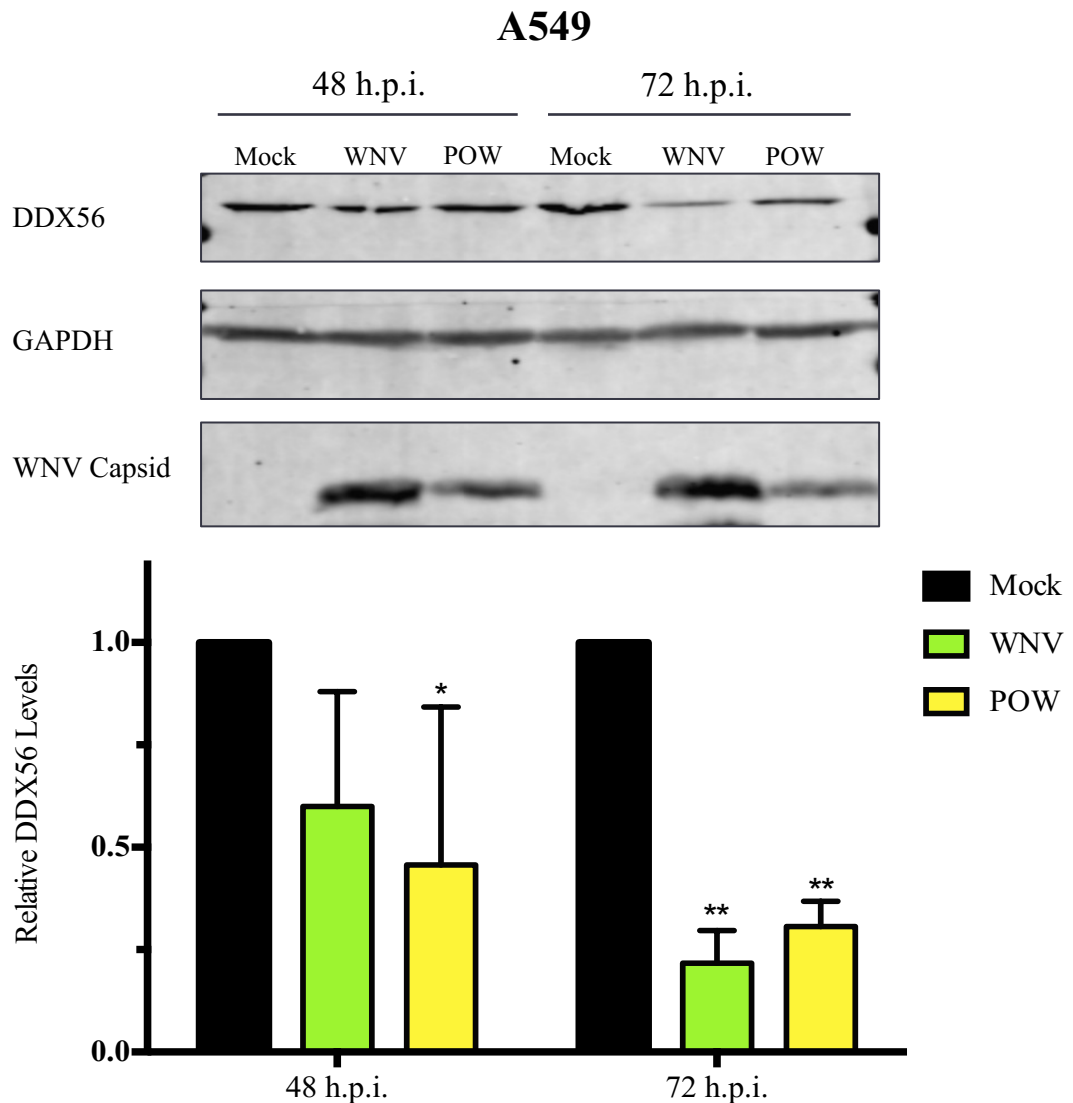


Figure 4.2 Flaviviruses WNV, POW, and SLEV induce degradation of DDX56 during infection. (A) Vero cells or (B) HEK 293T cells were infected with WNV (MOI, 3), POW (MOI,1) or SLEV (MOI, 3), and 48 or 72 hours post infection (h.p.i.) cell lysates were subjected to immunoblot analysis for DDX56 and GAPDH. Data from three independent experiments were used to determine the normalized level of DDX56 (relative to GAPDH). Lysates of mock treated and SLEV infected cells were also subjected to immunoblot analysis from non-reducing conditions for detection of SLEV envelope and β -actin. (C) A549 cells were infected with WNV (MOI, 3) or POW (MOI, 1), and 48 or 72 hours later cell lysates were subjected to immunoblot analysis for DDX56 and GAPDH. Data from three independent experiments were used to determine the normalized level of DDX56 (relative to GAPDH). Note: WNV capsid antibody was able to detect POW capsid. Statistical analysis by 2-way ANOVA with Tukey's multiple comparison function is shown by mean difference > 0.5 (*) and 0.65 (**).

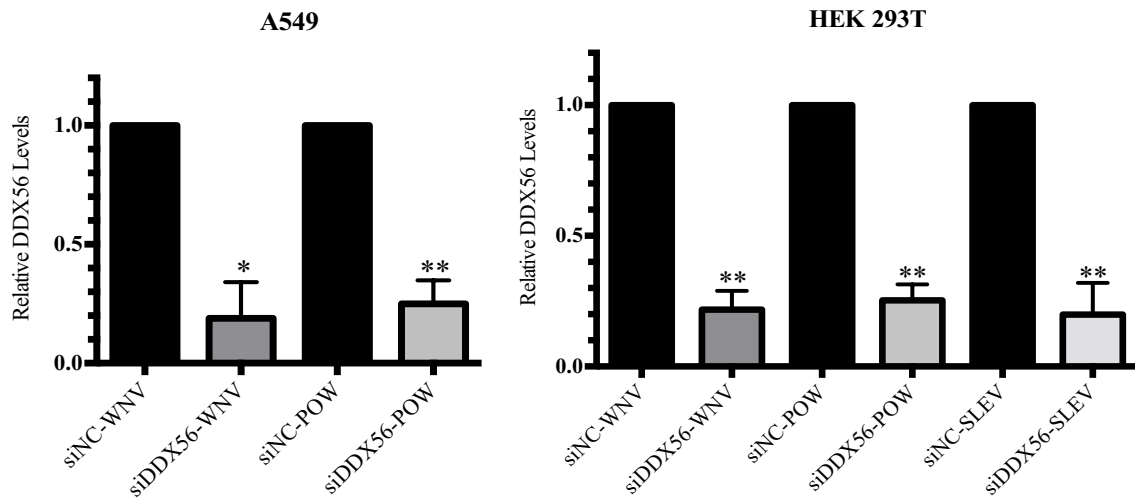
4.2.2 Reducing expression of DDX56 does not significantly affect the infectivity of POW and SLEV

Our laboratory showed that DDX56 is required for the production of infectious WNV virions, likely by enhancing packaging viral RNA at assembly sites (Xu, Anderson et al. 2011). To determine if DDX56 was also required for production of infectious POW and SLEV virions, I transiently knocked down expression of DDX56 in A549 and HEK 293T cells (Section 2.2.3) prior to infection with WNV, POW, or SLEV. Forty-eight hours after infection, cell media were collected and passed through 0.45 μ m PVDF filters before titer determination on Vero and BHK-21 cells (Section 2.2.4.3). Immunoblotting was used to assess DDX56 levels in control siRNA (siNC) and DDX56 siRNA (siDDX56) transfected cell lysates that were collected at 48 h.p.i. (72 hours post knock down). Transient knock down of DDX56 was successful in that protein levels were reduced 75-85% compared to siNC-transfected cells (Figure 4.3, A).

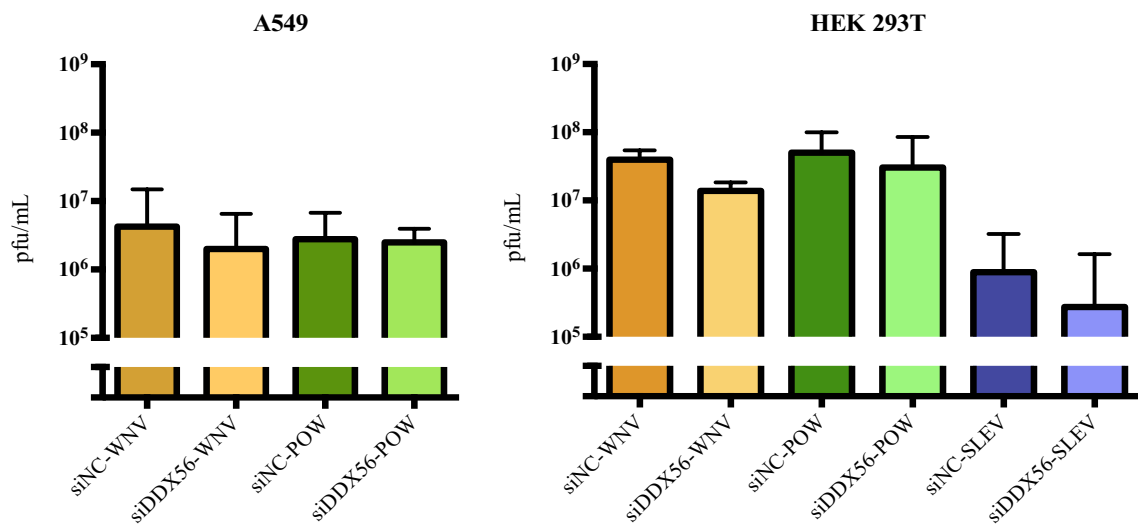
In light of our previous report that decreased DDX56 expression dramatically affects production of infectious WNV virions (Xu, Anderson et al. 2011), it was surprisingly to find that there were no significant differences when the cell supernatants were titered on Vero cells (Figure 4.3 B). This was the case for WNV, POW, or SLEV produced in A549 or HEK 293T cells transfected with control siRNA or DDX56 targeting siRNA. However, it is important to point out that Xu *et al*, used BHK-21 cells for the plaque assays and I was able to verify that WNV virions produced in siDDX56 cells were ~100 times less infectious than those produced in control cells when plaque assays were performed on BHK-21 cells (Figure 4.3, C).

In contrast to the WNV titer experiments in BHK-21 cells, there was no significant decrease in the amount of infectious POW virions released from DDX56-depleted A549 or HEK 293T cells. Similar results were observed from SLEV infection of HEK 293T cells transfected with DDX56-specific siRNA. Taken together, these data suggest that unlike WNV, neither POW nor SLEV require DDX56 for production of infectious virions.

A.



B.



C.

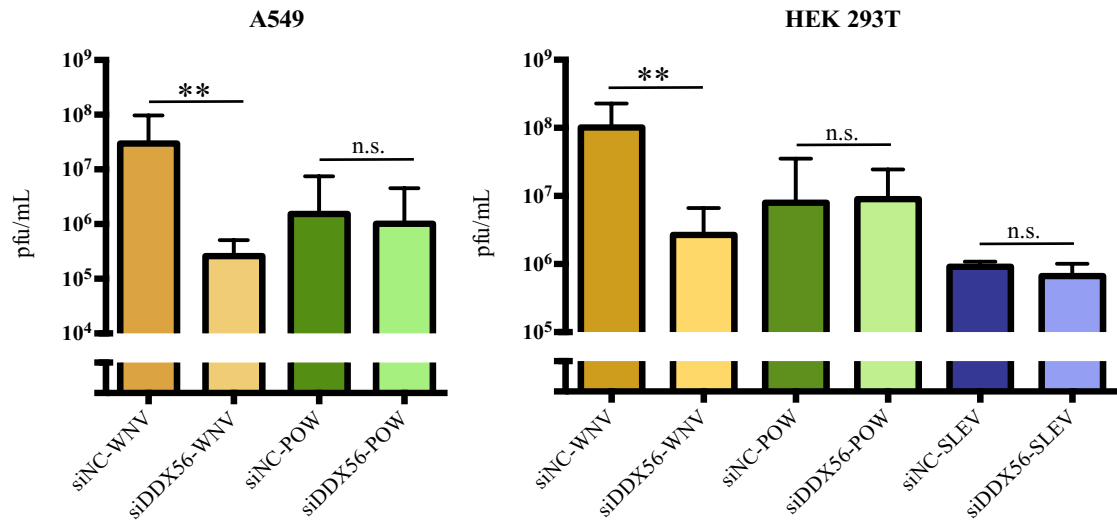


Figure 4.3 Flaviviruses POW and SLEV do not require DDX56 for infectious virion production. A) A549 or HEK 293T cells were transfected with 10nM non-silencing control siRNA (siNC) or DDX56-targeting siRNA (si-DDX56) 24h before infection with WNV, POW, or SLEV (MOI, 2). 48 hours later supernatants were saved for titer determination and cellular lysates were subjected to immunoblot analysis for DDX56 and β -actin. Data from three independent experiments were used to determine the normalized level of DDX56 (relative to β -actin). B) Levels of infectious virions produced from A549 or HEK293T siNC or siDDX56 cells was determined by a plaque assay in Vero cells. C) Levels of infectious virions produced from A549 or HEK293T siNC or siDDX56 cells was determined by a plaque assay in BHK-21 cells. Statistical analysis of differences was determined by pair *t*-tests with Welch's correction. *, $P < 0.05$ and **, $P < 0.01$.

4.3 Conclusion

In this chapter, using confocal microscopy, I provide evidence that DDX56 is lost from the nucleolus during infection with POW and SLEV. DDX56 is also degraded during infection of A549, HEK 293T, or Vero cells with POW and SLEV. The pathway for degradation of DDX56 in these cells remains to be determined. The experimental observations described here are consistent with what we have previously reported regarding stability of nuclear-localized DDX56 during WNV infection. Contrary to WNV infection, reducing DDX56 expression did not significantly affect the infectivity of POW or SLEV virions. This is in contrast to WNV, which requires DDX56 for efficient packaging of viral RNA and does not support our original hypothesis that SLEV based on its high degree of relatedness to WNV, requires DDX56 for infectivity. Together, these data suggest that DDX56 degradation and loss from the nucleolus is a separate phenomenon and is not indicative of a requirement for this host factor in the production of infectious virions. Accordingly, DDX56 seems to be a specific host factor for WNV due to its apparent lack of requirement by other *Flaviviruses*.

Chapter 5

Discussion

5.1 Overview

Flaviviruses are important human pathogens that significantly contribute to the global burden of viral disease. Research focused on the intricacies of flaviviral infection in host cells has identified important host factors through large genetic and proteomic screens (Saha 2003, Krishnan, Ng et al. 2008, Sessions, Barrows et al. 2009, Mishra, Diwaker et al. 2012, Mairiang, Zhang et al. 2013, Zhang, Chai et al. 2013, Campbell, Harrison et al. 2014, Sengupta, Ghosh et al. 2014). However, in many cases, functional and mechanistic data are lacking for these host factors. Understanding the specific manipulations by these viruses during infection will provide insight into how the necessary host factors are utilized, possibly allowing for the development of new antivirals. To this end, our group previously identified a nucleolar RNA helicase, DDX56, as an important WNV capsid-binding host factor. WNV virions produced in DDX56-KD cells or those expressing helicase-dead mutants are ~100x less infectious and contain 3-4x less viral RNA. This was interpreted to mean that the ATP-dependent helicase activity of DDX56 is required during virus assembly (Xu, Anderson et al. 2011, Xu and Hobman 2012). Consistent with this scenario, the nucleolar pool of DDX56 is depleted during WNV infection and the helicase accumulates in the cytoplasm, which is where replication and assembly of flaviviruses occurs.

In the first part of my thesis research, I used quantitative imaging to determine precisely where DDX56 localized in the cytoplasm of WNV infected cells. My data indicate that the enzyme localizes to regions of the ER that are enriched in the viral assembly marker, envelope (E) protein. The second part of my thesis research was to determine whether DDX56 was important for infectivity of the related *Flaviviruses*,

SLEV and POW. I found that both SLEV and POW infection induces loss of DDX56 from the nucleolus as well as degradation, which is similar to our observations for WNV. However, siRNA-mediated depletion of DDX56 did not significantly affect the infectivity of POW or SLEV virions. Accordingly, DDX56 appears to be a specific host factor for WNV assembly, but not related flaviviruses.

5.2 Unraveling the role of DDX56 during WNV Assembly

5.2.1 Characterizing DDX56 localization during WNV infection

As with all +RNA viruses, *Flaviviruses* remodel host cellular membranes, in particular those derived from the ER, however, little is known about how this occurs. Identifying the key components of these dynamic environments, such as viral and host proteins, will further our understanding of how these complexes form and may identify host factors that are suitable targets for antiviral therapy. To date there has not been a systematic study to characterize these sites during WNV infection by imaging techniques. Often nonstructural proteins, such as NS3 or NS5, or dsRNA antibodies are used to characterize sites of viral replication. In my study, I observed a lack of colocalization between dsRNA and E or capsid protein which indicates that these markers for replication and assembly respectively, are confined to distinct regions of the cytoplasm and can be resolved from each other using light microscopy. These markers overlapped with the resident ER protein calnexin, indicating that they in fact localized to the ER where replication and assembly occur. The results are consistent with previous tomographic studies of DENV infected cells, which indicated that these ER-localized sites are distinct but do occur in close proximity (Welsch, Miller et al. 2009). To my knowledge, this is the first study suggesting that WNV replication and assembly

complexes can be resolved by confocal microscopy imaging methods utilizing these markers, however, whether these are active assembly or replication sites remains to be determined.

Previously, DDX56 was visualized at capsid-positive puncta in the cytoplasm of WNV-infected cells treated with a proteasome inhibitor (Xu, Anderson et al. 2011). I expected to detect DDX56 at viral assembly sites (where RNA packaging occurs) and indeed, both confocal microscopy and 3D-SIM detected DDX56 in perinuclear clusters that overlapped with E and calnexin. Unexpectedly, I was not able to detect interaction or colocalization between DDX56 and WNV capsid protein in the cytoplasm. Instead, DDX56-capsid protein interactions occur primarily in the nucleus. At first glance, my results do not appear to support the original model in which genomic RNA packaging is enhanced by interaction of capsid with DDX56 at virus assembly sites (Xu and Hobman 2012), however, there are a number of factors to consider. One possibility is that the interaction between capsid and DDX56 in the cytoplasm is very unstable and/or transient. Alternatively, capsid-DDX56 interaction in the nucleus may affect other aspects of virus-host interactions such as blocking a nuclear-specific function of DDX56.

Multiple cellular pathways and host factors are important for the remodeling of host membranes during viral infection. For example, alterations in lipid metabolism are often required to aid in membrane proliferation and the production of specific lipids for their composition (Reviewed in (Belov and van Kuppeveld 2012)). To date, helicases have not been implicated in this complex process for WNV at least. In the case of HCV, the host cell DEAD-box RNA helicase, DDX3X, increases lipid droplet formation, resulting in greater association between lipid droplets and HCV core and ultimately

enhanced virion production (Li, Pène et al. 2013, Pène, Li et al. 2015). In contrast, my data indicate that DDX56 is not important for the formation of WNV VPs (replication sites) and CMs (proteolytic processing sites) as their size and abundance does not change in the absence of DDX56 protein expression. These structures are similar to what has been described previously for DENV and WNV (Welsch, Miller et al. 2009, Whiteman, Popov et al. 2015). In retrospect, this is not altogether surprising because the formation of these structures occurs early in infection, likely before the bulk of DDX56 moves from the nucleolus to the cytoplasm.

Previously, the Src-family kinase, c-Yes was shown to be important for the release of infectious WNV virions as pharmacological inhibition reduced viral titers 2-4 logs (Hirsch, Medigeschi et al. 2005). Examination of infected cells (by EM) in which c-Yes was inhibited, revealed a build up of virions in the ER suggesting that this kinase is important for virion egress. In contrast, I did not observe any differences in the accumulation of virions within DDX56-KD cells; further confirming that virion morphogenesis and egress do not require this helicase.

In summary, during WNV infection a pool of DDX56 localizes to the ER and colocalizes with E protein, likely at viral assembly sites. I was also able to demonstrate that presumed markers of virus replication and assembly localize to distinct regions of the ER. This further supports our hypothesis that DDX56 localizes to the ER during infection where it enhances the packaging of viral RNA.

5.2.2 Mechanisms of DDX56 relocalization

Often, host factors that are utilized by viruses are relocalized from their normal subcellular site. For example, many nuclear proteins that are relocalized to the cytoplasm during *Flavivirus* infection are involved in enhancing replication (reviewed in (Lloyd 2015)). DDX56 is different from other flavivirus-specific host factors, as its role seems to be confined to assembly of infectious virions. In non-infected cells, DDX56 has no known function in the cytoplasm. Rather, it localizes to the nucleolus where it is thought to facilitate biogenesis of 60S ribosomes (Zirwes, Eilbracht et al. 2000). As such, it was of interest to understand how WNV infection results relocalization of DDX56 from the nucleolus to subdomains of the ER where virus assembly occurs.

DDX56 and WNV capsid colocalize and interact in the nucleus, however, previous results suggest that capsid expression alone cannot alter the localization of DDX56 (Xu, Anderson et al. 2011). Thus, I assessed whether expression of other WNV proteins were sufficient for this process. Of interest, a pool of NS5 has been reported to localize to the nucleus during infection with DENV-2 or -3 serotypes (Hannemann, Sung et al. 2013). Expression of WNV nonstructural proteins, including NS5, with or without capsid did not alter DDX56 localization or stability. Moreover, expression of a cassette encoding the three WNV structural proteins C/prM/E alone or co-expressed with WNV nonstructural proteins (from two separate plasmids) did not affect DDX56 localization. However, it is important to point out that expression of the structural proteins in these cases was limited and therefore, I cannot definitively rule out their potential role in DDX56 localization.

While the mechanism by which WNV infection leads to DDX56 relocalization still needs to be elucidated, one can imagine two possibilities in which this occurs. First, there may be a general block of nuclear import, such as degradation of importins, preventing nuclear transport DDX56 following translation. Degradation of importins and blocking nuclear transport is a feature of many viruses, and is an important process used by some *Picornaviruses*, another +RNA virus family, to prevent antiviral signaling (reviewed in ((Yarborough, Mata et al. 2014))). Recently, it has been reported that HCV disrupts the nuclear pore complex by relocalizing many of these proteins to the membranous web, a process that seems to be important for viral replication (Neufeldt, Joyce et al. 2013). So far, very little is known whether *Flaviviruses* alter nuclear transport during infection. In this first scenario, WNV may sequester newly synthesized DDX56 at the ER for RNA packaging, preventing it from entering the nucleus, and nucleolar loss and degradation of DDX56 would be due to normal protein turnover. This model is consistent with my data showing that viral protein expression for 24h does not cause loss of DDX56 from the nucleolus. However, the fact that another host nuclear protein, nucleolin, is not relocalized or degraded during WNV infection, suggests that host nuclear import/export are not disrupted on a global scale (Xu, Anderson et al. 2011). Indeed, blocking the CRM-1 dependent nuclear import/export pathway did not prevent DDX56 degradation in WNV infected cells either. It is important to note that at 61 kDa, DDX56 is on the cusp of the size limit for passive diffusion through nuclear pores and may not be actively transported (reviewed in (Allen, Cronshaw et al. 2000))).

A second possibility is that DDX56 is actively recruited from the nucleolus and sequestered at the ER. In this scenario, a host factor and/or viral protein would facilitate

trafficking of DDX56 out of the nucleus. Given that we did not find evidence to suggest viral protein expression is sufficient, if this scenario is correct, it would appear that changes in cell physiology triggered by viral replication contributes to this process. For example, the redistribution of the host cell nuclear proteins TIA-1 and TIAR, which function in biogenesis of stress granules, to the cytoplasm is attributed to the stress caused by WNV or DENV infection (Li, Li et al. 2002, Emara and Brinton 2007). Their sequestration in the perinuclear region is also thought to aid in replication of these viruses. Finally, the two scenarios I have proposed need not be mutually exclusive, as both recruitment of nascent DDX56 to the ER and simultaneous inhibition of its nuclear import would result in increased DDX56 localization to the cytoplasm.

5.3 DDX56 is a specific host factor for WNV infectivity

As discussed previously, many *Flaviviruses*, including those studied here, cause similar clinical symptoms (i.e. neuroinvasion). Accordingly, development of broad-spectrum antivirals that could be used even before the specific viral pathogen is identified during early clinical onset. With this in mind, I focused on determining if DDX56 was an important host factor for related viruses, SLEV and POW.

Similar to WNV infection, DDX56 is lost from the nucleoli of cells infected with POW or SLEV. In contrast to WNV infection though, DDX56 is not required for production of infectious POW or SLEV virions. Therefore, the virus-induced change in DDX56 localization and stability is not necessarily indicative of its role in WNV assembly. This provides evidence in support of the scenario where viral infection itself, rather than a specific recruitment process, is responsible for nucleolar DDX56 loss and

degradation. One possible scenario is that during infection with WNV, POW, or SLEV, newly synthesized DDX56 is prevented from entering the nucleus; a situation that may result in increased degradation because the helicase is not in its normal subcellular location. This could explain why loss of DDX56 from the nucleolus occurs later in infection (>24 hours).

In the case of WNV, there seems to be cell type-specific factors that affect titer measurements. For example, when Vero cells were used for plaque assays, loss of DDX56 expression did not affect the infectivity of WNV. In contrast, when BHK-21 cells were used, up to 100-fold reduction in infectivity of WNV was observed when DDX56 levels were reduced. Of note, when WNV was plaqued on Vero cells, the titers were invariably lower than when BHK-21 cells were used. One possible explanation is that WNV uses different receptors for entry into Vero and BHK-21 cells. Moreover, Vero cells may be less permissive to virions that have altered protein and/or lipid composition (due to loss of DDX56 activity). Clearly, further investigation is needed to understand this phenomenon.

In summary, this study confirms that DDX56 is an important host factor that is specific for WNV infectivity but not POW or SLEV. However, virus-induced changes to its localization and stability are not limited to WNV infection, but rather appear to be the result of some common cellular response to flavivirus infection. Further characterization of this effect may provide insight into common host manipulations by *Flaviviruses*, which may help in the development of broad-spectrum antivirals.

5.4 Future Directions

Functional and localization studies of host factors can provide insight into their mechanistic function during viral infection. During my graduate studies I examined the localization of DDX56 during WNV infection. While I found that DDX56 localizes to ER-derived membranes and colocalizes with E protein, a marker of viral assembly, further investigation is needed. First, examination of viral assembly marker staining patterns in WNV infected DDX56-KD cells will determine if DDX56 influences the localization of these proteins. Second, while DDX56 is not packaged into virions, it is not clear whether this helicase affects the protein and/or lipid composition of WNV virions. Thus, it would be interesting to examine purified virions from both control and DDX56-KD cells by mass spectrometry. The outcome of these studies may provide evidence for additional roles of DDX56 during WNV infection.

Understanding the essential host factors used by the *Flavivirus* genus may lead to new targets for broad-spectrum antivirals. In the second study of my thesis, I showed that DDX56 is dispensable for the production of infectious POW or SLEV virions, however, DDX56 is lost from the nucleolus and degraded during infection. Further work into understanding why DDX56 is lost in the nucleolus of these viruses may give insight into the process of DDX56 relocalization and what factors contribute to this process. Additionally, production of infectious JEV, HCV, and DENV virions in DDX56-KD cells will determine if this host factor is dispensable for these related viruses as well, and is a viable target for antivirals during these infections.

References

Akey, D. L., W. C. Brown, S. Dutta, J. Konwerski, J. Jose, T. J. Jurkiw, J. DelProposto, C. M. Ogata, G. Skiniotis, R. J. Kuhn and J. L. Smith (2014). "Flavivirus NS1 structures reveal surfaces for associations with membranes and the immune system." Science **343**(6173): 881-885.

Allen, T. D., J. M. Cronshaw, S. Bagley, E. Kiseleva and M. W. Goldberg (2000). "The nuclear pore complex: mediator of translocation between nucleus and cytoplasm." J Cell Sci **113** (Pt 10): 1651-1659.

Angus, A. G. N., D. Dalrymple, S. Boulant, D. R. McGivern, R. F. Clayton, M. J. Scott, R. Adair, S. Graham, A. M. Owsianka, P. Targett-Adams, K. Li, T. Wakita, J. McLauchlan, S. M. Lemon and A. H. Patel (2010). "Requirement of cellular DDX3 for hepatitis C virus replication is unrelated to its interaction with the viral core protein." J Gen Virol **91**(Pt 1): 122-132.

Ariumi, Y., M. Kuroki, K.-i. Abe, H. Dansako, M. Ikeda, T. Wakita and N. Kato (2007). "DDX3 DEAD-box RNA helicase is required for hepatitis C virus RNA replication." J Virol **81**(24): 13922-13926.

Ariumi, Y., M. Kuroki, Y. Kushima, K. Osugi, M. Hijikata, M. Maki, M. Ikeda and N. Kato (2011). "Hepatitis C virus hijacks P-body and stress granule components around lipid droplets." J Virol **85**(14): 6882-6892.

Assenberg, R., E. Mastrangelo, T. S. Walter, A. Verma, M. Milani, R. J. Owens, D. I. Stuart, J. M. Grimes and E. J. Mancini (2009). "Crystal structure of a novel conformational state of the flavivirus NS3 protein: implications for polyprotein processing and viral replication." J Virol **83**(24): 12895-12906.

Assenberg, R., J. Ren, A. Verma, T. S. Walter, D. Alderton, R. J. Hurrelbrink, S. D. Fuller, S. Bressanelli, R. J. Owens, D. I. Stuart and J. M. Grimes (2007). "Crystal structure of the Murray Valley encephalitis virus NS5 methyltransferase domain in complex with cap analogues." J Gen Virol **88**(Pt 8): 2228-2236.

Belov, G. A. and F. J. van Kuppeveld (2012). "(+)RNA viruses rewire cellular pathways to build replication organelles." Curr Opin Virol **2**(6): 740-747.

Bhattacharyya, S., H. Yu, C. Mim and A. Matouschek (2014). "Regulated protein turnover: snapshots of the proteasome in action." Nat Rev Mol Cell Biol **15**(2): 122-133.

Bhuvanakantham, R. and M.-L. Ng (2013). "West Nile virus and dengue virus capsid protein negates the antiviral activity of human Sec3 protein through the proteasome pathway." Cell Microbiol **15**(10): 1688-1706.

- Biedenbender, R., J. Bevilacqua, A. M. Gregg, M. Watson and G. Dayan (2011). "Phase II, randomized, double-blind, placebo-controlled, multicenter study to investigate the immunogenicity and safety of a West Nile virus vaccine in healthy adults." J Infect Dis **203**(1): 75-84.
- Brinton, M. A. (2001). "Host factors involved in West Nile virus replication." Ann N Y Acad Sci **951**: 207-219.
- Calisher, C. H. (1994). "Medically important arboviruses of the United States and Canada." Clin Microbiol Rev **7**(1): 89-116.
- Campbell, C. L., T. Harrison, A. M. Hess and G. D. Ebel (2014). "MicroRNA levels are modulated in *Aedes aegypti* after exposure to Dengue-2." Insect Mol Biol **23**(1): 132-139.
- Chable-Bessia, C., O. Meziane, D. Latreille, R. Triboulet, A. Zamborlini, A. Wagschal, J.-M. Jacquet, J. Reynes, Y. Levy, A. Saib, Y. Bennasser and M. Benkirane (2009). "Suppression of HIV-1 replication by microRNA effectors." Retrovirology **6**: 26.
- Chahar, H. S., S. Chen and N. Manjunath (2013). "P-body components LSM1, GW182, DDX3, DDX6 and XRN1 are recruited to WNV replication sites and positively regulate viral replication." Virology **436**(1): 1-7.
- Chambers, T. J., A. Grakoui and C. M. Rice (1991). "Processing of the yellow fever virus nonstructural polyprotein: a catalytically active NS3 proteinase domain and NS2B are required for cleavages at dibasic sites." J Virol **65**(11): 6042-6050.
- Chatel-Chaix, L., M.-A. Germain, A. Motorina, É. Bonneil, P. Thibault, M. Baril and D. Lamarre (2013). "A host YB-1 ribonucleoprotein complex is hijacked by hepatitis C virus for the control of NS3-dependent particle production." J Virol **87**(21): 11704-11720.
- Chen, C. J., M. D. Kuo, L. J. Chien, S. L. Hsu, Y. M. Wang and J. H. Lin (1997). "RNA-protein interactions: involvement of NS3, NS5, and 3' noncoding regions of Japanese encephalitis virus genomic RNA." J Virol **71**(5): 3466-3473.
- Chen, Y., T. Maguire, R. E. Hileman, J. R. Fromm, J. D. Esko, R. J. Linhardt and R. M. Marks (1997). "Dengue virus infectivity depends on envelope protein binding to target cell heparan sulfate." Nat Med **3**(8): 866-871.
- Cheong, Y. K. and M.-L. Ng (2011). "Dephosphorylation of West Nile virus capsid protein enhances the processes of nucleocapsid assembly." Microbes Infect **13**(1): 76-84.

- Chiu, W.-W., R. M. Kinney and T. W. Dreher (2005). "Control of translation by the 5'- and 3'-terminal regions of the dengue virus genome." *J Virol* **79**(13): 8303-8315.
- Choi, Y.-J. and S.-G. Lee (2012). "The DEAD-box RNA helicase DDX3 interacts with DDX5, co-localizes with it in the cytoplasm during the G2/M phase of the cycle, and affects its shuttling during mRNP export." *J Cell Biochem* **113**(3): 985-996.
- Chu, J. J. and M. L. Ng (2004). "Infectious entry of West Nile virus occurs through a clathrin-mediated endocytic pathway." *J Virol* **78**(19): 10543-10555.
- Chu, P. W. and E. G. Westaway (1987). "Characterization of Kunjin virus RNA-dependent RNA polymerase: reinitiation of synthesis in vitro." *Virology* **157**(2): 330-337.
- Cui, T., R. J. Sugrue, Q. Xu, A. K. Lee, Y. C. Chan and J. Fu (1998). "Recombinant dengue virus type 1 NS3 protein exhibits specific viral RNA binding and NTPase activity regulated by the NS5 protein." *Virology* **246**(2): 409-417.
- Davis, C. W., H.-Y. Nguyen, S. L. Hanna, M. D. Sánchez, R. W. Doms and T. C. Pierson (2006). "West Nile virus discriminates between DC-SIGN and DC-SIGNR for cellular attachment and infection." *J Virol* **80**(3): 1290-1301.
- Day, J. F. (2001). "Predicting St. Louis encephalitis virus epidemics: lessons from recent, and not so recent, outbreaks." *Annu Rev Entomol* **46**: 111-138.
- Durbin, A. P., P. F. Wright, A. Cox, W. Kagucia, D. Elwood, S. Henderson, K. Wanionek, J. Speicher, S. S. Whitehead and A. G. Pletnev (2013). "The live attenuated chimeric vaccine rWN/DEN4Δ30 is well-tolerated and immunogenic in healthy flavivirus-naïve adult volunteers." *Vaccine* **31**(48): 5772-5777.
- Ebel, G. D. (2010). "Update on Powassan virus: emergence of a North American tick-borne flavivirus." *Annu Rev Entomol* **55**: 95-110.
- Edeling, M. A., M. S. Diamond and D. H. Fremont (2014). "Structural basis of Flavivirus NS1 assembly and antibody recognition." *Proc Natl Acad Sci U S A* **111**(11): 4285-4290.
- Egloff, M.-P., D. Benarroch, B. Selisko, J.-L. Romette and B. Canard (2002). "An RNA cap (nucleoside-2'-O-)-methyltransferase in the flavivirus RNA polymerase NS5: crystal structure and functional characterization." *EMBO J* **21**(11): 2757-2768.
- Emara, M. M. and M. A. Brinton (2007). "Interaction of TIA-1/TIAR with West Nile and dengue virus products in infected cells interferes with stress granule formation and processing body assembly." *Proc Natl Acad Sci U S A* **104**(21): 9041-9046.

- Gangodkar, S., P. Jain, N. Dixit, K. Ghosh and A. Basu (2010). "Dengue virus-induced autophagosomes and changes in endomembrane ultrastructure imaged by electron tomography and whole-mount grid-cell culture techniques." J Electron Microsc (Tokyo) **59**(6): 503-511.
- Geissler, R., R. P. Golbik and S.-E. Behrens (2012). "The DEAD-box helicase DDX3 supports the assembly of functional 80S ribosomes." Nucleic Acids Res **40**(11): 4998-5011.
- Gillespie, L. K., A. Hoenen, G. Morgan and J. M. Mackenzie (2010). "The endoplasmic reticulum provides the membrane platform for biogenesis of the flavivirus replication complex." J Virol **84**(20): 10438-10447.
- Girard, Y. A., V. Popov, J. Wen, V. Han and S. Higgs (2005). "Ultrastructural study of West Nile virus pathogenesis in *Culex pipiens quinquefasciatus* (Diptera: Culicidae)." J Med Entomol **42**(3): 429-444.
- Goh, P.-Y., Y.-J. Tan, S. P. Lim, Y. H. Tan, S. G. Lim, F. Fuller-Pace and W. Hong (2004). "Cellular RNA helicase p68 relocalization and interaction with the hepatitis C virus (HCV) NS5B protein and the potential role of p68 in HCV RNA replication." J Virol **78**(10): 5288-5298.
- Gray, T. J. and C. E. Webb (2014). "A review of the epidemiological and clinical aspects of West Nile virus." Int J Gen Med **7**: 193-203.
- Grun, J. B. and M. A. Brinton (1986). "Characterization of West Nile virus RNA-dependent RNA polymerase and cellular terminal adenylyl and uridylyl transferases in cell-free extracts." J Virol **60**(3): 1113-1124.
- Guyatt, K. J., E. G. Westaway and A. A. Khromykh (2001). "Expression and purification of enzymatically active recombinant RNA-dependent RNA polymerase (NS5) of the flavivirus Kunjin." J Virol Methods **92**(1): 37-44.
- Hannemann, H., P.-Y. Sung, H.-C. Chiu, A. Yousuf, J. Bird, S. P. Lim and A. D. Davidson (2013). "Serotype-specific differences in dengue virus non-structural protein 5 nuclear localization." J Biol Chem **288**(31): 22621-22635.
- Hayes, E. B. and D. R. O'Leary (2004). "West Nile virus infection: a pediatric perspective." Pediatrics **113**(5): 1375-1381.
- Hayes, E. B., J. J. Sejvar, S. R. Zaki, R. S. Lanciotti, A. V. Bode and G. L. Campbell (2005). "Virology, pathology, and clinical manifestations of West Nile virus disease." Emerg Infect Dis **11**(8): 1174-1179.

Hirsch, A. J., G. R. Medigeshi, H. L. Meyers, V. DeFilippis, K. Früh, T. Briese, W. I. Lipkin and J. A. Nelson (2005). "The Src family kinase c-Yes is required for maturation of West Nile virus particles." *J Virol* **79**(18): 11943-11951.

Hunt, T. A., M. D. Urbanowski, K. Kakani, L. M. Law, M. A. Brinton and T. C. Hobman (2007). "Interactions between the West Nile virus capsid protein and the host cell-encoded phosphatase inhibitor, I2PP2A." *Cell Microbiol* **9**(11): 2756-2766.

Ishaq, M., J. Hu, X. Wu, Q. Fu, Y. Yang, Q. Liu and D. Guo (2008). "Knockdown of cellular RNA helicase DDX3 by short hairpin RNAs suppresses HIV-1 viral replication without inducing apoptosis." *Mol Biotechnol* **39**(3): 231-238.

Ishikawa, T., A. Yamanaka and E. Konishi (2014). "A review of successful flavivirus vaccines and the problems with those flaviviruses for which vaccines are not yet available." *Vaccine* **32**(12): 1326-1337.

Jan, L. R., C. S. Yang, D. W. Trent, B. Falgout and C. J. Lai (1995). "Processing of Japanese encephalitis virus non-structural proteins: NS2B-NS3 complex and heterologous proteases." *J Gen Virol* **76** (Pt 3): 573-580.

Jangra, R. K., M. Yi and S. M. Lemon (2010). "DDX6 (Rck/p54) is required for efficient hepatitis C virus replication but not for internal ribosome entry site-directed translation." *J Virol* **84**(13): 6810-6824.

Junjhon, J., T. J. Edwards, U. Utaipat, V. D. Bowman, H. A. Holdaway, W. Zhang, P. Keelapang, C. Puttikhunt, R. Perera, P. R. Chipman, W. Kasinrerk, P. Malasit, R. J. Kuhn and N. Sittisombut (2010). "Influence of pr-M cleavage on the heterogeneity of extracellular dengue virus particles." *J Virol* **84**(16): 8353-8358.

Kaufmann, B. and M. G. Rossmann (2011). "Molecular mechanisms involved in the early steps of flavivirus cell entry." *Microbes Infect* **13**(1): 1-9.

Kaufusi, P. H., J. F. Kelley, R. Yanagihara and V. R. Nerurkar (2014). "Induction of endoplasmic reticulum-derived replication-competent membrane structures by West Nile virus non-structural protein 4B." *PLoS One* **9**(1): e84040.

Khromykh, A. A., A. N. Varnavski, P. L. Sedlak and E. G. Westaway (2001). "Coupling between replication and packaging of flavivirus RNA: evidence derived from the use of DNA-based full-length cDNA clones of Kunjin virus." *J Virol* **75**(10): 4633-4640.

Khromykh, A. A. and E. G. Westaway (1997). "Subgenomic replicons of the flavivirus Kunjin: construction and applications." *J Virol* **71**(2): 1497-1505.

Kimura, T. and A. Ohya (1988). "Association between the pH-dependent conformational change of West Nile flavivirus E protein and virus-mediated membrane fusion." J Gen Virol **69** (Pt 6): 1247-1254.

Krishnan, M. N. and M. A. Garcia-Blanco (2014). "Targeting host factors to treat West Nile and dengue viral infections." Viruses **6**(2): 683-708.

Krishnan, M. N., A. Ng, B. Sukumaran, F. D. Gilfoy, P. D. Uchil, H. Sultana, A. L. Brass, R. Adametz, M. Tsui, F. Qian, R. R. Montgomery, S. Lev, P. W. Mason, R. A. Koski, S. J. Elledge, R. J. Xavier, H. Agaisse and E. Fikrig (2008). "RNA interference screen for human genes associated with West Nile virus infection." Nature **455**(7210): 242-245.

Lazear, H. M. and M. S. Diamond (2015). "New insights into innate immune restriction of West Nile virus infection." Curr Opin Virol **11**: 1-6.

Lee, E. and M. Lobigs (2000). "Substitutions at the putative receptor-binding site of an encephalitic flavivirus alter virulence and host cell tropism and reveal a role for glycosaminoglycans in entry." J Virol **74**(19): 8867-8875.

Lee, E. and M. Lobigs (2002). "Mechanism of virulence attenuation of glycosaminoglycan-binding variants of Japanese encephalitis virus and Murray Valley encephalitis virus." J Virol **76**(10): 4901-4911.

Lee, J. W.-M., J. J.-H. Chu and M.-L. Ng (2006). "Quantifying the specific binding between West Nile virus envelope domain III protein and the cellular receptor alphaVbeta3 integrin." J Biol Chem **281**(3): 1352-1360.

Levin, A., C. J. Neufeldt, D. Pang, K. Wilson, D. Loewen-Dobler, M. A. Joyce, R. W. Wozniak and D. L. J. Tyrrell (2014). "Functional characterization of nuclear localization and export signals in hepatitis C virus proteins and their role in the membranous web." PLoS One **9**(12): e114629.

Li, C., L. L. Ge, P. P. Li, Y. Wang, J. J. Dai, M. X. Sun, L. Huang, Z. Q. Shen, X. C. Hu, H. Ishag and X. Mao (2014). "Cellular DDX3 regulates Japanese encephalitis virus replication by interacting with viral un-translated regions." Virology **449**: 70-81.

Li, C., L. L. Ge, P. P. Li, Y. Wang, M. X. Sun, L. Huang, H. Ishag, D. D. Di, Z. Q. Shen, W. X. Fan and X. Mao (2013). "The DEAD-box RNA helicase DDX5 acts as a positive regulator of Japanese encephalitis virus replication by binding to viral 3' UTR." Antiviral Res **100**(2): 487-499.

Li, H., S. Clum, S. You, K. E. Ebner and R. Padmanabhan (1999). "The serine protease and RNA-stimulated nucleoside triphosphatase and RNA helicase functional domains of dengue virus type 2 NS3 converge within a region of 20 amino acids." J Virol **73**(4): 3108-3116.

Li, Q., V. Pène, S. Krishnamurthy, H. Cha and T. J. Liang (2013). "Hepatitis C virus infection activates an innate pathway involving IKK- α in lipogenesis and viral assembly." Nat Med **19**(6): 722-729.

Li, W., Y. Li, N. Kedersha, P. Anderson, M. Emara, K. M. Swiderek, G. T. Moreno and M. A. Brinton (2002). "Cell proteins TIA-1 and TIAR interact with the 3' stem-loop of the West Nile virus complementary minus-strand RNA and facilitate virus replication." J Virol **76**(23): 11989-12000.

Lieberman, M. M., V. R. Nerurkar, H. Luo, B. Cropp, R. Carrion, M. de la Garza, B.-A. Coller, D. Clements, S. Ogata, T. Wong, T. Martyak and C. Weeks-Levy (2009). "Immunogenicity and protective efficacy of a recombinant subunit West Nile virus vaccine in rhesus monkeys." Clin Vaccine Immunol **16**(9): 1332-1337.

Lim, S. P. and P.-Y. Shi (2013). "West Nile virus drug discovery." Viruses **5**(12): 2977-3006.

Linder, P. and E. Jankowsky (2011). "From unwinding to clamping - the DEAD box RNA helicase family." Nat Rev Mol Cell Biol **12**(8): 505-516.

Liu, W. J., H. B. Chen, X. J. Wang, H. Huang and A. A. Khromykh (2004). "Analysis of adaptive mutations in Kunjin virus replicon RNA reveals a novel role for the flavivirus nonstructural protein NS2A in inhibition of beta interferon promoter-driven transcription." J Virol **78**(22): 12225-12235.

Liu, W. J., X. J. Wang, D. C. Clark, M. Lobigs, R. A. Hall and A. A. Khromykh (2006). "A single amino acid substitution in the West Nile virus nonstructural protein NS2A disables its ability to inhibit alpha/beta interferon induction and attenuates virus virulence in mice." J Virol **80**(5): 2396-2404.

Lloyd, R. E. (2015). "Nuclear proteins hijacked by mammalian cytoplasmic plus strand RNA viruses." Virology **479-480C**: 457-474.

Lorenz, I. C., S. L. Allison, F. X. Heinz and A. Helenius (2002). "Folding and dimerization of tick-borne encephalitis virus envelope proteins prM and E in the endoplasmic reticulum." J Virol **76**(11): 5480-5491.

Macdonald, J., J. Tonry, R. A. Hall, B. Williams, G. Palacios, M. S. Ashok, O. Jabado, D. Clark, R. B. Tesh, T. Briese and W. I. Lipkin (2005). "NS1 protein secretion during the acute phase of West Nile virus infection." *J Virol* **79**(22): 13924-13933.

Mackenzie, J. M., M. K. Jones and E. G. Westaway (1999). "Markers for trans-Golgi membranes and the intermediate compartment localize to induced membranes with distinct replication functions in flavivirus-infected cells." *J Virol* **73**(11): 9555-9567.

Mackenzie, J. M., M. K. Jones and P. R. Young (1996). "Immunolocalization of the dengue virus nonstructural glycoprotein NS1 suggests a role in viral RNA replication." *Virology* **220**(1): 232-240.

Mackenzie, J. M., M. T. Kenney and E. G. Westaway (2007). "West Nile virus strain Kunjin NS5 polymerase is a phosphoprotein localized at the cytoplasmic site of viral RNA synthesis." *J Gen Virol* **88**(Pt 4): 1163-1168.

Mairiang, D., H. Zhang, A. Sodja, T. Murali, P. Suriyaphol, P. Malasit, T. Limjindaporn and R. L. Finley, Jr. (2013). "Identification of new protein interactions between dengue fever virus and its hosts, human and mosquito." *PLoS One* **8**(1): e53535.

Makino, Y., M. Tadano, T. Anzai, S. P. Ma, S. Yasuda and T. Fukunaga (1989). "Detection of dengue 4 virus core protein in the nucleus. II. Antibody against dengue 4 core protein produced by a recombinant baculovirus reacts with the antigen in the nucleus." *J Gen Virol* **70** (Pt 6): 1417-1425.

McGivern, D. R. and S. M. Lemon (2009). "Tumor suppressors, chromosomal instability, and hepatitis C virus-associated liver cancer." *Annu Rev Pathol* **4**: 399-415.

Miller, S., S. Kastner, J. Krijnse-Locker, S. Buhler and R. Bartenschlager (2007). "The non-structural protein 4A of dengue virus is an integral membrane protein inducing membrane alterations in a 2K-regulated manner." *J Biol Chem* **282**(12): 8873-8882.

Mishra, K. P., D. Diwaker and L. Ganju (2012). "Dengue virus infection induces upregulation of hn RNP-H and PDIA3 for its multiplication in the host cell." *Virus Res* **163**(2): 573-579.

Miyaji, K., Y. Nakagawa, K. Matsumoto, H. Yoshida, H. Morikawa, Y. Hongou, Y. Arisaka, H. Kojima, T. Inoue, I. Hirata, K. Katsu and Y. Akao (2003). "Overexpression of a DEAD box/RNA helicase protein, rck/p54, in human hepatocytes from patients with hepatitis C virus-related chronic hepatitis and its implication in hepatocellular carcinogenesis." *J Viral Hepat* **10**(4): 241-248.

- Moesker, B., I. A. Rodenhuis-Zybert, T. Meijerhof, J. Wilschut and J. M. Smit (2010). "Characterization of the functional requirements of West Nile virus membrane fusion." J Gen Virol **91**(Pt 2): 389-393.
- Mori, Y., T. Okabayashi, T. Yamashita, Z. Zhao, T. Wakita, K. Yasui, F. Hasebe, M. Tadano, E. Konishi, K. Moriishi and Y. Matsuura (2005). "Nuclear localization of Japanese encephalitis virus core protein enhances viral replication." J Virol **79**(6): 3448-3458.
- Mostashari, F., M. L. Bunning, P. T. Kitsutani, D. A. Singer, D. Nash, M. J. Cooper, N. Katz, K. A. Liljebjelke, B. J. Biggerstaff, A. D. Fine, M. C. Layton, S. M. Mullin, A. J. Johnson, D. A. Martin, E. B. Hayes and G. L. Campbell (2001). "Epidemic West Nile encephalitis, New York, 1999: results of a household-based seroepidemiological survey." Lancet **358**(9278): 261-264.
- Moureau, G., S. Cook, P. Lemey, A. Nougairede, N. L. Forrester, M. Khasnatinov, R. N. Charrel, A. E. Firth, E. A. Gould and X. de Lamballerie (2015). "New insights into flavivirus evolution, taxonomy and biogeographic history, extended by analysis of canonical and alternative coding sequences." PLoS One **10**(2): e0117849.
- Mukhopadhyay, S., R. J. Kuhn and M. G. Rossmann (2005). "A structural perspective of the flavivirus life cycle." Nat Rev Microbiol **3**(1): 13-22.
- Mulhern, O. and A. G. Bowie (2010). "Unexpected roles for DEAD-box protein 3 in viral RNA sensing pathways." Eur J Immunol **40**(4): 933-935.
- Nagy, P. D. and J. Pogany (2012). "The dependence of viral RNA replication on co-opted host factors." Nat Rev Microbiol **10**(2): 137-149.
- Nash, D., F. Mostashari, A. Fine, J. Miller, D. O'Leary, K. Murray, A. Huang, A. Rosenberg, A. Greenberg, M. Sherman, S. Wong, M. Layton and W. N. O. R. W. Group (2001). "The outbreak of West Nile virus infection in the New York City area in 1999." N Engl J Med **344**(24): 1807-1814.
- Navarro-Sanchez, E., R. Altmeyer, A. Amara, O. Schwartz, F. Fieschi, J.-L. Virelizier, F. Arenzana-Seisdedos and P. Desprès (2003). "Dendritic-cell-specific ICAM3-grabbing non-integrin is essential for the productive infection of human dendritic cells by mosquito-cell-derived dengue viruses." EMBO Rep **4**(7): 723-728.
- Neufeldt, C. J., M. A. Joyce, A. Levin, R. H. Steenbergen, D. Pang, J. Shields, D. L. Tyrrell and R. W. Wozniak (2013). "Hepatitis C virus-induced cytoplasmic organelles use the nuclear transport machinery to establish an environment conducive to virus replication." PLoS Pathog **9**(10): e1003744.

- Offerdahl, D. K., D. W. Dorward, B. T. Hansen and M. E. Bloom (2012). "A three-dimensional comparison of tick-borne flavivirus infection in mammalian and tick cell lines." PLoS One **7**(10): e47912.
- Oliphant, T., M. Engle, G. E. Nybakken, C. Doane, S. Johnson, L. Huang, S. Gorlatov, E. Mehlhop, A. Marri, K. M. Chung, G. D. Ebel, L. D. Kramer, D. H. Fremont and M. S. Diamond (2005). "Development of a humanized monoclonal antibody with therapeutic potential against West Nile virus." Nat Med **11**(5): 522-530.
- Owsianka, A. M. and A. H. Patel (1999). "Hepatitis C Virus core protein interacts with a human DEAD box protein DDX3." Virology **257**: 330-340.
- Pène, V., Q. Li, C. Sodroski, C.-S. Hsu and T. J. Liang (2015). "Dynamic Interaction of Stress Granules, DDX3X, and IKK- α Mediates Multiple Functions in Hepatitis C Virus Infection." J Virol **89**(10): 5462-5477.
- Pérez-Vilaró, G., N. Scheller, V. Saludes and J. Díez (2012). "Hepatitis C virus infection alters P-body composition but is independent of P-body granules." J Virol **86**(16): 8740-8749.
- Ray, D., A. Shah, M. Tilgner, Y. Guo, Y. Zhao, H. Dong, T. S. Deas, Y. Zhou, H. Li and P.-Y. Shi (2006). "West Nile virus 5'-cap structure is formed by sequential guanine N-7 and ribose 2'-O methylations by nonstructural protein 5." J Virol **80**(17): 8362-8370.
- Reed, J. C., B. Molter, C. D. Geary, J. McNevin, J. McElrath, S. Giri, K. C. Klein and J. R. Lingappa (2012). "HIV-1 Gag co-opts a cellular complex containing DDX6, a helicase that facilitates capsid assembly." J Cell Biol **198**(3): 439-456.
- Reid, C., A. Airo and T. Hobman (2015). "The Virus-Host Interplay: Biogenesis of +RNA Replication Complexes." Viruses **7**(8): 2825.
- Reisen, W. K., H. D. Lothrop, S. S. Wheeler, M. Kennsington, A. Gutierrez, Y. Fang, S. Garcia and B. Lothrop (2008). "Persistent West Nile virus transmission and the apparent displacement St. Louis encephalitis virus in southeastern California, 2003-2006." J Med Entomol **45**(3): 494-508.
- Rhee, C., E. F. Eaton, W. Concepcion and B. G. Blackburn (2011). "West Nile virus encephalitis acquired via liver transplantation and clinical response to intravenous immunoglobulin: case report and review of the literature." Transpl Infect Dis **13**(3): 312-317.
- Rocak, S. and P. Linder (2004). "DEAD-box proteins: the driving forces behind RNA metabolism." Nat Rev Mol Cell Biol **5**(3): 232-241.

Roe, K., M. Kumar, S. Lum, B. Orillo, V. R. Nerurkar and S. Verma (2012). "West Nile virus-induced disruption of the blood-brain barrier in mice is characterized by the degradation of the junctional complex proteins and increase in multiple matrix metalloproteinases." J Gen Virol **93**(Pt 6): 1193-1203.

Roosendaal, J., E. G. Westaway, A. Khromykh and J. M. Mackenzie (2006). "Regulated cleavages at the West Nile virus NS4A-2K-NS4B junctions play a major role in rearranging cytoplasmic membranes and Golgi trafficking of the NS4A protein." J Virol **80**(9): 4623-4632.

Saha, S. (2003). "Common host genes are activated in mouse brain by Japanese encephalitis and rabies viruses." Journal of General Virology **84**(7): 1729-1735.

Scheller, N., L. B. Mina, R. P. Galão, A. Chari, M. Giménez-Barcons, A. Noueir, U. Fischer, A. Meyerhans and J. Díez (2009). "Translation and replication of hepatitis C virus genomic RNA depends on ancient cellular proteins that control mRNA fates." Proc Natl Acad Sci U S A **106**(32): 13517-13522.

Schermelleh, L., R. Heintzmann and H. Leonhardt (2010). "A guide to super-resolution fluorescence microscopy." J Cell Biol **190**(2): 165-175.

Sejvar, J. J. (2014). "Clinical manifestations and outcomes of West Nile virus infection." Viruses **6**(2): 606-623.

Selisko, B., H. Dutartre, J.-C. Guillemot, C. Debarnot, D. Benarroch, A. Khromykh, P. Desprès, M.-P. Egloff and B. Canard (2006). "Comparative mechanistic studies of de novo RNA synthesis by flavivirus RNA-dependent RNA polymerases." Virology **351**(1): 145-158.

Sengupta, N., S. Ghosh, S. V. Vasaikar, J. Gomes and A. Basu (2014). "Modulation of neuronal proteome profile in response to Japanese encephalitis virus infection." PLoS One **9**(3): e90211.

Sessions, O. M., N. J. Barrows, J. A. Souza-Neto, T. J. Robinson, C. L. Hershey, M. A. Rodgers, J. L. Ramirez, G. Dimopoulos, P. L. Yang, J. L. Pearson and M. A. Garcia-Blanco (2009). "Discovery of insect and human dengue virus host factors." Nature **458**(7241): 1047-1050.

Sips, G. J., J. Wilschut and J. M. Smit (2012). "Neuroinvasive flavivirus infections." Rev Med Virol **22**(2): 69-87.

- Soto-Rifo, R., P. S. Rubilar, T. Limousin, S. de Breyne, D. Décimo and T. Ohlmann (2012). "DEAD-box protein DDX3 associates with eIF4F to promote translation of selected mRNAs." *EMBO J* **31**(18): 3745-3756.
- Suthar, M. S., M. S. Diamond and M. Gale, Jr. (2013). "West Nile virus infection and immunity." *Nat Rev Microbiol* **11**(2): 115-128.
- Suzuki, K., P. Bose, R. Y. Leong-Quong, D. J. Fujita and K. Riabowol (2010). "REAP: A two minute cell fractionation method." *BMC Res Notes* **3**: 294.
- Tadano, M., Y. Makino, T. Fukunaga, Y. Okuno and K. Fukai (1989). "Detection of dengue 4 virus core protein in the nucleus. I. A monoclonal antibody to dengue 4 virus reacts with the antigen in the nucleus and cytoplasm." *J Gen Virol* **70 (Pt 6)**: 1409-1415.
- Tan, B. H., J. Fu, R. J. Sugrue, E. H. Yap, Y. C. Chan and Y. H. Tan (1996). "Recombinant dengue type 1 virus NS5 protein expressed in Escherichia coli exhibits RNA-dependent RNA polymerase activity." *Virology* **216**(2): 317-325.
- Tassaneeritthep, B., T. H. Burgess, A. Granelli-Piperno, C. Trumpfheller, J. Finke, W. Sun, M. A. Eller, K. Pattanapanyasat, S. Sarasombath, D. L. Birx, R. M. Steinman, S. Schlesinger and M. A. Marovich (2003). "DC-SIGN (CD209) mediates dengue virus infection of human dendritic cells." *J Exp Med* **197**(7): 823-829.
- Tilgner, M., T. S. Deas and P.-Y. Shi (2005). "The flavivirus-conserved penta-nucleotide in the 3' stem-loop of the West Nile virus genome requires a specific sequence and structure for RNA synthesis, but not for viral translation." *Virology* **331**(2): 375-386.
- Treffers, E. E., A. Tas, F. E. M. Scholte, M. N. Van, M. T. Heemskerk, A. H. de Ru, E. J. Snijder, M. J. van Hemert and P. A. van Veelen (2015). "Temporal SILAC-based quantitative proteomics identifies host factors involved in chikungunya virus replication." *Proteomics* **15**(13): 2267-2280.
- Uchil, P. D. and V. Satchidanandam (2003). "Architecture of the flaviviral replication complex. Protease, nuclease, and detergents reveal encasement within double-layered membrane compartments." *J Biol Chem* **278**(27): 24388-24398.
- Urbanowski, M. D. and T. C. Hobman (2013). "The West Nile virus capsid protein blocks apoptosis through a phosphatidylinositol 3-kinase-dependent mechanism." *J Virol* **87**(2): 872-881.
- Villordo, S. M. and A. V. Gamarnik (2009). "Genome cyclization as strategy for flavivirus RNA replication." *Virus Res* **139**(2): 230-239.

Ward, A. M., K. Bidet, A. Yinglin, S. G. Ler, K. Hogue, W. Blackstock, J. Gunaratne and M. A. Garcia-Blanco (2011). "Quantitative mass spectrometry of DENV-2 RNA-interacting proteins reveals that the DEAD-box RNA helicase DDX6 binds the DB1 and DB2 3' UTR structures." RNA Biol **8**(6): 1173-1186.

Watterson, D., B. Kobe and P. R. Young (2012). "Residues in domain III of the dengue virus envelope glycoprotein involved in cell-surface glycosaminoglycan binding." J Gen Virol **93**(Pt 1): 72-82.

Weaver, S. C. (2005). "Host range, amplification and arboviral disease emergence." Arch Virol Suppl(19): 33-44.

Welsch, S., S. Miller, I. Romero-Brey, A. Merz, C. K. Bleck, P. Walther, S. D. Fuller, C. Antony, J. Krijnse-Locker and R. Bartenschlager (2009). "Composition and three-dimensional architecture of the dengue virus replication and assembly sites." Cell Host Microbe **5**(4): 365-375.

Westaway, E. G., A. A. Khromykh, M. T. Kenney, J. M. Mackenzie and M. K. Jones (1997). "Proteins C and NS4B of the flavivirus Kunjin translocate independently into the nucleus." Virology **234**(1): 31-41.

Westaway, E. G., A. A. Khromykh and J. M. Mackenzie (1999). "Nascent flavivirus RNA colocalized in situ with double-stranded RNA in stable replication complexes." Virology **258**(1): 108-117.

Westaway, E. G. M., J. M.; Kenny, M. T.; Jones, M. K.; Khromykh, A. A.; (1997). "Ultrastructure of Kunjin Virus-Infected Cells: Colocalization of NS1 and NS3 with Double-Stranded RNA, and of NS2B with NS3, in Virus-Induced Membrane Structures." Journal of Virology **71**(9): 6650-6661.

Weston, A. and J. Sommerville (2006). "Xp54 and related (DDX6-like) RNA helicases: roles in messenger RNP assembly, translation regulation and RNA degradation." Nucleic Acids Res **34**(10): 3082-3094.

Whiteman, M. C., V. Popov, M. B. Sherman, J. Wen and A. D. T. Barrett (2015). "Attenuated West Nile virus mutant NS1130-132QQA/175A/207A exhibits virus-induced ultrastructural changes and accumulation of protein in the endoplasmic reticulum." J Virol **89**(2): 1474-1478.

Williams, C. A., T. E. M. Abbink, K.-T. Jeang and A. M. L. Lever (2015). "Identification of RNA helicases in human immunodeficiency virus 1 (HIV-1) replication - a targeted small interfering RNA library screen using pseudotyped and WT HIV-1." J Gen Virol **96**(Pt 6): 1484-1489.

Winston, D. J., H. R. Vikram, I. B. Rabe, G. Dhillon, D. Mulligan, J. C. Hong, R. W. Busuttil, M. J. Nowicki, T. Mone, R. Civen, S. A. Tecle, K. K. Trivedi, S. N. Hocevar and W. N. V. T.-A. T. I. Team (2014). "Donor-derived West Nile virus infection in solid organ transplant recipients: report of four additional cases and review of clinical, diagnostic, and therapeutic features." Transplantation **97**(9): 881-889.

Wu, R.-H., M.-H. Tsai, D.-Y. Chao and A. Yueh (2015). "Scanning mutagenesis studies reveal a potential intramolecular interaction within the C-terminal half of dengue virus NS2A involved in viral RNA replication and virus assembly and secretion." J Virol **89**(8): 4281-4295.

Xie, X., J. Zou, C. Puttikhunt, Z. Yuan and P.-Y. Shi (2015). "Two distinct sets of NS2A molecules are responsible for dengue virus RNA synthesis and virion assembly." J Virol **89**(2): 1298-1313.

Xu, T., A. Sampath, A. Chao, D. Wen, M. Nanao, P. Chene, S. G. Vasudevan and J. Lescar (2005). "Structure of the Dengue virus helicase/nucleoside triphosphatase catalytic domain at a resolution of 2.4 Å." J Virol **79**(16): 10278-10288.

Xu, Z. (2013). "Functional Analyses of West Nile Virus-Host Interactions " PhD Thesis.

Xu, Z., R. Anderson and T. C. Hobman (2011). "The capsid-binding nucleolar helicase DDX56 is important for infectivity of West Nile virus." J Virol **85**(11): 5571-5580.

Xu, Z. and T. C. Hobman (2012). "The helicase activity of DDX56 is required for its role in assembly of infectious West Nile virus particles." Virology **433**(1): 226-235.

Xu, Z., R. Waeckerlin, M. D. Urbanowski, G. van Marle and T. C. Hobman (2012). "West Nile virus infection causes endocytosis of a specific subset of tight junction membrane proteins." PLoS One **7**(5): e37886.

Yarbrough, M. L., M. A. Mata, R. Sakthivel and B. M. Fontoura (2014). "Viral subversion of nucleocytoplasmic trafficking." Traffic **15**(2): 127-140.

Yasuda-Inoue, M., M. Kuroki and Y. Ariumi (2013). "DDX3 RNA helicase is required for HIV-1 Tat function." Biochem Biophys Res Commun **441**(3): 607-611.

Yasuda-Inoue, M., M. Kuroki and Y. Ariumi (2013). "Distinct DDX DEAD-box RNA helicases cooperate to modulate the HIV-1 Rev function." Biochem Biophys Res Commun **434**(4): 803-808.

- Yedavalli, V. S. R. K., C. Neuveut, Y.-H. Chi, L. Kleiman and K.-T. Jeang (2004). "Requirement of DDX3 DEAD box RNA helicase for HIV-1 Rev-RRE export function." Cell **119**(3): 381-392.
- Yedavalli, V. S. R. K., N. Zhang, H. Cai, P. Zhang, M. F. Starost, R. S. Hosmane and K.-T. Jeang (2008). "Ring expanded nucleoside analogues inhibit RNA helicase and intracellular human immunodeficiency virus type 1 replication." J Med Chem **51**(16): 5043-5051.
- You, L.-R., C.-M. Chen, T.-S. Yeh, T.-Y. Tsai, R.-T. Mai, C.-H. Lin and Y.-H. W. Lee (1999). "Hepatitis C virus core protein interacts with cellular putative RNA Helicase." J Virol **73**(4): 2841-2853.
- Youn, S., R. L. Ambrose, J. M. Mackenzie and M. S. Diamond (2013). "Non-structural protein-1 is required for West Nile virus replication complex formation and viral RNA synthesis." Virology **450**: 339.
- Zhang, C., L. He, K. Kang, H. Chen, L. Xu and Y. Zhang (2014). "Screening of cellular proteins that interact with the classical swine fever virus non-structural protein 5A by yeast two-hybrid analysis." J Biosci **39**(1): 63-74.
- Zhang, L. and R. Padmanabhan (1993). "Role of protein conformation in the processing of dengue virus type 2 nonstructural polyprotein precursor." Gene **129**(2): 197-205.
- Zhang, L. K., F. Chai, H. Y. Li, G. Xiao and L. Guo (2013). "Identification of host proteins involved in Japanese encephalitis virus infection by quantitative proteomics analysis." J Proteome Res **12**(6): 2666-2678.
- Zhang, Y., J. Corver, P. R. Chipman, W. Zhang, S. V. Pletnev, D. Sedlak, T. S. Baker, J. H. Strauss, R. J. Kuhn and M. G. Rossmann (2003). "Structures of immature flavivirus particles." EMBO J **22**(11): 2604-2613.
- Zhang, Y., B. Kaufmann, P. R. Chipman, R. J. Kuhn and M. G. Rossmann (2007). "Structure of immature West Nile virus." J Virol **81**(11): 6141-6145.
- Zhou, X., J. Luo, L. Mills, S. Wu, T. Pan, G. Geng, J. Zhang, H. Luo, C. Liu and H. Zhang (2013). "DDX5 facilitates HIV-1 replication as a cellular co-factor of Rev." PLoS One **8**(5): e65040.
- Zhou, Y., D. Ray, Y. Zhao, H. Dong, S. Ren, Z. Li, Y. Guo, K. A. Bernard, P.-Y. Shi and H. Li (2007). "Structure and function of flavivirus NS5 methyltransferase." J Virol **81**(8): 3891-3903.

Zirwes, R., J. Eilbracht, S. Kneissel and M. Schmidt-Zachmann (2000). "A novel helicase-type protein in the nucleolus: protein NOH61." Molecular Biology of the Cell **11**(4): 1153-1167.